

INVESTIGATIONS ON ULTRASONIC TRANSDUCER ARRAY SYSTEMS FOR NDE OF UNDERWATER PIPELINES

A THESIS SUBMITTED BY
SUMANGALA R.

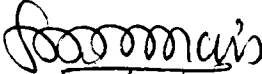
IN PARTIAL FULFILMENT OF THE
REQUIREMENTS FOR THE DEGREE OF
DOCTOR OF PHILOSOPHY

**DEPARTMENT OF ELECTRONICS
FACULTY OF TECHNOLOGY
COCHIN UNIVERSITY OF SCIENCE AND TECHNOLOGY
COCHIN-682 022, INDIA**

DECEMBER 1996

CERTIFICATE

This is to certify that the thesis entitled "**Investigations on Ultrasonic Transducer Array Systems for NDE of Underwater Pipelines**" is a bona fide record of the research work carried out by Ms. Sumangala.R under my supervision in the *Department of Electronics, Cochin University of Science & Technology*. The results embodied in this thesis or part of it have not been presented for any other degree.


16/12/96

DR.P.R.SASEENDRAN PILLAI
(Supervising Teacher)
Professor
Department of Electronics
Cochin University of Sci. & Tech.

Cochin
16th December 1996

CONTENTS

Chapter 1 Introduction

1.1. Historical development	3
1.2 Ultrasonic transducers	7
1.2.1 Ceramic Transducers	7
1.2.2 Piezopolymer Transducers	8
1.2.3 Radiated fields	9
1.2.4 Focusing	9
1.2.5 Sound levels and decibel scale	9
1.3 Properties of transducer arrays	10
1.3.1 Array gain	11
1.3.2 Shading and Superdirectivity	11
1.3.3 Array Beamsteering	11
1.3.4 Directivity index	11
1.4 Ultrasonic testing techniques	12
1.4.1 Ultrasonic probes	12
1.4.2 Through transmission technique	12

1.4.3 Resonance Technique	13
1.4.4 Pulse echo technique	14
1.4.5 Modes of display	14
1.5 Motivation for the present work	14
1.6 Brief description of the present work	16
Chapter 2 Review of past work	
2.1 Transducer design	20
2.2 PVDF transducers	24
2.3 Sound field	27
2.4 Pulsed transducers	29
2.5 High frequency transducers	30
2.6 Transducer arrays	31
Chapter 3 Methodology	
3.1 Ultrasonic waves	36
3.1.1 Compressional waves	37
3.1.2 Shear waves	37
3.1.3 Surface waves	38
3.1.4 Plate waves	38
3.1.5 Plane waves at solid liquid interface	39
3.2 Methods and instrumentation	42
3.2.1 Design considerations	42
3.2.2 Single crystal vertical (0°) probes	43
3.2.3 Single crystal angle probe	44
3.2.4 Transmitter receiver (TR) probes or twin probes	45

3.3 Ultrasonic testing techniques	45
3.3.1 Through transmission technique	46
3.3.2 Resonance Technique	47
3.3.3 Pulse echo method	48
3.3.4 Modes of display	49
3.4 Properties of transducer arrays	50
3.4.1 Array gain	50
3.4.2 Beam Pattern	52
3.4.3 Shading and Superdirectivity	52
3.4.4 Array beamsteering	54
3.4.5 Directivity index	55
3.4.6 Acoustic pressure field	56

Chapter 4 Beam characteristics of annular ring and annular cylindrical arrays

4.1 Inspection system	58
4.2 Crosscorrelation coefficients	60
4.2.1 Annular ring array	61
4.2.2 Annular cylindrical array	61
4.3 Array gain	62
4.4 Beam pattern	63
4.4.1 Annular ring array	63
4.4.2 Annular cylindrical array	71

Chapter 5 Effective acoustic pressure of annular ring and annular cylindrical arrays

5.1 Computation of effective acoustic pressure at a point	76
---	----

5.1.1 Multiple point source	76
5.1.2 Annular ring array	77
5.1.3 Annular cylindrical array	84
5.2 Impulse response	89
5.2.1 Impulse response of a circular piston	90
5.2.2 Impulse response of annular ring and annular cylindrical arrays	91
5.3 Transient response	92
Chapter 6 Conclusions	
6.1 Highlights	95
6.2 Scope for further work	99
Appendix 1 Performance evaluation of (3,3) Mode PVDF transducer elements for Ultrasonic NDE	
A.1 Design	100
A.2 Measurement set-up	103
A.3 Reciprocity theorem	104
A.4 Reciprocity calibration	104
A.5 Results	105
A.6 Conclusions	106
References	113
Index	128
List of publications of the author	134
Reprints of journal papers published	135

**Investigations on Ultrasonic Transducer Array
Systems for NDE of Underwater Pipelines**

Introduction

Structural integrity of his shelter, defence, transportation and energy resources has been of great concern to man from time immemorial. Earliest instance of testing techniques can be traced back to the prehistoric man where a sharp tug on a vine could ensure its load bearing capacity. Though testing techniques have come a long way from that, the basic philosophy of proof testing remains the same even today. The field of Nondestructive testing(NDT) is related to other technical disciplines involving instrument development, health physics, laser technology, medicine, process control, corrosion monitoring and nuclear power. Some of the nondestructive testing techniques available today are, radiography, magnetic particle tests, magnetic flux

leakage technique, ultrasonic testing, neutron radiographic technique, liquid penetrant technique, remote field eddy current technique, leak testing, acoustic emissions, visual inspection and holography [1].

Ultrasonic testing technique is found to be the best suited for underwater applications. Electromagnetic waves get easily attenuated in water hence cannot penetrate. The use of ultrasound for nondestructive characterisation of metals and other materials was one of the first applications of ultrasound and dates back to the 1950s. The detailed properties of materials that can be measured with ultrasound include microstructure, surface characteristics, elastic properties, density, porosity, mechanical properties, process characteristics and flaws. Ultrasonic waves transmitted may take the form of longitudinal, shear and surface waves. Wave characteristics include ultrasonic velocities and frequency dependence of ultrasonic attenuation/ absorption. Specific reaction occurring within a tested material may include ultrasound reflection, transmission, refraction, diffraction, interference, scattering and absorption. In applying ultrasound to testing, the characteristics of the radiation source that can be manipulated include wave type, frequency, bandwidth, pulse shape and pulse size.

Ultrasound is the only technique that is applicable to a wide range of materials compared to other nondestructive characterisation methods such as liquid penetrant examination, magnetic particle, eddy current testing and radiography [2]. Of the various Non Destructive Evaluation techniques, ultrasonic method plays a vital role in defect detection, characterisation, estimation as well as in medical diagnostics and therapy. The success of an ultrasonic nondestructive testing application depends on the selection of the best qualified transducer, with optimum frequency response, pulse

width and shape. Some of the applications of ultrasound are in detection of fluid flow, liquid level, viscosity, density, proximity and material thickness. Industrial applications are in cleaning, drilling, emulsifying, soldering, welding as well as in some security systems to detect intruders. In surgery it is used in extracorporeal lithotripsy, for breaking up gall stones into fragments. Ultrasonic density sensors are used in density measurement of lime slurries, for the purpose of adjusting pH. These sensors can be fully immersed in an agitated slurry, without the sensor surface being coated or clogged. The suspended solids present in the slurry attenuate the ultrasonic beam. Ultrasonic waves transmitted from a transducer gets reflected or scattered at a surface or discontinuity which can be received by another transducer. The time elapsed between the transmitted and reflected signal is a measure of the distance of the discontinuity or crack. The amplitude of the reflected signal is proportional to the dimension of the defect.

1.1 HISTORICAL DEVELOPMENT

Ultrasonic testing of defects in solid materials was first proposed by Sokolov in the year 1929[1]. In 1931 Mühlhäuser obtained the first patent for an instrument working with the shadow method. Kruse, Meyer, Bock, Czerlinsky, Götz and Shraiber have also been working with transducers made from piezoelectric quartz plates. During the second world war, ultrasonic instruments designed by Berthold and Trost were used for the first practical testing of steel boiler plates. After the second world war, the companies ACEC of Charloi, Belgium and Dr. Lehfeldt and Co. of Heppenheim, Germany started the production of ultrasonic instruments using the shadow method.

The experiments for imaging methods were started in the 1930s with Pohlman cell being the first to transform the sound pressure into visual image. A complete device using this cell, the Schallsichtgerät was developed with a large visual field of 500mm. It was used to test steel plates. Ogura et al. Cunningham and Quate have used the principle of the Pohlman cell in 1972 with a frequency of 1000 MHz for ultrasonic microscopy. Sokolov in 1936 introduced the relief method in which the image of the ripples generated on the water surface by the reflection of high intensity ultrasound by immersed specimen, can be observed with special illumination. In the 50-100MHz range it is used in commercial applications as an ultrasonic microscope (SLAM-scanning laser acoustic microscope) or sonomicroscope by Sonoscan, USA.

The phase-measuring method of Hatfield, was used for thickness and velocity measurements in which the phase of an outgoing wave is compared with that of a reflected one. Kaiser put forth sound-emission analysis as a possible means of nondestructive testing of materials. Mason, Mc Skimin and Shockley made first trials to use this method. In the 1940s, materials testing by continuous waves was replaced by pulses and wall thickness measurements were carried out using the resonance method. Resonance method makes use of the fact that the resonance frequency of a plate depends on its thickness.

Resonance based instruments were later on replaced by pulse echo instruments. The transit time of the pulse gives the required information about the thickness of plate or location of flaw for wall- thickness measurements. Spallanza in 1798 suggested that bats can orientate using inaudible sound signals, but this was proved only in 1938 by Pierce and Griffin. The discovery of piezoelectric effect by Jacques and Pierre Curie

facilitated the technical realisation of the pulse echo method, using quartz crystals as transmitters and receivers.

Between 1885 and 1910, Lord Rayleigh enunciated the scientific fundamentals of the propagation of sound in solids. Langevin and Chilowski between 1915 and 1917, solved the problem of detecting submarines and icebergs by using ultrasonic pulses. Though this method found many applications in measuring sea-depths, it could effectively be used for materials testing only after the rapid developments of electronic engineering during the period 1935 to 1938.

In 1940 Firestone (USA) put forward the first proposal to use pulse echo techniques for materials testing. In England, Sproule used this method in 1942. Kruse in Germany developed a pulse echo system.

In 1943, Sperry Products Inc., Danbury, USA and Kelvin and Hughes Ltd., London, built the first commercial apparatus for pulse echo method, based on the works of Firestone and Sproule. Though considerable success was achieved in testing large forgings using longitudinal waves at perpendicular incidence, new applications like testing of tubes and welds became feasible by transverse waves produced by filling plastic wedges to the longitudinal wave probes. Piezoceramics and piezopolymers have replaced quartz due to their higher sensitivity.

The first experiments with ultrasonic holography were carried out by Greguss, Mueller, Sheridan and Thurstone in 1965 and 1966, after the invention of the laser optical holography.

In 1974, Mezrich and his collaborators invented a scanning method with lasers using interferometry. A very thin metallic foil immersed in a cell filled with liquid, forms one of the twin mirrors of Michelson interferometer, which can follow the particle movement in an ultrasonic wave. A laser beam scans its surface to produce an image. This is the principle used in ultrasonovision. In schlieren method, the optical refractive index of transparent media is modified by the pressure oscillations of ultrasound. This finds application in imaging the sound fields and propagation of sound in liquids or transparent models of specimen.

Piezoelectric scanning displays the amplitude and transit time of the echo from the specimen, like the human body, at each probe position. Dussik in 1942, Wild and Neal in 1951, Donald in 1955, Suckling and McLean in 1955 have contributed to this development. These were mechanical scanning devices, which are very slow. Bradfield in 1954 proposed the phased array in which the beam is electronically tuned, this was later on used by Somer in 1968. Improvements have been made to obtain real time images for medical diagnostics etc.

The SAFT-UT or the Synthetic Aperture Focusing Technique for Ultrasonic Testing is the latest development in digital image systems. In the early 1970s Quate et. al, and Korpel et. al, developed ultrasonic microscopy for practical applications. 1974 saw the first applications of ultrasonic tomography by Greanleaf and collaborators. In the late 1980's and quite recently, developments in high frequency transducer arrays for hyperthermia cancer treatment has been reported. The conventional piezoelectric materials like quartz and ceramics are being replaced by piezopolymers and composites.

1.2 ULTRASONIC TRANSDUCERS

A transducer is a device which converts one form of energy into another. Piezoelectric transducers convert mechanical energy into electrical energy and vice-versa. Piezoelectric transducers are used for underwater applications and ultrasonic nondestructive testing. Transducers solely used for reception are called hydrophones and those used as transmitters are called projectors. Linearity and reversibility are essential requirements of a transducer. In piezoelectric crystals, a mechanical stress applied to it results in the separation of the centres of positive and negative charges producing electric dipoles within the crystal which in turn induce surface charges [6]. Also when an electric potential is applied to a piezoelectric material, it changes shape. If the electric potential is alternating, a mechanical oscillation is produced in the piezoelectric material. Quartz, Lithium sulphate, Barium titanate, PZT(Lead zirconate titanate), Lead Niobate and PVDF(Polyvinylidene fluoride) are some of the piezoelectric materials.

1.2.1 Ceramic Transducers

Piezoelectric ceramics are available in a wide variety of elastic, electric and piezoelectric constants, which are suited for a wide range of applications. Piezoelectric ceramics can be moulded into various shapes and sizes with their polar axis directed according to the geometry and mode of vibration. Various commercial versions of PZT are manufactured in different countries [6]. Barium titanate, Lead metaniobate and Sodium niobate are also being used as transducer materials. Lead zirconate titanate has gained popularity among ceramic materials due to its strong piezoelectric effect and high Curie point.

1.2.2 Piezopolymer Transducers

PVDF is a semi crystalline polymer of molecular structure $\text{CH}_2\text{-CF}_2\text{-(CH}_2\text{-CF}_2\text{)}_n\text{-CH}_2\text{-CF}_2$ with a nonpolar α form with antiparallel dipole chains and a highly polar β form with a parallel dipole chain. The piezofilm is stretched and poled under intense electric field. The electrodes are coated on the film by vacuum deposition. Apart from NDT transducers, piezofilm finds application in military, industry, medicine and sports utilities. Some of them are hydrophones, computer keyboards, tactile sensors, micropositioners in manipulator devices, imaging and osteogenesis in medicine, microphone and tone generators, sports equipments, acoustic speakers etc. Some of the attractive features of PVDF as a transducer material are

- ★ wide frequency range from 0.005Hz to 10^9 Hz
- ★ vast dynamic range ie., sensitive from 10^{-8} to 10^6 psi
- ★ low acoustic impedance
- ★ high elastic compliance
- ★ high voltage output of about 10 times that of piezoceramic
- ★ high dielectric strength with a capacity to withstand strong fields($75\text{V}/\mu\text{m}$)
- ★ high mechanical strength and stability
- ★ relatively low fabrication costs

All these factors together make PVDF an excellent active material for transducer design.

Piezoelectric composites of ceramic and polymeric materials are also being used for transducer fabrication. They are two phase materials in which the ceramic contributes to the piezoelectric effect and the polymer phase helps in reducing density and permittivity of the material and increases elastic compliance.

1.2.3 Radiated fields

The acoustic field distribution for sinusoidal excitation is given by the Rayleigh's integral [8] [9]. The intensity remains fairly constant in the near field, but the intensity decreases with distance from the source in the far field due to the presence of a spherical wave. The field distribution in the near field is complex, while the far field axial distribution of a disc can be expressed as the product of the spherical wave and the directivity function.

1.2.4 Focusing

A plane piston transducer produces an unfocused beam which spreads radially due to diffraction. The acoustic pressure becomes too low with distance and the beam diameter becomes too large making it difficult to obtain a good transverse definition when probing an object. Focused acoustic beams can provide a good transverse definition and high acoustic intensity at a point of interest. Focusing in a single element transducer can be achieved by shaping the transducer using a lens and in multielement transducer, focusing can be achieved by adjusting the relative phases of the signals from each element.

1.2.5 Sound levels and decibel scale

A logarithmic scale is commonly used to represent the strength of sound. In the acoustic phenomena wide range of frequencies are to be handled. The audible intensities range from 10^{-12} to 10 watts/m². The decibel scale is the most generally used logarithmic scale[5]. The intensity level of a sound of intensity I is defined as

$$IL = 10 \log_{10}(I/I_0)$$

IL is expressed in decibel(dB) and I_0 is the reference intensity.

1.3 PROPERTIES OF TRANSDUCER ARRAYS

Transducer arrays find wide ranging applications from underwater communication, target detection, mine hunting etc in the kHz range to flaw detection, imaging and ultrasonic holography in the MHz range. The advantages of using an array over a single hydrophone are

- ★ focusing effect
- ★ better sensitivity
- ★ directionality
- ★ improved signal to noise ratio

Since there are more number of elements in an array, more voltage or current is generated, improving the sensitivity than a single element exposed to the same acoustic field. The directionality of the transducer enables the identification of sound arriving at a particular direction. An improved signal to noise ratio capacitates the discrimination of isotropic noise against signals.

Different configurations and designs of arrays suited for different applications are emerging day by day such as the linear array, ring array, cylindrical section array, annular cylindrical array etc [10].

Some of the important parameters of transducer arrays are

- ★ array gain
- ★ shading and superdirectivity
- ★ array beamsteering
- ★ directivity index

1.3.1 Array gain

One of the most important factors in the detection of underwater targets is the improvement in the signal to noise ratio. This is measured by the array gain of the transducer array in decibels, expressed as a ratio of the signal to noise ratio of the array to that of a single element.

1.3.2 Shading and Superdirectivity

A transducer array whose elements have equal weighting may produce a radiation pattern with high sidelobe levels comparable with the main lobe so that target detection is hindered. For such applications the beam pattern may be tailored by giving proper weighting or adjusting the spacing between the elements. This technique is called shading. An extreme form of shading to obtain narrow beam with arrays of limited size is termed superdirectivity [11].

1.3.3 Array Beamsteering

Beamsteering is a technique to direct the beam to a particular angle. This finds use in sonar and NDT applications. The phase of the elements are adjusted to introduce a delay between the elements so that the main lobe is directed to a desired angle.

1.3.4 Directivity index

The transmitting directivity index of a projector at a point on the axis of the beam pattern is the difference between the sound level generated by the projector and the level that would be generated by a nondirectional projector radiating the same amount of total acoustic pressure [11].

1.4 ULTRASONIC TESTING TECHNIQUES

Ultrasonic testing techniques widely being used for defect detection are the through transmission technique, pulse echo technique and resonance methods using a normal or angle beam of ultrasound. Suitable probes have to be designed considering the flaw size, sensitivity, beam divergence, penetration and resolution.

1.4.1 Ultrasonic probes

Different types of probes have been designed for different testing problems. A transmitting probe transmits ultrasound into the object, which then investigates the test material and a receiving probe receives the ultrasound which carries the information of the test object. In certain cases a single probe can be used as both transmitter and receiver [12]. In through transmission two separate probes are used for transmission and reception. In the pulse echo method the various probe configurations are the single probe, twin probe and angle probes which can be operated in the single and multiple reflection modes.

1.4.2 Through transmission technique

Material discontinuities in the path of ultrasonic waves create an obstacle for the ultrasound, through which only a small fraction of the incident energy can penetrate. Even very thin cracks of the order of a micrometer creates an impenetrable barrier to the ultrasonic waves used in nondestructive testing. An ultrasonic transmitter probe is placed on one side of the test object and a receiver probe on the other side with good coupling and alignment, and the intensity of the ultrasound received is monitored. A defect in the path of the ultrasound casts an acoustic shadow on the receiver, resulting in a drop or absence of the received signal. This reveals the

presence of the defect. Some of the requirements for successful and reliable defect detection with through transmission are the following

- ★ The acoustic wavelength in the object must be less than the diameter of the smallest defect to be detected, because of diffraction around the edges of the defect. The minimum noticeable flaw size also depends on the distance from the surface of detection.
- ★ A good acoustic coupling and consistent alignment of the transmitter and receiver should be ensured.

Through transmission technique is used in detection of defects in laminations etc.

1.4.3 Resonance Technique

In the resonance testing the transducer coupled to the plate is driven with continuous waves of varying frequency below its resonance. The transducer is loaded more heavily than at other frequencies when the wave passes through a fundamental or harmonic resonance of the plate. The increase of load causes a corresponding increase of driving alternating current. Thus the resonant frequency can be detected. The plate thickness can be determined knowing the acoustic velocity in the material.

This technique is used in checking the thickness of plates, sheet material, pipe wall etc. This is a time consuming process since the adjacent resonances are to be located.

1.4.4 Pulse echo technique

A short burst of ultrasound is sent into the test object and the echoes from the discontinuities, defects or boundaries of the object are amplified and displayed on a cathode ray oscilloscope. The time of flight of a pulse gives the information of the distance or depth in the object. The echo amplitude is affected by the reflectivity of the interface, its size, its orientation, distance from the probe, attenuation along the path, acoustic coupling between probe and the test surface, as well as probe characteristics.

This is the most versatile and most widely used ultrasonic method of nondestructive testing. It is used in weld testing, testing of bars, rods, sheets, pipes, rails etc.

1.4.5 Modes of display

Acoustic visualisation is much different from its optical counterpart. An optical image normally corresponds to the visualisation of the surface of an object, but most materials are at least partially transparent to acoustic waves, hence views the entire interior through which it passes and provides more information than that is optically observable. Some of the standard visualisation techniques employed in NDT and medical diagnosis are the A-Scan, B-scan and C-scan.

1.5 MOTIVATION FOR THE PRESENT WORK

A lot of emphasis is laid on the structural integrity of materials during production as well as during operation. The need for evaluation of defects becomes severe as the complexity of the structure increases. Very precise and accurate methods have become essential for detection localisation and estimation of defects such as cracks

or inclusions. As inspection techniques become more and more accurate and reliable, smaller and smaller defects become detectable. Accuracy, reliability and inspection time are some of the problems encountered in testing techniques [14]. Inspection of underwater pipelines and offshore structures poses many challenges. Sophisticated unmanned systems equipped with various sensors, manipulator arms, closed circuit television camera and other tools are needed for working in the ocean environment which is too harsh for humans. There is a need to develop highly sensitive and efficient sensor systems.

Various types of probes have been developed for detection of flaw in pipes. Those commonly used are the focused probe or the single probe, which has to be moved about the pipeline. A widely spaced point source ultrasound ring array working in the near field was designed by Whittington and Cox to reduce the necessity for mechanical rotation of the probes for tube inspection [15].

The motivation to carry out this work is to develop a better ultrasonic transducer system for testing underwater pipelines. An annular ring array and an annular cylindrical array have been designed which can inspect underwater pipelines without being mechanically rotated about the pipe. The inspection time can be considerably reduced. A section of the annular ring or annular cylindrical array is selectively energised which focuses a beam of ultrasound on the pipeline. A similarly grouped section of the array can act as receivers. Then the next set of transmitters and receivers are energised and so on, thereby inspecting the whole contour of the pipeline.

1.6 BRIEF DESCRIPTION OF THE PRESENT WORK

Schematic of the work done with chapter wise details is given below.

Earlier work carried out by various authors in the field of piezoelectrics, transducers, ultrasonic nondestructive testing etc. are presented as literature survey in Chapter 2. A review of the important contributions in the field of piezoelectric materials, as well as in the design and fabrication of different transducers and transducer arrays, for various ultrasonic applications is carried out in this chapter. The revolutionary discovery of piezoelectric effect, its impact on the new generation of sensors and contribution to modern technology can be glimpsed while going through a review of the past work in this field.

The methodology adopted in the design of transducer arrays used for inspection of defects in underwater pipelines is featured in Chapter 3. Different types of ultrasonic waves, plane waves at solid liquid interface, radiated sound field and modes of display are also described. Different types of probes and inspection methods for ultrasonic testing and computation method of array gain, beam pattern and effective acoustic pressure are also depicted.

Chapter 4 highlights the formulation and computation results of array gain and beam pattern of an annular ring array and annular cylindrical array suited for pipeline inspection. The inspection system comprises an annular ring array or an annular cylindrical array placed concentric over the pipeline and selectively activated with the ultrasound focused on the contour of the pipeline. A similarly grouped set of elements of the remaining array acts as the receiver to collect the information of the defect. The array gain and beam pattern are computed for a selectively energised section of an

annular ring and annular cylindrical array. The computations are carried out for different configurations and array radius of the annular ring and annular cylindrical array. The sidelobe level and 3dB beamwidth are determined for different configurations of the array. The sidelobe level and 3dB beamwidth are found to remain constant when the array radius is $> 40\lambda$.

Chapter 5 concentrates on the formulation and computation of effective acoustic pressure of an annular ring array and an annular cylindrical array for continuous as well as pulse excited signals. An ultrasonic transducer array comprising a selectively energised section of an annular ring array or an annular cylindrical array concentric to the test pipeline, with the ultrasound focused on its contour is used for underwater inspection. The impulse response of the array $h_a(r,t)$ is computed to evaluate the effective acoustic pressure. The pressure field is evaluated as the Fourier Transform of the impulse function. The transient effective acoustic pressure is evaluated for different configurations of the array. The effective acoustic pressure at a point on the contour of the pipeline is evaluated as the sum of the contributions from individual elements. The effective acoustic pressure is determined for different configurations of the array, and by varying the pipeline radius, array radius and axial distance between the pipeline and array.

Various conclusions drawn from the outcome of the investigations are discussed in Chapter 6. An annular ring array and an annular cylindrical array are designed for inspection of underwater pipelines. Substantial reduction in inspection time and a focusing effect can be achieved using an annular ring or annular cylindrical array compared to the conventional single probe technique. The scope for further work in

this field and also the suitability of similar arrays in biomedical applications like hyperthermia cancer treatment is also discussed in this chapter.

Transducer elements have been developed using PVDF film of $110\mu\text{m}$ thickness operating in the (3,3) mode. The design, calibration and experimental set-up are discussed in Annexure I.

Review of past work in the field

A review of the past work connected with piezoelectric materials, design and fabrication of different transducers and transducer arrays suited for various ultrasonic applications are discussed in this chapter. A lot of literature is available on ultrasonics and non-destructive testing. Non-destructive testing is a challenging field for research and development. Ultrasonic technologies have tremendous potential for providing advanced techniques of detection, characterisation, localisation and estimation of material anomalies. Different methods of computation of acoustic field of transducers have been formulated. Ultrasonics as an effective tool for non-destructive testing is being widely established in industry as well as biomedical applications. The wide range of applications of ultrasonics as unrivalled and indispensable testing and gauging method for production, quality control and preventive maintenance reaching into almost

all branches of industry is demonstrated by Steinberg. Steinberg has given a review of various applications of ultrasound in industry, defence and medical fields [16].

Posakony has analyzed the challenges, capabilities and limitations of today's ultrasonic nondestructive testing system. The present testing techniques can be made more efficient by improving reliability and reproducibility. Future breakthrough can be achieved by technological research [17]. Papadakis has described the future prospects of nondestructive evaluation with emphasis on cost savings in quality control, materials, energy, manpower, etc. [18], while Buckley [19] has given an account of its economic significance.

Alan. A. Winder has given a detailed account of transducers for underwater communication [20]. Sound energy is the most effective tool for underwater communication and inspection. A review of underwater sound transducers was given by Sherman [21]. Different transduction mechanisms were compared and discussed. The advantages and disadvantages of piezoceramic transducers were also dealt with.

2.1 TRANSDUCER DESIGN

In the design of transducers, various parameters to be considered are the piezoelectric properties of the material, different vibration modes, effects of backing and matching, multilayered stacking of materials, power limitations of the transducer and calibration. Various transducer designs, their characteristics, performance and array configurations are reported in literature.

The study of piezoelectric properties of different transducer materials is essential

for the design of transducers and arrays for specific applications. Gallego has given a review of the basic piezoelectric characteristics and transducer properties of different types of ceramics and their application in practical ultrasonic transducers [6]. Multielement sandwich transducers, flexural mode transducers and transducer arrays are also discussed. Toulis has made modifications in the computation of electromechanical coupling constants for different composite structures of transducers [22]. The theory of vibration of longitudinally polarised thin-walled ferroelectric ceramic tubes, including the lateral influence on the longitudinal vibrations was derived by Martin [23]. Miller has demonstrated that in a typical transducer a very soft spring can provide a very large force and still retain its low stiffness, which in turn keeps the coupling coefficient almost intact [24]. Thus the overall tuned bandwidth of the transducer is preserved. Bui et. al conducted measurements on the acoustic loss factor and piezoelectric coupling coefficient of PVDF films suited for high frequency ultrasonic applications [25]. Brown et. al have presented a method for modelling the electromechanical performance of PVDF and polyvinylidene fluoride trifluoroethylene P(VDF-TrFE) ultrasound transducer [26]. Determination of piezoelectric frequency dependant constants and dielectric properties were discussed.

High efficiency broad band transducers can be designed by proper backing and matching of the transducer faces. A high acoustic impedance backing provides a broad bandwidth and a relatively low acoustic impedance matching layer provides a good acoustic coupling between the transducer and the medium, improving the efficiency. The theory and design criteria of a 10kW piezoelectric transducer was given by Minchenko [27]. The effect of backing and matching on the performance of transmitting and receiving water loaded transducers was studied by Kossoff [28].

Wider bandwidth were obtained by quarter wave matching the transducer to the backing. Transmission parameters of a multilayered stacked configuration of a transducer have been analyzed by Sittig [29]. At high frequencies the thickness of the bonding layer becomes comparable with the sound wavelength, hence a permissible layer thickness has to be considered in the design of ultrasonic delay lines. Sittig explains the effect of bonding and electrode layers on the transducers [30]. Asymmetric and complex multielement sandwich transducers are dealt with in detail by Neppiras [31]. A simplified mathematical model of a sandwich type transducer was discussed by Dominique et. al [32] [33]. Broad bandwidths were obtained for water loaded piezoelectric transducers by using properly chosen multiple layer impedance matching. A high efficiency, low ripple piezoelectric transduction into a water load was predicted by Goll et. al for transducers in a frequency range 1 to 40 MHz [34]. A design method for thickness mode transducers using experimental data and computer programme was discussed by Rubens et. al [35].

Thick block of ceramic materials, being poor thermal conductors, tend to retain heat generated within its volume due to electrical and mechanical losses. This problem can be overcome using a sandwich construction in which the piezoelectric material forms a part of a composite resonator. Narayana et.al have discussed the design and testing method of sandwich transducers [36]. Broadband transducers have been designed with high efficiency and good impulse response using a quarter wave matching layer between the piezoelectric material and the acoustic load. Desilets et. al have developed transducers based on this design using lead metaniobate and PZT [37]. The design of broadband transducers using thin ceramic disks with proper backing and matching is given by Goll [38]. Ultrasonic pulsed fields from circular and

square transducers are discussed by Hayman et.al[39]. The reciprocity principle between transmission and reception is verified. The discrepancies from the theory at short ranges near the axis is attributed to an extra head wave. The effects of backing, matching and tuning of ultrasonic probes are explained by Smith et. al. Measurement of transduction parameters based on frequency response analysis is also considered [40].

Souquet et. al deal with the design of low loss, wide band ultrasonic transducers for non invasive medical application [41]. The impedance matching of the front face with the medium is achieved using one or two quarter wave plates. Ultrasonic transducers using PVDF films with a non piezoelectric backing material and improved performance have been developed by Klaase [42].

Woollett has concentrated on the electrical, mechanical and thermal power limitations of sonic transducers in the audio and ultrasonic frequency ranges [43]. Martin et.al. have designed transducers with a Gaussian distribution of amplitudes across its face to produce a single beam having a Gaussian distribution across its width, thereby eliminating diffraction lobes [44]. A high power transducer of 40 W/cm^2 working in the frequency range 15-150 kHz has been designed by Hulst for macrosonic applications such as metal and plastic welding, drilling, wire drawing and cleaning. An acoustically loaded symmetric prestressed design was considered [45]. Du et. al have discussed the principle of designing a Gaussian transducer and the experimental measurements of the Gaussian fields produced by quartz and PZT Gaussian transducers. The transducers were designed with a curved back electrode [46].

Mollow has discussed a computation method for the calculation of directivity index for various types of radiators [47]. W. James Troff has designed a portable hydrophone calibrator with associated electronic circuitry for hydrophones in the frequency range from 1 Hz to 3.5 kHz [48]. For biomedical applications needle like miniature hydrophones using PVDF have been designed by Lewin [49]. Free field calibration of the hydrophone probe using a novel calibration technique based on time delay spectrometry was also developed.

Bindal et. al have discussed the design aspects of a resonator of exact half wavelength at a desired frequency [50]. Methods adopted to achieve this were highlighted. Generally the measurement of fields and characterisation of transducers rely on wide band point like hydrophones. Leeman et al have suggested an alternative approach based on the use of very large aperture hydrophones [51]. Hoen puts forth the idea of aperture apodization to reduce the off axis intensity of pulsed mode directivity function of linear arrays. In aperture apodization, the excitation of outer elements were reduced [52].

2.2 PVDF TRANSDUCERS

The piezoelectric effect of PVDF was studied by Kawai in 1969 [53]. PVDF films were made significantly piezoelectric and pyroelectric by poling them in a strong electric field. Piezoelectric properties comparable to crystalline quartz and pyroelectric properties comparable to single crystal LiNbO_3 were reported by McFee et. al [54]. Gallantree has given a brief report on the properties of PVDF membrane hydrophones [55]. The design, sensitivity, frequency response, transmission and reflection coefficient etc. were discussed for various hydrophones. Inderherbergh has discussed

in detail the general properties and processing of PVDF [56]. The properties which make PVDF a good transducer material were highlighted. Edelman et. al. used polyvinylchloride as the active material for underwater sound receiver and obtained a response of -112 dB re 1V/ μ bar [57]. Woodward made an attempt to assess the suitability of PVDF for use as an underwater transducer [58].

A review of ultrasonic materials suitable for medical applications such as surgery, therapy and diagnosis were discussed by Hadjicostis et. al [59]. PVDF is discussed as a promising material due to its low acoustic impedance. Electrical, biological and acoustical safety considerations are also taken into account. Dario et. al have designed catheter tip transducers used in medical applications such as measurement of intracardiac pressure and sound [60]. A vinylidene fluoride and trifluoroethylene copolymer, linear array transducer has been developed by Kimura et. al with high resolution and energy conversion efficiency. Its practical application is in medical echograms etc.[61]. An ultrasonic compression sensor using compliant rubber array elements was developed by Schoenberg et. al for application in tactile force sensors [62]. The use of PVDF film as the transducer material provides flexibility and ruggedness.

Electroacoustic transducer using piezopolymer PVDF film for applications such as tweeters and microphones was reported by Masahiko Tamura et.al [63]. Composite resonators using PVDF films have been fabricated by Chubachi et. al for applications at VHF from 10 MHz to 65 MHz [64].

Murayama et. al have carried out a survey on the development and application

of piezoelectric polymer films [65]. The applicability of PVDF in the thickness mode for construction of high frequency transducers was shown by Sasady [66]. PVDF films of thickness 7 micron and 30 micron, with unpoled PVDF as backing were used in this design.

A piezopolymer flexural disk hydrophone has been developed by Sullivan and Powers using PVDF demonstrating its feasibility for underwater application [67]. Lerch has carried out theoretical and experimental analysis of cylindrical and spherical PVDF diaphragm [68]. The response of PVDF microphone to airborne sound was calculated as a function of diaphragm geometry, acoustic impedance, coupling volume and excitation.

Lerch et. al have reported about piezoelectric microphones with rigidly supported piezopolymer membrane [69]. The advantages of these microphone structures are the well defined geometry of the membrane along with its good mechanical and thermal stability. A 25 micron thick PVDF film was used which was spherically preformed by stretching it over a steel sphere at 100°C and then poling it. Shock resistant hydrophones capable of surviving explosive shocks and working in 5 to 50 kHz range have been designed using tubular PVDF by Henriquez [70].

De Reggi et. al have developed and tested piezoelectric polymer probes for ultrasonic application [71]. A spot poled PVDF membrane design was used for ultrasonic field characterisation in the low MHz region. Point supported piezoelectric foil membrane transducers have been studied by Lerch [72]. An improved thermal and mechanical stability were observed. Such transducers designed using PVDF find

application in microphones and headphones. Foster has presented an investigation into the properties and application of piezoelectric thin films used in the generation and detection of bulk and surface waves [73]. The physical properties of PVDF are reviewed and the various applications discussed on the basis of transduction mechanism by Marcus [74]. The sensitivity considerations of spot poled PVDF membrane hydrophones were studied by Harris [75]. The effect of different lead geometries on sensitivity were also discussed.

Varying the compositions of tungsten and vinyl powders in tungsten-vinyl composites it was possible to formulate a composite with specified specific acoustic impedance. Sidney Lees et.al measured the velocity, density and specific acoustic impedance for different compositions [76]. Hossack et. al discussed the modelling and design of composite piezoelectric arrays [77]. The field characteristics and electromechanical performance were also evaluated.

The design of transducers for ultrasonic delay lines was given by Mc Skimin [78]. A unified analysis of ultrasonic delay lines was presented based on equivalent circuits by Morio Onoe [79]. The effect of acoustic mismatching at bonding points on the signal to noise ratio and on the ringing in the output were also presented.

2.3 SOUND FIELD

Goodman has given an introduction to the foundations of scalar diffraction theory using Green's function and the Rayleigh Sommerfeld formulation of diffraction [80]. The radiation pattern of a narrow strip acoustic transducer was derived by Selfridge et. al using Rayleigh-Sommerfeld formula [81]. Computation of the sound field due to a

concave spherical radiator along the axis of symmetry and in the vicinity of the focal plane has been carried out by O'Neil [82]. Stepanishen has presented a computation method for the near and far field transient radiation from pistons, based on Green's function development [83]. He also described a method for computing the interaction forces and mutual radiation impedance [84].

Lockwood and Willette have presented a method to calculate the pressure variations at any point in the field of a baffled piston using the impulse response and Fourier transform technique [85]. Penttinen et. al carried out an analysis of the impulse response of a curved radiator based on the time dependent Green's function approach [86]. Hunt et. al used the impulse response technique for the computation of ultrasound field of plane, spherical and conical transducers [87].

A fast algorithm to compute the ultrasound pressure field from a circular, single element transducer was developed by Yao et. al [88]. This algorithm performs well in calculating the pressure in the near field and points at large distance off axis. Ocheltree et. al developed a method for determining the field of a plane source [89]. The source was divided into a number of rectangular elements chosen to be small enough for far field approximation. The total pressure is the sum of the contribution from each element. Wang et. al have put forward a high speed method for exactly calculating the time dependant pressure of the radiated acoustic field from pulse excited axisymmetrically curved surface or lens transducer [90].

Jensen et. al have devised a fast and accurate method of calculating pulsed pressure field emitted from an arbitrarily shaped, apodized and excited ultrasound

transducer [91]. The field was calculated by dividing the surface into small rectangles and then summing their response. Yoon et. al presented an efficient method to calculate the sound field radiated from a linear phased array transducer through a liquid lens [92]. A variable geometry focusing capability was achieved by adjusting the volume of the liquid lens.

2.4 PULSED TRANSDUCERS

Pulsed ultrasonic equipment is widely being used for various applications. A measurement of the peak acoustic intensity of pulsed ultrasonic equipment was illustrated by Kossoff [93]. Its advantage is that the biological effects caused by ultrasonic radiation generally occur in those portions of the beam of highest intensity. A complete description of the ultrasonic dosage can be had only by knowing the peak intensity. The design and characterisation of short pulse ultrasound transducers and computation of transient pressure using convolution or Fourier Transform technique was done by Foster and Hunt [94].

Pulsed ultrasonic fields produced by several ultrasonic sources were measured by spot poled PVDF membrane hydrophone receivers. The pulses were observed to be composed of plane wave as well as edge wave. Two head waves arising from the reradiation of longitudinal and transverse lateral waves were also observed by Harris et. al [95]. Hutchins et. al discussed the radiated pressure fields of pulsed PVDF transducers determined experimentally and their comparison with theory [96]. Smith et. al summarised the performance of different PVDF pulse echo transducers, their frequency response and depth resolution capabilities were also studied [97]. Stepanishen has presented an approach to evaluate the transmit/receive response of

pulsed ultrasonic transducers [98]. Transient response of a plate transducer in the thickness and length vibration mode was described by Redwood [99].

2.5 HIGH FREQUENCY TRANSDUCERS

A wide band PZT ultrasound transducer operating in the frequency range 0.5-20 MHz was designed by Brown and Weight [100] and PVDF broadband transducers were discussed by Bui et.al [101]. A PVDF membrane hydrophone operating in the 0.5 to 15 MHz range was described by Schotton et. al for measuring the spatial and temporal distribution of pressure within the fields from medical ultrasound equipment [102].

Bacons has described an improved design and characteristics of a PVDF membrane hydrophone for use in the 1-100 MHz range [103]. These transducers find application in measurement of ultrasonic fields from medical and NDT equipment.

Rajendra et. al have described the design fabrication and application of high frequency ultrasonic transducer employing ZnO-film/Al-foil composite structure [104]. The fabrication of a concave transducer and its application in scanning acoustic microscope was also dealt with. Swartz et. al illustrated the suitability of PVDF in the generation of high frequency acoustic energy [105]. They can be very useful in medical imaging when combined with the integrated circuit technology. A multiple layer stack was proposed as a method for increasing the available output power.

Thompson et. al has given a review on ultrasonics in nondestructive evaluation [106]. Onozawa et. al have discussed ultrasonic testing for near surface flaws in castings. A multi transducer probe has been used for this purpose [107]. Specially designed transducers are required for high temperature NDT applications. Garcia et.

al have reported a 91-30 PZT polymer compound designed to work at temperatures over 100°C [108].

Piezoelectric zinc oxide films of 10 micron thickness were deposited on metal sheet to develop transducers for NDT. White et. al have done a theoretical analysis of these transducers [109].

2.6 TRANSDUCER ARRAYS

A phased array of transducers with elements of different dimensions and operated near their resonant frequencies, having a flat power response over a broad band were described by Greenspan et.al. [110]. A two dimensional transmit receive piezoelectric transducer array suitable for medical imaging and NDT application operating at 2.4 MHz was developed by Plummer et.al [111]. Wei-Ming Wang has discussed the radiation patterns of acoustic transducer elements in an infinite array [112].

A number of probe designs for ultrasonic phased arrays for NDE application was described by McNab et. al [113]. Cochran et. al have presented experimental and theoretical results of beam forming in solids using monolithic ultrasonic arrays [114]. Such arrays were suitable for real time NDT applications due to their attractive beam characteristics.

A spatially shaded PVDF acoustic transducer was discussed by Mcgehee et. al, with reduced side lobes [115]. The uniformly driven array elements were randomly distributed along the transducer with a density distribution that matches the desired

shading. A divided ring array for 3-D beam steering in ultrasonic NDT was discussed by Schwarz [116]. Computation of directivity pattern, theoretical optimization etc. were also carried out.

A coaxial circular spherical array designed for C mode visualization by using low frequency ultrasonic waves was designed by Shibata et. al [117]. An ultrasonic curved transducer array that enables the beam pattern to be randomly directed over a large angular range without altering the beam shape was discussed by Huissan et. al [118]. A curved transducer array has been developed by Ylitalo et. al for the transskull brain imaging [119].

A cylindrical section ultrasound phased array has been designed and constructed for hyperthermia applications by Ebbini et. al [120]. The ultrasonic energy is focused at its geometric focus. 2-dimensional cylindrical section phased array system was discussed by Wang et. al to examine the role of implantable acoustic sensors for phase aberration correction and motion compensation in ultrasound hyperthermia [121].

A variable focus ultrasonic transducer using PVDF film in which the focal point may be scanned along the transducer axis by controlled deformation of the stretched film is demonstrated by Bennett et. al. [122]. Kino has given a description of electrically scanned and focused systems used in acoustic imaging [123].

Beam steering and focusing with linear array in the transmit and receive modes were discussed along with techniques for improving ultrasound image quality using

phased array by Von Ramm et.al [124]. A theoretical investigation of the focusing and steering properties of pulsed 2-D arrays was carried out by Turnbull et. al [125]. Details of computation methods were also presented. Schwarz et. al developed an ultrasonic array for application in medicine and NDT [126]. The sound beam was steered around 360° and a radar like picture was obtained. The effective geometrical parameter for weakly focused ultrasonic transducers were investigated by Adach et. al [127]. Problems encountered in the experimental determination of effective parameters were also discussed.

Ultrasonic transducers using PVDF film has been designed by Hurmila et. al for NDT and medical applications [128]. Focused conical transducer for NDT and array transducer for medical holographic B scan imaging were discussed.

Qin et. al introduces a technique to reconstruct a circular array using the linear array imaging [129]. The resolution of this imaging method was found to be better than that of a linear array system. Kim et. al have developed an ultrasonic contact transducer generating point-focused Rayleigh waves along the flat surface of the specimen [130]. These transducers find application in detection, sizing and imaging of surface cracks and subsurface defects.

A phasing method for direct synthesis of multiple focus field patterns using ultrasonic arrays was developed by Ebbini et. al [131]. These arrays find application in ultrasound hyperthermia cancer therapy. Desired or specified field levels could be produced at a set of control points in treatment volume.

An $n \times n$ square element ultrasound phased array was designed by Ibbini et. al for simultaneously focusing the ultrasound beam at different points uniformly distributed along the tumour periphery in hyperthermia applications [132]. A rectangular strip like focusing transducer was evaluated by Reibold et. al. The radiated fields were explained in terms of direct waves and edge waves [133], [134]. A theoretical investigation of the focusing and steering properties of pulsed 2-D arrays to characterise the parameters required for medical imaging, such as element size, spacing and number of elements were carried out by Turnbull et.al [135]. The effect of apodization and element cross coupling on the beam properties were also studied. A multi frequency, multi focal length ultrasonic transducer has been designed for clinical hyperthermia application by Singh et. al [136]. The focusing was achieved using a plano convex perspex lens on the front surface of the transducer.

The general characteristics of underwater acoustic imaging was presented by Sutton [137]. The limitations and prospects for the future in underwater acoustic imaging are explained. An analysis of direct imaging arrays in which the individual arrays are fired in sequence and phased arrays in which the outputs are appropriately delayed and summed, was carried out by Macovski [138]. This analysis is very useful in the design of ultrasonic imaging arrays.

An electron beam scanned piezoelectric sensor can be used to achieve real time, high resolution, reflection and transmission ultrasonic imaging. Brown has discussed a substantial improvement in image quality using electroactive PVDF sensors [139]. Smith et. al have discussed the design, fabrication and evaluation of two dimensional transducer arrays for medical imaging [140]. An improved B-scan

imaging has been achieved for a 4 x 32 element array operating at 2.8 MHz array.

O'Donnell suggests that substantial improvements in resolution can be obtained using a simple annular array imaging system [141]. In the receive mode it simulates a spherically focused transducer.

Methodology

The methodology adopted for the design of transducer arrays for inspection of defects in underwater pipelines is featured in this chapter. Some of the factors to be taken into account for ultrasonic testing are different types of ultrasonic waves, plane waves at interface, radiated sound field and piezoelectric properties. Different types of probes and inspection methods for ultrasonic testing, computation method of array gain, beam pattern and effective acoustic pressure are also described.

3.1 ULTRASONIC WAVES

Ultrasonic waves are produced by the mechanical vibrations of the particles

of an elastic medium of frequency greater than 20,000 Hz. Some of the basic characteristics of ultrasonic waves which are of significance in industrial ultrasonic testing are reflection and refraction at interfaces, mode conversion, attenuation, wavelength, frequency, velocity, beamsread, near and far fields. Unlike electromagnetic waves, the wavelength of ultrasonic waves varies with the medium due to the variations in the elastic properties of the medium[3]. There is a fundamental upper limit of frequency based on the closest atomic spacing in solids of about 10^{13} Hz.

Different types of ultrasonic waves are

- ★ compressional or longitudinal waves
- ★ shear or transverse waves
- ★ surface waves
- ★ plate waves

Sound of frequency below 20 Hz is termed infrasound. Seismic waves accompanying an earth quake belong to this category [4].

3.1.1 Compressional waves

Compressional or longitudinal waves are compressional in nature. Particle displacement is in the direction of wave propagation.

3.1.2 Shear waves

In shear or transverse waves, particle vibration is transverse to the direction of wave propagation. Shear waves are generated when ultrasound beam is passed through a material at an angle.

3.1.3 Surface waves

In surface waves, the particle displacement follows an elliptical path. The wave travels with little attenuation in the direction of wave propagation. Their energy decreases rapidly as the wave penetrates below the surface. Surface velocity is about 0.9 times the longitudinal wave velocity in most solids and the particle motion is practically zero for depths greater than one wavelength below the surface.

A surface wave at a liquid/solid interface produces leaky waves and a part of ultrasonic energy is transferred back into the liquid medium.

Creeping waves are lateral waves formed at an interface between two solids of different impedances and are similar to a glancing angle compressional wave.

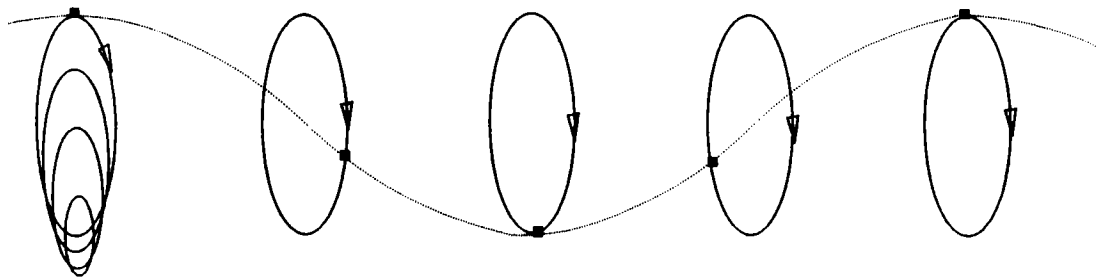


Fig.3.1 Rayleigh waves

3.1.4 Plate waves

In thin plates ultrasonic energy propagates as plate waves since pure surface waves cannot exist unless their wavelength is considerably smaller than the plate thickness. They have multiple or varying wave velocities dependent on the thickness

of the material and frequency. A number of modes of particle vibration are possible; most common modes of vibration are symmetrical and antisymmetrical.

Love waves are transverse waves with a direction of oscillation parallel to the surface. Lamb waves have a component of oscillation at right angles to the surface. Plate waves are often termed as rod waves in a specimen with circular crosssection. Head waves are longitudinally polarised shear waves. They are also known as *P* waves.

3.1.5 Plane waves at solid liquid interface

The effect of boundaries on the propagation of sound are of vital importance in materials testing. The acoustic wave from the ultrasonic probe has to penetrate the boundaries when passing into the specimen and vice versa when being received. Detection of defects in specimens is carried out by their effect on boundaries. Propagation of acoustic waves can be influenced by other boundaries of the specimen also. They are interfering reflections, intentional guiding such as in plates and rods and by reflecting waves into areas otherwise inaccessible. For an acoustic wave propagating in medium I and incident on medium II, there is a transmitted wave in medium II and a reflected wave in medium I similar to that in optics.

An acoustic wave incident in material I at an angle α_i is reflected at an angle α_r and α_d is the angle of the transmitted wave as seen in Figure 3.2. c_1 and c_2 are the acoustic velocities in the two media.

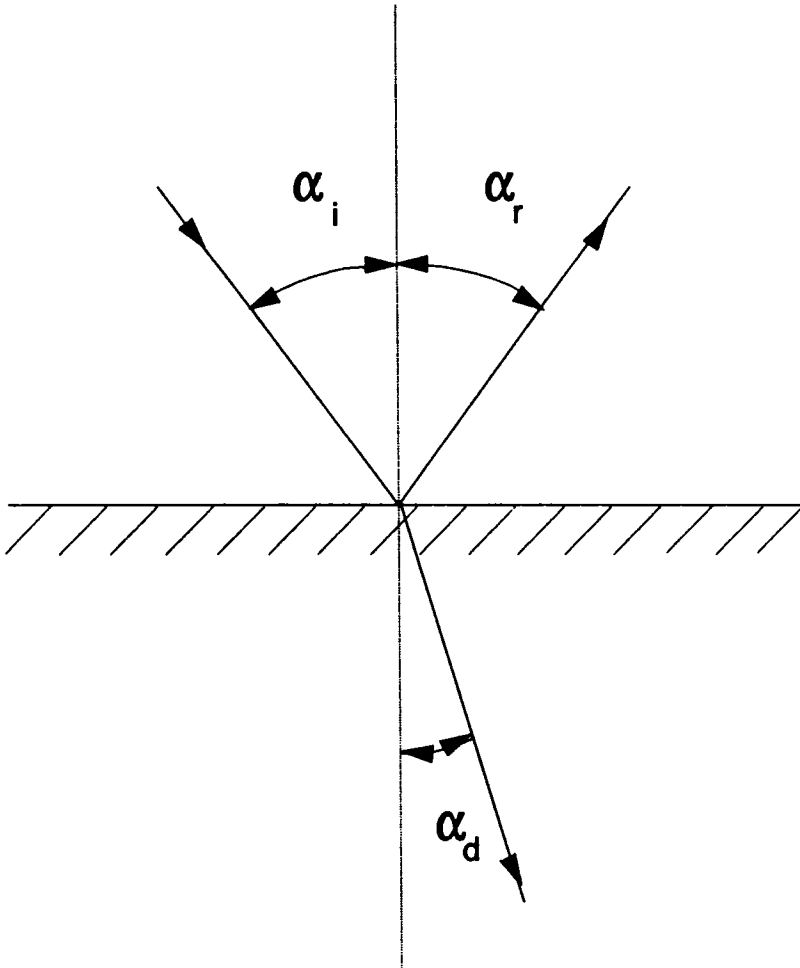


Fig.3.2 Acoustic waves at an interface of two media

The direction of reflected and transmitted waves are determined by Snell's Law.

$$\frac{\sin\alpha_i}{\sin\alpha_d} = \frac{c_1}{c_2} \tag{3.1}$$

Knowing α_i , α_d is determined from

$$\sin\alpha_d = \frac{c_2}{c_1} \sin\alpha_i \tag{3.2}$$

In acoustics, unlike in optics, one kind of wave gets transformed into another. A longitudinal wave into transverse and vice versa. This phenomenon is called mode conversion. The liquid/solid and solid/liquid interfaces are of most interest in materials testing. For a longitudinal wave travelling in water and incident on a solid like aluminium, both longitudinal and transverse waves are produced.

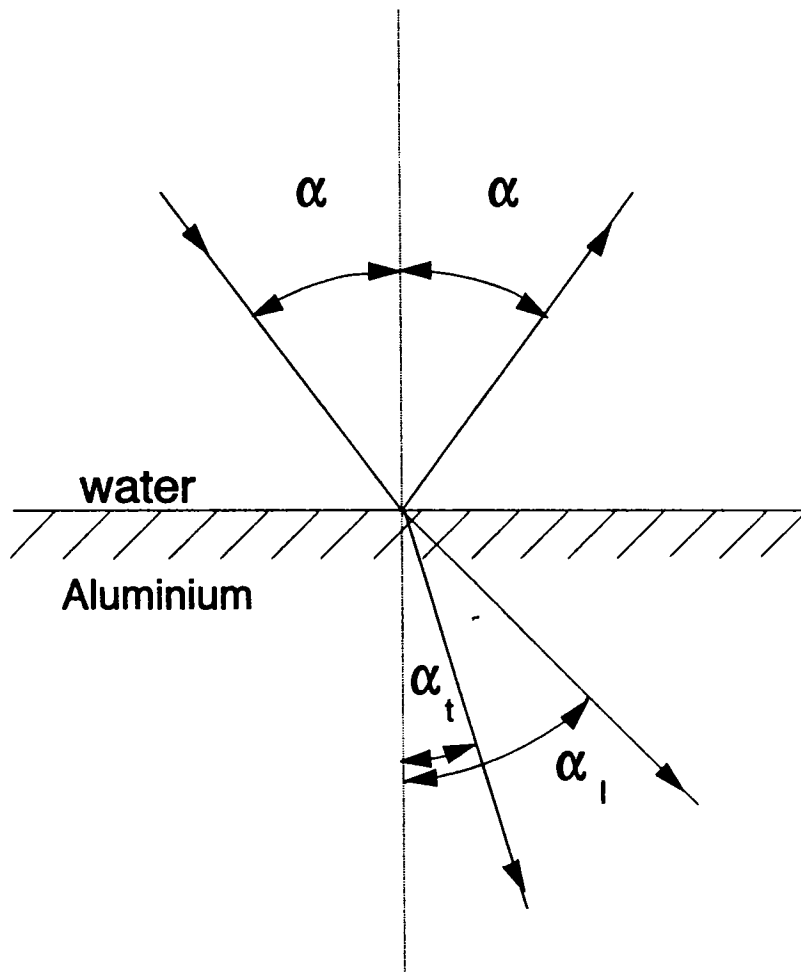


Fig.3.3 Acoustic waves at liquid solid interface

For small angles of incidence, longitudinal waves and weak transverse waves are produced simultaneously. The sound pressure and angle of refraction increases rapidly with the angle of incidence and reaches a maximum at 20° in aluminium. This corresponds to the critical angle, for the longitudinal wave. The longitudinal wave in

aluminium disappears at this angle, immediately a stronger transverse wave appears and remains with increasing sound pressure from about 30° - 90° in aluminium, while the angle of incidence increases to 29.2° which is the second critical angle, the critical angle for transverse wave. Above this angle however no waves are found in aluminium and is of no interest for testing purposes. The incident longitudinal wave is totally reflected beyond this.

3.2 METHODS AND INSTRUMENTATION

The discovery of piezoelectric effect in 1880 was instrumental in the development of ultrasonic transducers. Piezoelectric materials such as piezoceramics, piezopolymers and composites have facilitated the development of highly sensitive sensors. Transducer elements have to be designed, based on the requirement for different applications. Some of the aspects to be considered in the design of transducers are effects of backing and matching, piezoelectric properties of the materials, mode of vibration, stacking of materials, bonding, electrode connections, coupling of the probe with the test material etc.

3.2.1 Design considerations

The ultrasonic transducer probe mainly consists of a piezoelectric material with a thin metallised layer on both surfaces to act as electrodes. A protective layer on the front surface which also acts as acoustic impedance match between the transducer and the medium, and a backing of high attenuation to damp the energy radiated backwards. The backing also provides a mechanical support to the transducer. The transducer is enclosed in a housing with a waterproof cable which protects the transducer from mechanical damage, the operator from electrical shocks and makes

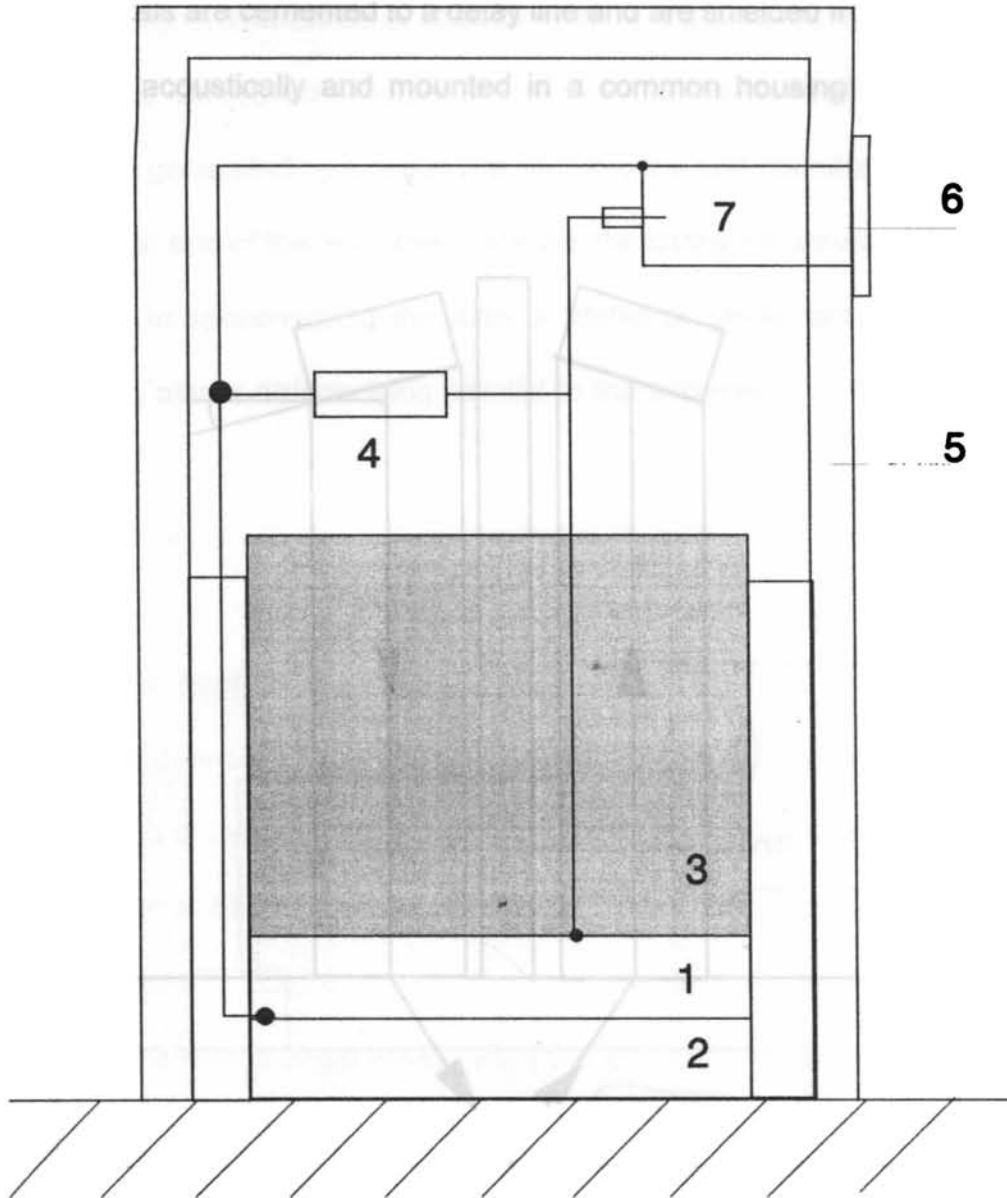
the transducer more suitable for various applications.

The thickness of the piezoelectric material is chosen according to the required frequency of operation. Generally a $\lambda/4$ thickness is considered where λ is the wavelength. The electrode layers must be as thin as possible so as not to cause a loading effect on the transducer. Ceramic surfaces are painted with silver emulsion and heated to about 800°C or a nickel or gold layer of about one micron thickness is chemically deposited onto which contact leads can be soldered. Other piezoelectric materials have a sprayed conductive paint layer or electrodes produced by metal evaporation. In these cases the contact wires are fixed by conductive cement.

The acoustic impedance and attenuation of the backing material are of considerable significance in improving the required degree of damping. When the acoustic impedance of the backing block and the crystal are equal, the energy of the backward travelling wave is absorbed without reflection. A high attenuation and thickness of the material suppress any reflections from the back face of the damping block. A mixture of resins and powdered tungsten has shown very good impedance values. A proper choice of the resin and admixtures of fine grained materials of high absorption can influence the attenuation.

3.2.2 Single crystal vertical (0°) probes

The ultrasonic waves generated by a single crystal vertical(0°) probe; also called normal probe, propagates into the surface of the specimen in perpendicular direction. A liquid coupling layer is used to couple the specimen.



1 oscillator, 2 protecting layer, 3 damping block, 4 electric matching, 5 wire, 6 housing, 7 connection socket

Fig.3.4 Transducer probe

3.2.3 Single crystal angle probe

A proper wedge inserted between a normal probe and the test object forms the angle probe. The geometry of the wedge is adjusted to obtain the desired angle of incidence.

3.2.4 Transmitter receiver (TR) probes or twin probes

The crystals are cemented to a delay line and are shielded from each other both electrically and acoustically and mounted in a common housing with two separate connectors

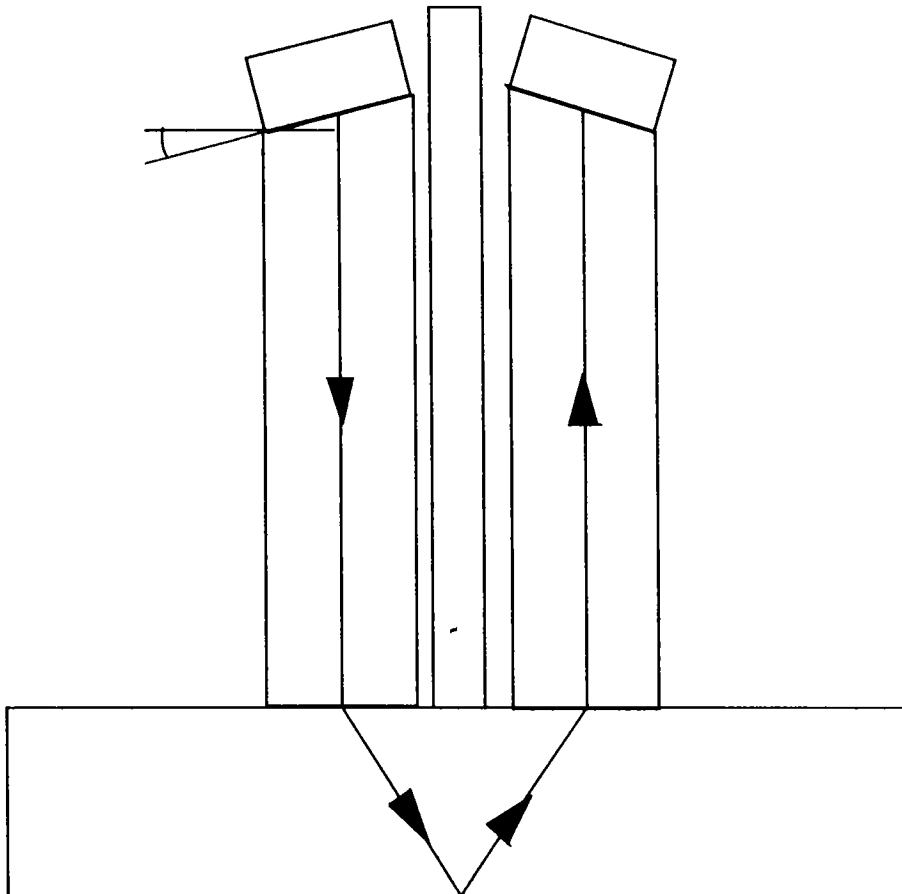


Fig.3.5 Transmitter receiver probe

3.3 ULTRASONIC TESTING TECHNIQUES

The different ultrasonic testing techniques can be categorized according to the type of primary measured quantity, the form of radiated ultrasound used and the effect of the inhomogeneity in the test material. Some of the current testing techniques are through transmission method, resonance method and pulse echo method.

3.3.1 Through transmission technique

In the through transmission or shadow method, the shadow of an inhomogeneity in the path of the ultrasound reduces the intensity of the received ultrasonic wave. Ultrasonic waves generated by a probe are sent into the test object and another probe placed at the other end of the test object receives the ultrasonic waves. This technique finds application in specimens in the form of plates or shells, accessible from both sides and having planar defects lying parallel to the surfaces.

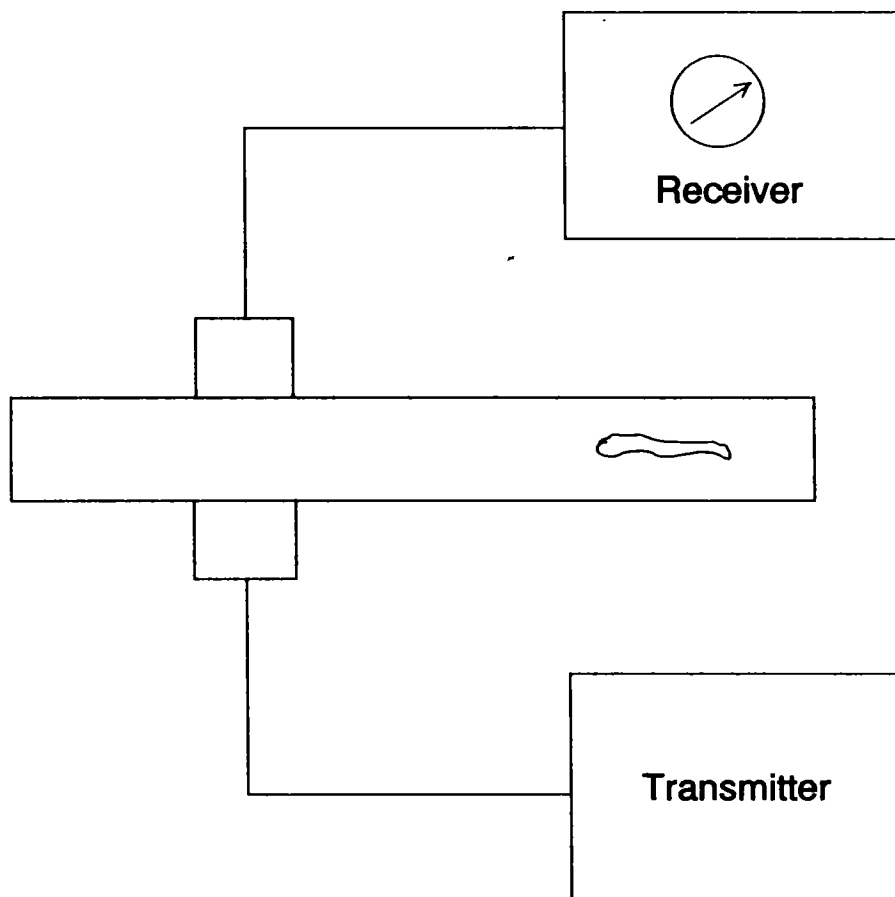


Fig.3.6a. Flaw detection in through transmission

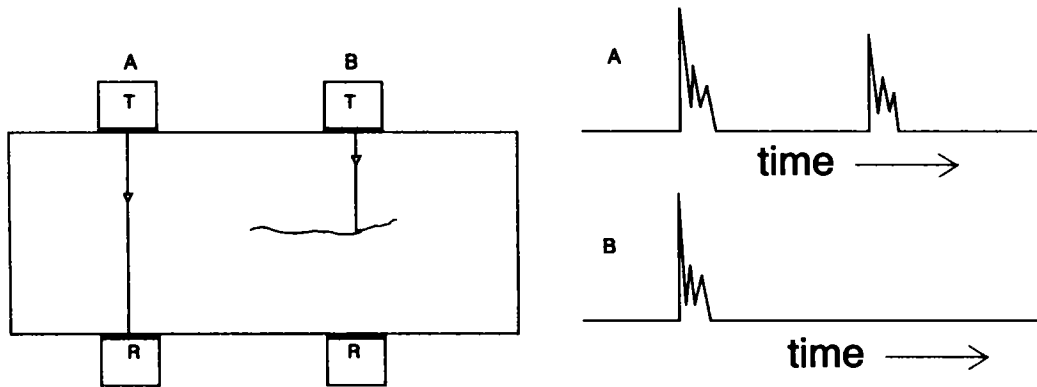


Fig.3.6b. Flaw detection in through transmission

3.3.2 Resonance Technique

In the resonance testing the transducer coupled to the plate is driven with continuous waves of varying frequency below its resonance. The transducer is loaded more heavily than at other frequencies when the wave passes through a fundamental or harmonic resonance of the plate. The increase of load causes a corresponding increase of driving alternating current. Thus the resonant frequency can be detected. The plate thickness can be determined knowing the acoustic velocity in the material. If f_n and f_{n+1} are two adjacent resonances and c is the acoustic velocity,

$$f_{n+1} - f_n = \Delta f \quad (3.3)$$

thickness $t = c/2\Delta f \quad (3.4)$

This technique finds application in checking the thickness of plates, sheet material, pipe wall etc. This is a time consuming process since the adjacent resonances are to be located.

3.3.3 Pulse echo method

The pulse echo method is the most important of testing techniques. A pulsed ultrasonic wave is generated by a transducer probe and it propagates into the test material with the ultrasonic velocity corresponding to the material concerned. If the ultrasound encounters an inhomogeneity which is not too large, a part of it will be reflected and the remainder will travel further to the boundary of the specimen and will be reflected back. The signal obtained from the receiver gives the information about the position of the defect which is displayed as a peak on a baseline of a CR tube.

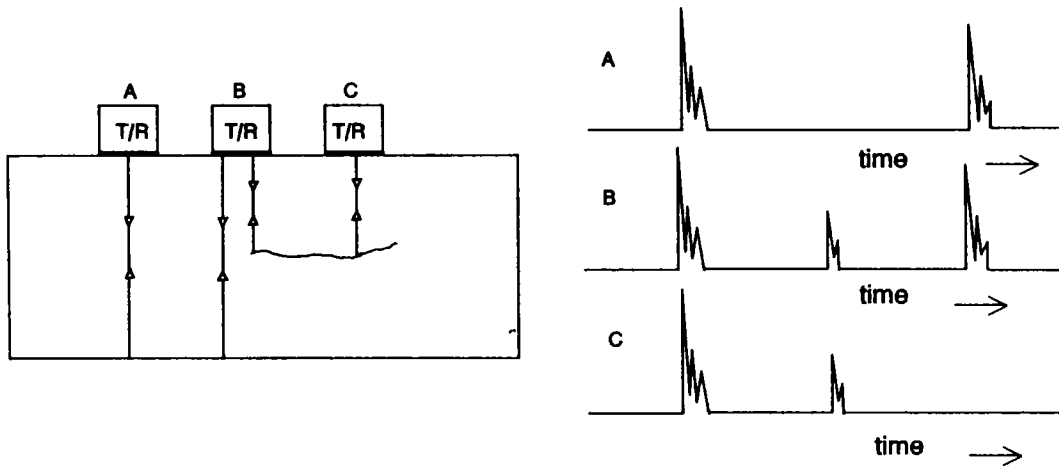


Fig 3.7 Flaw detection in pulse echo method

The horizontal sweep is a measure of the transit time. The baseline is calibrated in time per unit length. The distance d of any reflector can be calculated knowing the acoustic velocity c and transit time t as

$$2d/t=c \quad (3.5)$$

The amplitude of the received echo depends on;

- ★ transmitter pulse power entering the specimen
- ★ directivity of the transmitter probe

- ★ size of reflector
- ★ position of reflector
- ★ size and directivity of receiver probe
- ★ coupling losses
- ★ attenuation by absorption and scattering of the material
- ★ shadow effect of any defect in front of the reflector

3.3.4 Modes of display

The common modes of display are the A scan, B scan and C scan. In the amplitude scan or A-scan, the acoustic pulse generated by the excitation of an acoustic transducer is reflected by the acoustic impedance discontinuities caused by the presence of flaws or internal structures of the body [13]. The reflected echo signal received by the transducer is amplified and displayed as a function of time on an oscilloscope. The time delay t is given by;

$$t = \frac{2z}{c} \quad (3.6)$$

where z is the distance of the flaw from the surface and c is the acoustic wave velocity in the test material. The amplitude of the return echo is characteristic of the size and shape of the flaw.

In medical diagnosis, frequency of the order of 2-5 MHz is used to penetrate as much as 20 cm into the human body. Relatively high frequency of the order of 10 to 20MHz is used for observation of the human eye which is less than 3cm in extent. Very high frequency in the range 1-8 GHz is used for observing body cells and thin layers

of tissue.

Frequency of the order of 2.25 MHz is used for the nondestructive testing of nuclear reactor steel walls of thickness 25 cm. Higher frequency around 20 MHz is used in aircraft materials testing such as titanium or aluminium. 400 MHz signals have been used for examining structural ceramics and integrated circuits. Imaging with acoustic microscope employs a frequency of 2-3 GHz.

In brightness scan or B Scan method, the return echo signal is used to modify the intensity of the spot on the oscilloscope, while the horizontal position of the spot represents the time delay and the vertical position corresponds to the mechanical position along the surface of the object. An image of a cross section perpendicular to the body surface is obtained.

C Scan forms an image in a plane that is perpendicular to the direction of propagation of the acoustic beam. A focused transducer is used to transmit an acoustic beam through a thin object placed at its focus. Moving the beam back and forth, the object is mechanically scanned. Amplitude of the received signal is used to vary the intensity of light spot and is displayed. A good definition and high quality transmission image of thin objects is obtained.

3.4 PROPERTIES OF TRANSDUCER ARRAYS

3.4.1 Array gain

One of the most important factors in the detection of underwater targets is the improvement in the signal to noise ratio. This is measured by the array gain of the

transducer array in decibels, defined as

$$AG = 10 \log \frac{(S/N)_{array}}{(S/N)_{one\ element}} \quad (3.7)$$

where $(S/N)_{array}$ is the signal to noise ratio of the array and $(S/N)_{one\ element}$ is the signal to noise ratio of one element.

In terms of the crosscorrelation coefficients; the array gain,

$$AG = 10 \log \frac{\sum_i \sum_j a_i a_j (\rho_s)_{ij}}{\sum_i \sum_j a_i a_j (\rho_n)_{ij}} \quad (3.8)$$

Where ρ_s and ρ_n are the crosscorrelation coefficients of the signal and noise. a_i and a_j are the rms voltages produced by the i^{th} and j^{th} element respectively due to the signal or the noise.

For a single frequency unidirectional signal with time delay τ_e , the crosscorrelation coefficient is;

$$\rho_s = \cos \omega(\tau_\omega + \tau_e) \quad (3.9)$$

τ_ω is the transit time of the signal between array elements, $\omega = 2\pi f$; f being the frequency.

The crosscorrelation coefficient for the corresponding isotropic noise is

$$p_n = \frac{\sin\left(\frac{\omega d}{c}\right)}{\frac{\omega d}{c}} \cos\omega\tau_e \quad (3.10)$$

where d is the interelement spacing and c is the acoustic velocity.

3.4.2 Beam Pattern

Beam pattern specifies the directional response of an array. Directionality is a highly desirable factor in the design of arrays to determine the direction of arrival of a signal as well as to resolve closely adjacent signals. Directionality also reduces noise, relative to the signals arriving in other directions and enables to concentrate the emitted sound in a desired direction in projector arrays.

The response of an array as a function of angles θ and ϕ in polar coordinates is expressed as

$$R(\theta, \phi) = R(0, 0) v(\theta, \phi) \quad (3.11)$$

Where $R(0, 0)$ is the response in $\theta=0$ and $\phi=0$ direction and $v(\theta, \phi)$ is the response function normalised so that $v(0, 0)=1$

Then beam pattern or pattern function is

$$b(\theta, \phi) = v^2(\theta, \phi) \quad (3.12)$$

3.4.3 Shading and Superdirectivity

Shading is the technique of modifying the pattern of an array having some

particular geometry. The different types of shading are amplitude shading and phase shading. In amplitude shading the excitation of the array elements are adjusted to provide the desired pattern, while in phase shading, the spacing of the array elements is varied. Superdirectivity is an extreme form of shading to obtain narrow beam with arrays of limited size [11]. The elements are spaced less than $\lambda/4$ in superdirective arrays with the polarisation of adjacent elements reversed. Such arrays have a low array sensitivity due to the phase reversal of the elements, together with the relatively high side lobes. An array illuminated uniformly with equal weighting may produce a radiation pattern with a high side lobe level comparable with the main lobe which can hinder target detection. The sidelobe levels can be reduced by aperture shading

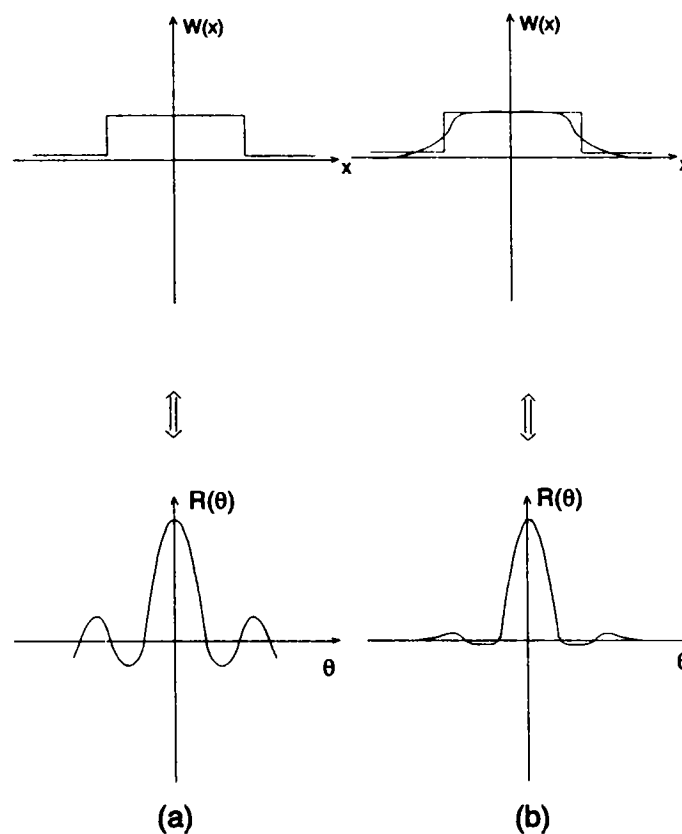


Fig.3.8 Aperture shading to reduce the sidelobe level of an aperture

a) with uniform illumination b) shaded aperture

The aperture distribution $W(x)$, produces a far field response which is a function of the normalised sine of the beam angle.

Hence,

$$R(\theta) = \int_{-\infty}^{\infty} W(x)e^{-j\theta x} dx \quad (3.13)$$

$$\theta = \frac{2\pi}{\lambda} \sin\theta \quad (3.14)$$

3.4.4 Array Beamsteering

The phase of the elements are adjusted so that the main lobe is directed at a desired angle.

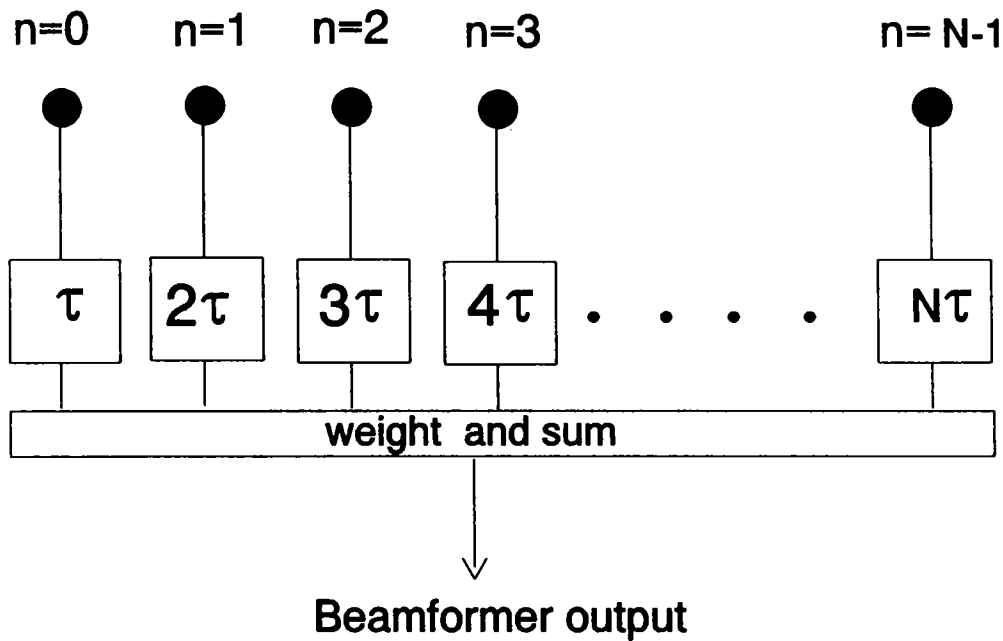


Fig 3.9 Beamsteering

The n^{th} element has a delay $n\tau$, then the beam will be directed at an angle θ , where;

$$\theta = \sin^{-1}(c\tau/d) \quad (3.15)$$

τ is the time delay, c is the acoustic velocity and d is the spacing between the elements.

The side lobes can be minimised and the main lobe shape can be tailored by proper shading of the elements

3.4.5 Directivity index

The transmitting directivity index of a projector at a point on the axis of the beam pattern is the difference between the sound level generated by the projector and the level that would be generated by a nondirectional projector radiating the same amount of total acoustic pressure [11].

$$DI_T = 10 \log \frac{I_D}{I_{Nond}} \quad (3.16)$$

where I_D is the sound level of the directional projector and I_{Nond} is that of the nondirectional projector.

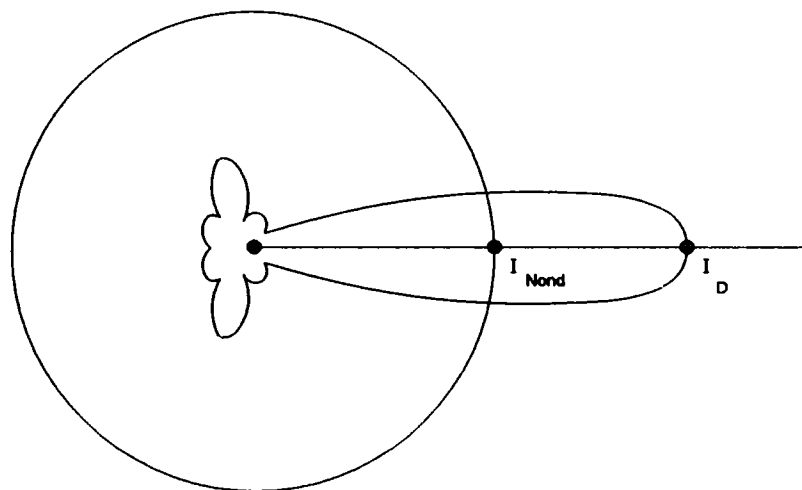


Fig.3.10 Directivity index

3.4.6 Acoustic pressure field

Effective acoustic pressure is the quantity usually recorded as the radiation pattern of a transmitter. The effective acoustic pressure p developed at a distance r from a simple source is expressed by

$$p = \frac{A}{r} e^{j(\omega t - kr)} \quad (3.17)$$

Where k is the wave number $2\pi/\lambda$ and A is the rms pressure amplitude at a reference distance r of one meter. When an array of elements are considered, total effective acoustic pressure is computed as the sum of the contributions from each element.

Beam Characteristics of Annular ring and Annular cylindrical arrays

A large number of ultrasonic probes suitable for various applications have been developed. Generally single probe transducers are being used for inspection and detection of underwater pipeline defects, but a substantial time saving in the inspection can be achieved by using suitable arrays. Fabrication of ultrasonic arrays is feasible using integrated circuit and hybrid construction techniques. The formulation and computation results of array gain and beam pattern of an annular ring array and annular cylindrical array suited for pipeline inspection are highlighted in this chapter. The array gain and beam pattern are computed for a selectively energised section of

an annular ring and annular cylindrical array. The computations are carried out for different configurations and array radius of the annular ring and annular cylindrical arrays. The sidelobe levels and 3dB beamwidths are determined for different configurations of the array.

4.1 INSPECTION SYSTEM

The transducer array designed for the inspection of underwater pipelines comprises transducer elements arranged in an annular ring or annular cylindrical fashion as in figures 4.1 and 4.2.

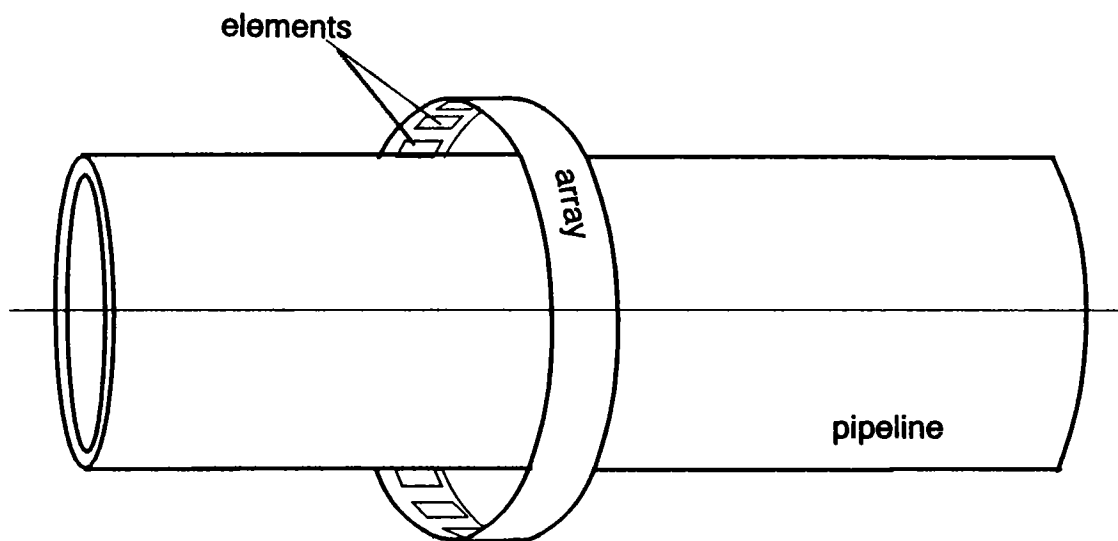


Fig.4.1 Configuration and orientation of an annular ring array around the pipeline

The configuration of the annular cylindrical array can be pictured as staves of elements arranged in such a way that they form a cylindrical structure concentric to the test pipeline as in Figure 4.2. Each staff consists of n elements arranged as a linear array. A consecutive set of staves focus the ultrasound at a point on the surface of

the pipeline.

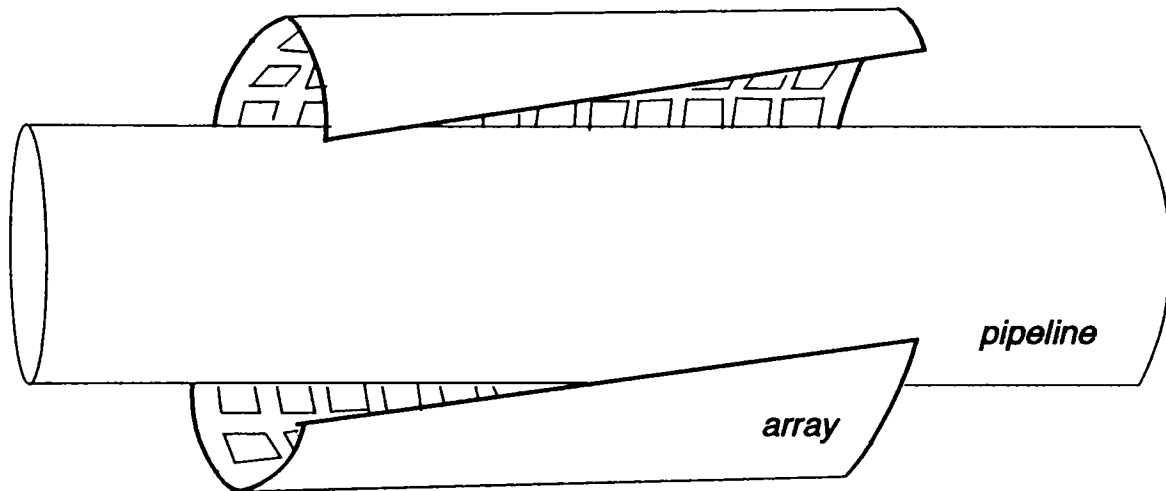


Fig.4.2 Configuration and orientation of an annular cylindrical array around the pipeline

The focused ultrasound has to be moved around the contour of the pipeline. For this, the next consecutive set of staves are energised to focus the beam at a point farther on the pipeline and so on until the whole contour of the pipeline is inspected. An $m \times n$ element annular cylindrical array is constituted by m staves of n elements each. For an annular ring array $n=1$. A similar set of elements form the receiving part of the array. Manual rotation of the array is not necessary due to electronic switching and there is a substantial reduction in inspection time compared to single probe system.

The transducer elements are excited by a sine wave of frequency between 1 to 10 MHz, in the continuous wave excitation. In the pulsed mode a gated sine wave is used. The assumptions made in the computation of the annular ring and annular cylindrical array are

- ★ The transducer elements are considered to be point source elements with half wavelength spacing between elements. Half wavelength spacing ensures, the elimination of grating lobes and minimum interelement interaction.
- ★ Since point source of elements are considered, the amount of energy reradiated and captured by the sources can be considered to be negligible.
- ★ Surface of the pipeline is assumed to be smooth so that scattering effect may be neglected.

However when a practical array is realised, the finite size of the elements are to be taken into account and the reradiation effects and interelement interaction are of considerable significance.

4.2 CROSSCORRELATION COEFFICIENTS

The cross correlation coefficients of signal ρ_s and that of noise ρ_n for an annular ring array or annular cylindrical array insonified by a single frequency sinusoidal wave with time delay τ_e is,

$$\rho_s = \cos \omega(\tau_w + \tau_e) \quad (4.1)$$

and

$$\rho_n = \frac{\sin(\omega d/c)}{\omega d/c} \cos \omega \tau_e \quad (4.2)$$

Where

$\omega=2\pi f$, f being the frequency of the acoustic wave incident on the array, τ_{ω} is the transit time of the signal between array elements, τ_e is the electrical time delay, c is the acoustic velocity and d is the spacing between the elements.

4.2.1 Annular ring array

The crosscorrelation coefficient of signal between i^{th} and j^{th} element $(\rho_s)_{ij}$ for a single frequency zero time delay acoustic signal incident at an angle θ on a reference element of the annular ring array is

$$(\rho_s)_{ij} = \cos(\omega\tau_{ij}) \quad (4.3)$$

where

$$\tau_{ij} = \frac{d_{ij}}{c} \cos\theta \quad (4.4)$$

and

$$d_{ij} = 2R \sin \left[|i-j| \frac{d}{2R} \right], \quad (4.5)$$

R being the radius of the array and d the interelement spacing. The crosscorrelation coefficient of noise $(\rho_n)_{ij}$ is

$$(\rho_n)_{ij} = \frac{\sin \left[\omega \frac{d_{ij}}{c} \right]}{\omega \frac{d_{ij}}{c}} \quad (4.6)$$

4.2.2 Annular cylindrical array

The crosscorrelation coefficient of signal for the annular cylindrical array

between $(ij)^{th}$ element and $(kl)^{th}$ element, where i and k represent linear positions and j and l represent positions along the annular ring is,

$$(\rho_s)_{ijkl} = \cos(\omega\tau_{ijkl}) \quad (4.7)$$

where

$$\tau_{ijkl} = \frac{d_{ijkl}}{c} \cos\theta \quad (4.8)$$

and

$$d_{ijkl} = \sqrt{\left[2R \sin\left[|i-k|\frac{d'}{2R}\right]\right]^2 + (|j-l|d)^2} \quad (4.9)$$

where R is the radius of the array and d the interelement spacing. The crosscorrelation coefficient of noise $(\rho_n)_{ijkl}$ is

$$(\rho_n)_{ijkl} = \frac{\sin\left[\omega \frac{d_{ijkl}}{c}\right]}{\omega \frac{d_{ijkl}}{c}} \quad (4.10)$$

4.3 ARRAY GAIN

The array gain of the annular ring and annular cylindrical arrays are computed from their respective crosscorrelation coefficients as

$$AG = 10 \log \frac{\sum_i \sum_j (\rho_s)_{ij}}{\sum_i \sum_j (\rho_n)_{ij}} \quad (4.11)$$

The array gain computed for different configurations of an annular ring array are shown in Table 4.2. The array gain for the annular cylindrical array is

$$AG = 10 \log \frac{\sum_i \sum_j \sum_k \sum_l (\rho_s)_{ijkl}}{\sum_i \sum_j \sum_k \sum_l (\rho_n)_{ijkl}} \quad (4.12)$$

The array gain computed for different configurations of the annular cylindrical array are shown in Table 4.4.

4.4 BEAM PATTERN

The beam pattern of a transducer array represents graphically its directional response to sound waves incident in a specified plane and at a specified frequency. The beam patterns of annular ring and annular cylindrical arrays are presented below.

4.4.1 Annular ring array

A plane sinusoidal wave is incident on an annular ring array. θ and ϕ are the incident angle and azimuth angle with which the wavefront is incident at the first element. The path difference of the wavefront incident on the two adjacent elements A and B is computed from the geometry of the array as

$$U = R \left[\sin \left[\theta' + \frac{d'}{R} \right] - \sin \theta' \right] \sin \phi \quad (4.13)$$

Where R is the radius of the annular ring, d is the interelement spacing and d' is the arclength between A and B.

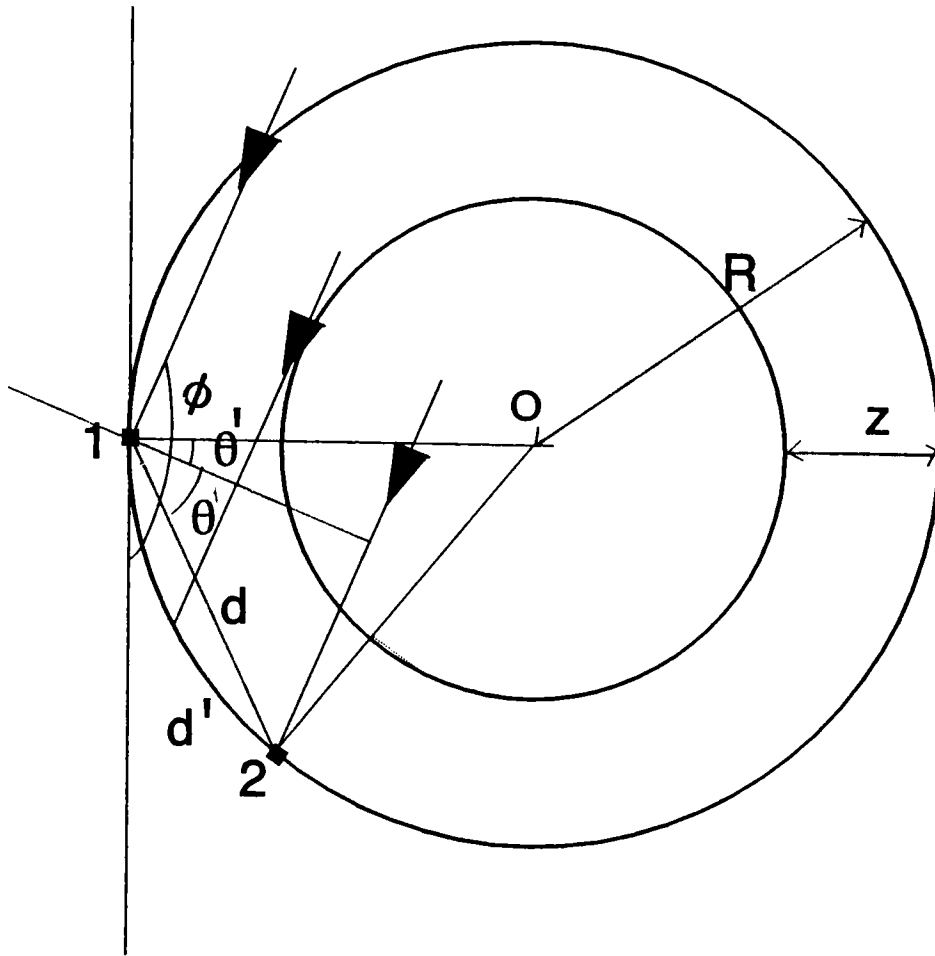


Fig.4.3 Geometrical variables used for the computation

The path difference of the wavefront for the m^{th} element relative to the first element is

$$U_{(m-1)} = R \left[\sin \left[\theta' + (m-1) \frac{d'}{R} \right] - \sin \theta' \right] \sin \phi \quad (4.14)$$

The beam pattern is computed as

$$b(\theta) = \left[\frac{V}{M} \right]^2 \quad (4.15)$$

Where V is the total output voltage from M element section of the receiving array.

Total output voltage is computed as

$$V = e^{ikU_0} + e^{ikU_1} + \dots + e^{ikU_{(M-1)}} \quad (4.16)$$

$$V = \sum_{m=0}^{M-1} \cos \left[kR \left[\sin(\theta' + \frac{md'}{R}) - \sin\theta' \right] \sin\phi \right] + j \sum_{m=0}^{M-1} \sin \left[kR \left[\sin(\theta' + \frac{md'}{R}) - \sin\theta' \right] \sin\phi \right] \quad (4.17)$$

$k=2\pi/\lambda$ the wave vector, λ being the acoustic wavelength

$$b(\theta) = \frac{1}{M^2} \left[\sum_{m=0}^{M-1} \cos \left[kR \left[\sin(\theta' + \frac{md'}{R}) - \sin\theta' \right] \sin\phi \right] \right]^2 + \frac{1}{M^2} \left[\sum_{m=0}^{M-1} \sin \left[kR \left[\sin(\theta' + \frac{md'}{R}) - \sin\theta' \right] \sin\phi \right] \right]^2 \quad (4.18)$$

$b(\theta)$ is plotted against $\sin(\theta)$ to obtain the beam pattern. Beam pattern for different configurations of an annular ring array with array radius 6cm and element spacing $\lambda/2$, operating at 1MHz are shown in Figures 4.4 and 4.5.

The array parameters like radius of the array, number of elements in the selected section of the array etc are varied and the beam pattern corresponding to these variations are plotted. Effect of array radius on the beam pattern is shown in

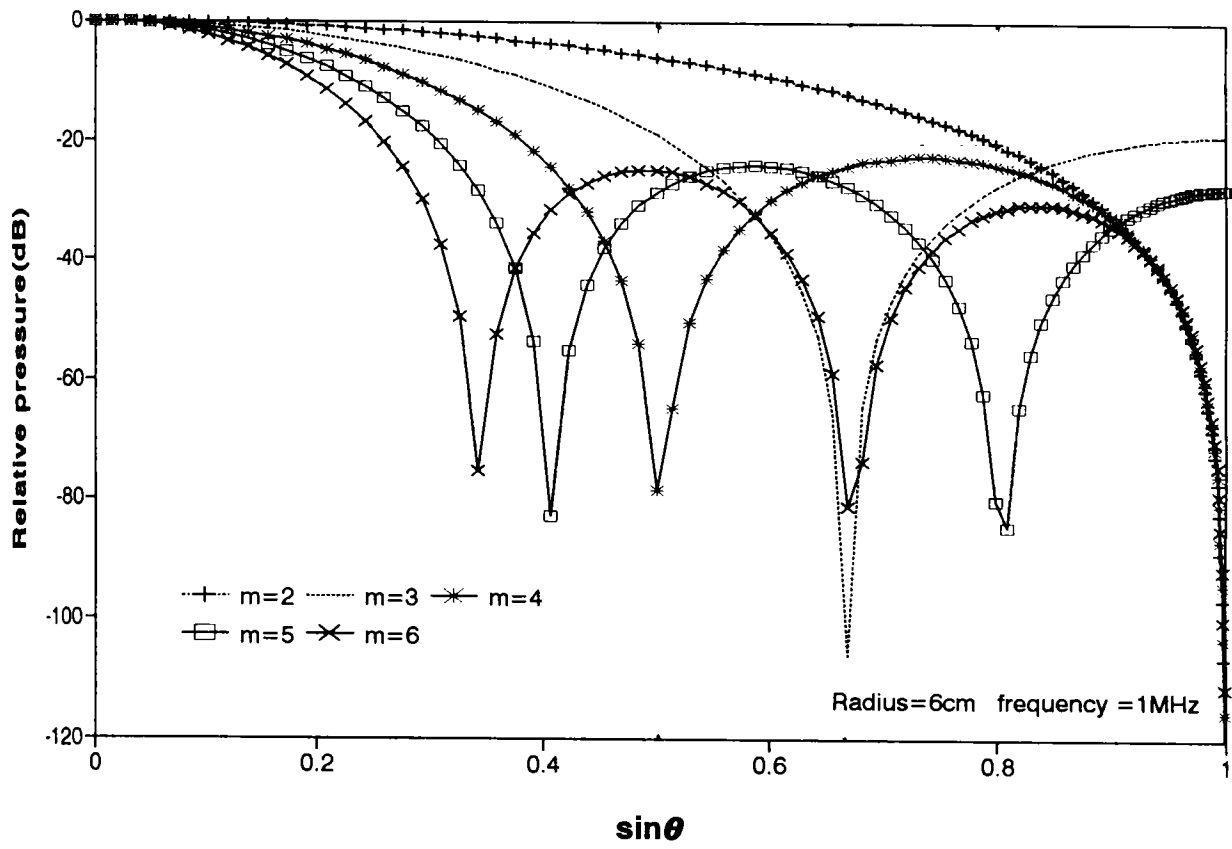


Fig.4.4 Beam pattern of an annular ring array for different configurations

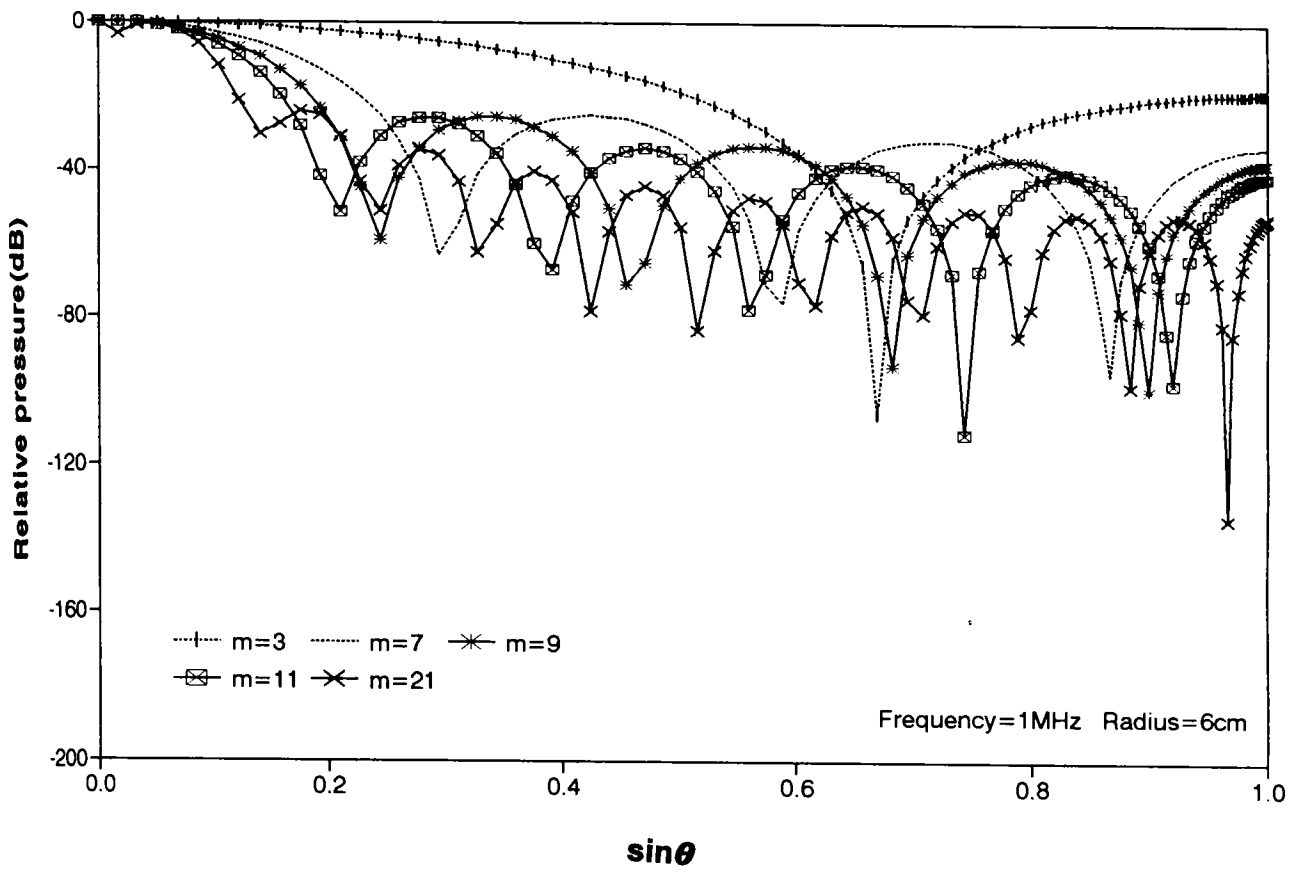


Fig.4.5 Beam pattern of an annular ring array for different configurations

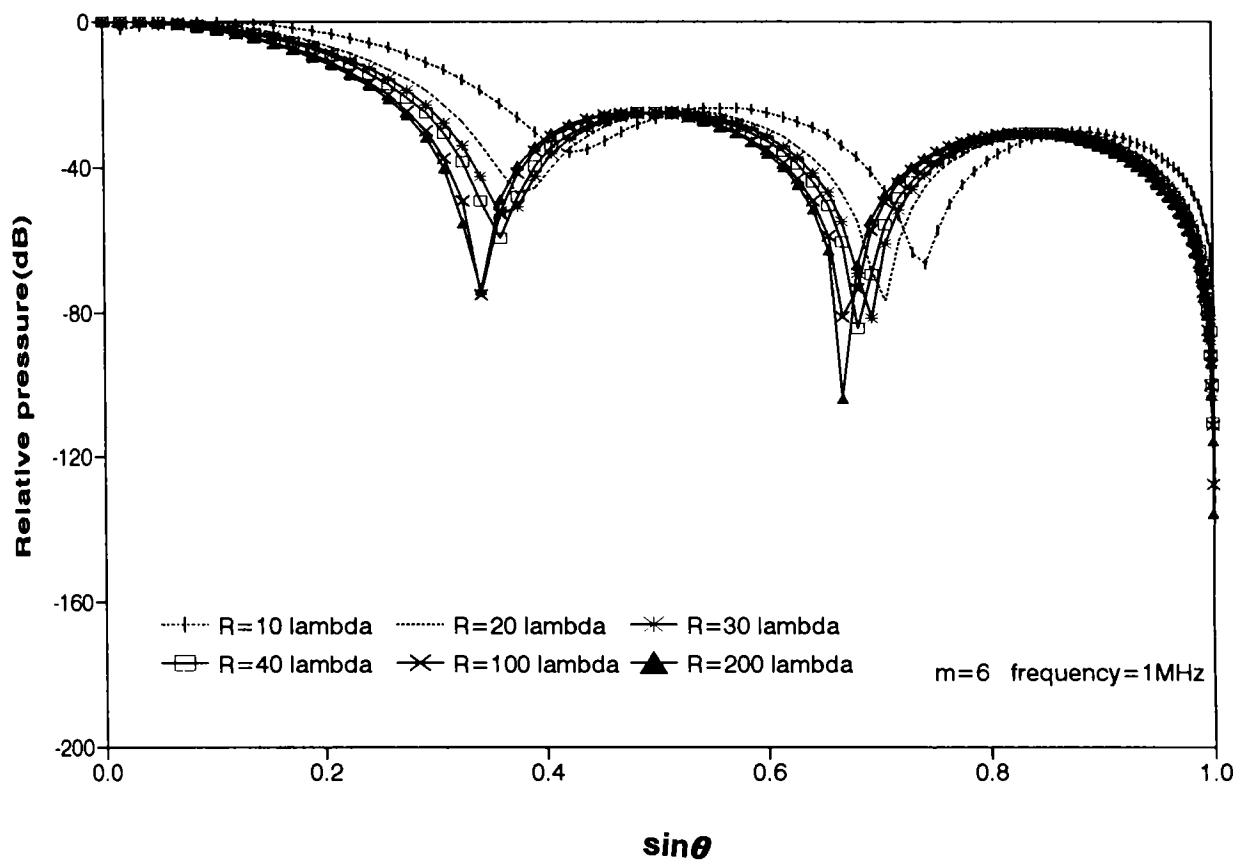


Fig.4.6 Effect of array radius on the beam pattern

Figure 4.6. The beam characteristics of a 5 element section of an annular ring array operating at 5 MHz for different array radii are shown in Table 4.1. Table 4.2 shows the beam characteristics for different configurations of an annular ring array.

Table 4.1

Beam characteristics of a 5 element annular ring array

Radius (λ)	Most Intense sidelobe level (dB)	Sidelobe level at 90°	3 dB Beamwidth (degrees)
10	-22.802	-28.107	22
20	-23.928	-28.623	20
30	-24.294	-28.719	18
40	-24.457	-28.753	17
50	-24.408	-28.768	17
60	-24.375	-28.777	17
70	-24.352	-28.782	16
80	-24.335	-28.785	16
90	-24.322	-28.788	16
100	-24.311	-28.789	16

Frequency=5MHz, $d=\lambda/2$, wavelength $\lambda=0.03\text{cm}$, $m=5$

Table 4.2

Beam characteristics for different configurations of annular ring array

No. of elements	Most Intense sidelobe level (dB)	Corresponding θ in degrees	Sidelobe level at 90°	3 dB Beamwidth (degrees)	Array Gain in dB
4	-22.609	50.40	-48.209	20.0	5.768
5	-24.071	36.00	-28.789	16.0	6.647
6	-24.816	30.60	-48.397	14.0	7.347
7	-25.232	26.10	-35.465	12.0	7.922
8	-25.490	22.50	-48.618	11.0	8.404
9	-25.569	20.25	-40.942	10.8	8.816
10	-25.567	18.45	-48.832	9.8	9.172
11	-25.492	17.10	-45.826	9.0	9.481

Frequency=5MHz, Radius=100 λ , $d=\lambda/2$, $\lambda=0.03\text{cm}$

From Table 4.1, the 3dB beamwidths and sidelobe levels are seen to remain constant when array radius is $\geq 40\lambda$

4.4.2 Annular cylindrical array

The annular cylindrical array can be pictured as staves of elements arranged in a cylindrical manner and concentric to the pipeline. The section of the annular cylindrical array comprising m elements along the curvature and n elements linear is energised. For a linear array constituted by n elements and element spacing d , the beam pattern is

$$b'(\theta) = \left[\frac{\sin \left[\frac{n\pi}{\lambda} d \sin\theta \sin\phi \right]}{n \sin \left[\frac{\pi}{\lambda} d \sin\theta \sin\phi \right]} \right]^2 \quad (4.19)$$

The beam pattern of an annular ring array constituted by m elements and element spacing d is

$$b(\theta) = \frac{1}{M^2} \left[\sum_{m=0}^{M-1} \cos \left[kR \left[\sin\left(\theta' + \frac{md'}{R}\right) - \sin\theta' \right] \sin\phi \right] \right]^2 + \frac{1}{M^2} \left[\sum_{m=0}^{M-1} \sin \left[kR \left[\sin\left(\theta' + \frac{md'}{R}\right) - \sin\theta' \right] \sin\phi \right] \right]^2 \quad (4.20)$$

The beam pattern $B(\theta)$ of the portion of the annular cylindrical array, can be expressed to a good approximation as [11],

$$B(\theta) = b(\theta) b'(\theta) \quad (4.21)$$

Where $b(\theta)$ is the beam pattern of an annular ring array of m elements and $b'(\theta)$

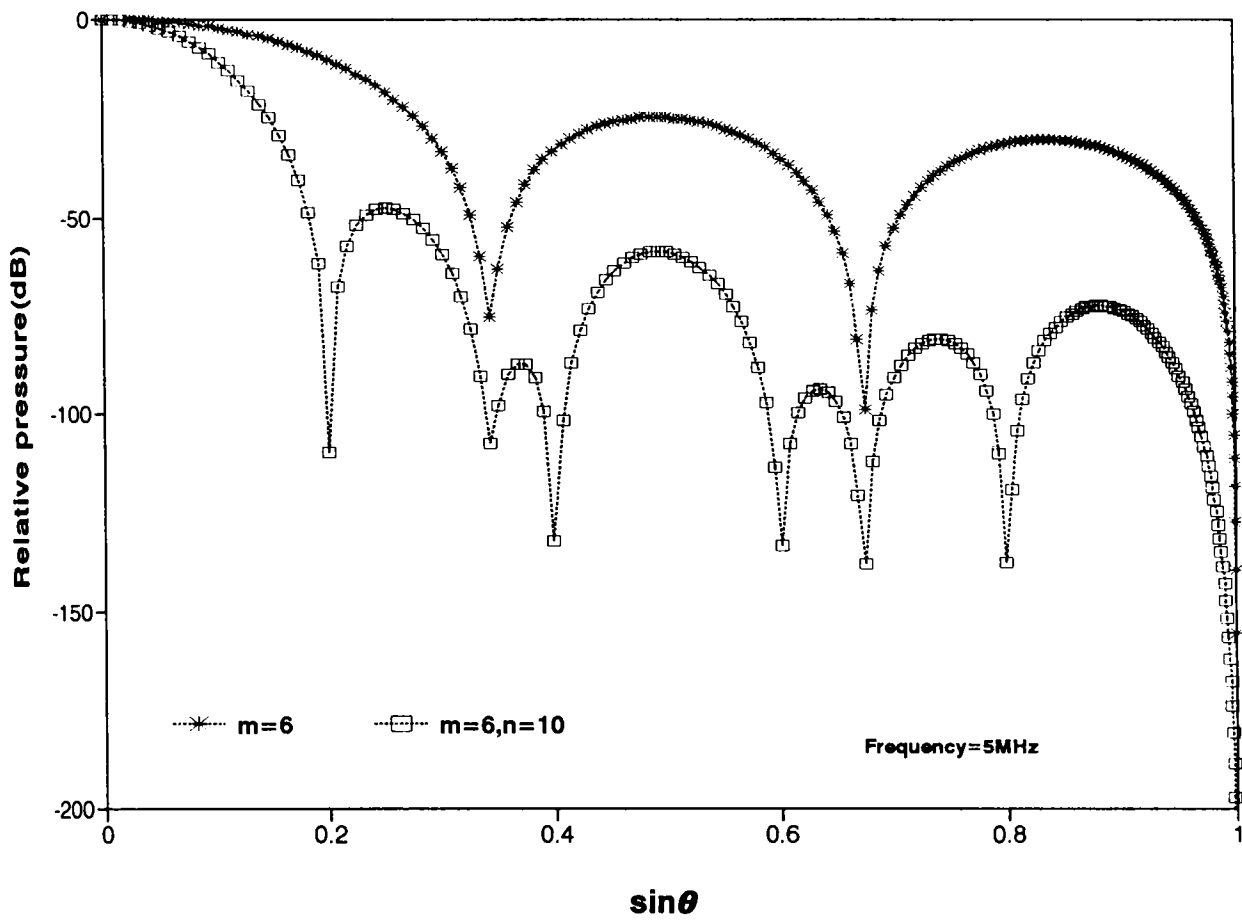


Fig.4.7 Beam pattern of an annular cylindrical array compared with an annular ring array

is the beam pattern of a linear array of n elements. Figure 4.7 shows the beam pattern of a 6x10 element annular cylindrical array compared with a 6 element annular ring array. The parameters like, the radius of the array and number of array elements selected are varied and the beam pattern is plotted. The results from these plots are tabulated in Tables 4.3 and 4.4.

Table 4.3

Beam characteristics of an annular cylindrical array

Radius (λ)	Most Intense sidelobe level (dB)	Sidelobe level at 90°	3 dB Beamwidth (degrees)
10	-15.14	-42.25	14.2
20	-15.29	-42.19	14.1
30	-15.34	-42.18	14.1
40	-15.36	-42.17	14.0
50	-15.38	-42.17	14.0
60	-15.39	-42.17	14.0
100	-15.40	-42.17	14.0

$m=3, n=10, \text{ Frequency}=1\text{MHz}, d=\lambda/2$

Table 4.4

Beam characteristics for different configurations of annular cylindrical array

No. of elements	Most Intense sidelobe level (dB)	Sidelobe level at 90°	3 dB Beamwidth (degrees)	Array Gain in dB $\theta=\pi/6, \phi=\pi/2$
2	-13.90	-26.17	14.2	11.69
3	-15.40	-42.17	14.0	12.92
4	-17.61	-30.53	13.6	13.69
5	-20.50	-35.67	13.2	14.23

Frequency=1MHz, $d=\lambda/2$, Radius $R=100\lambda$, Number of linear elements $n=10$

Effective Acoustic Pressure of Annular ring & Annular Cylindrical arrays

The formulation and computation of effective acoustic pressure of an annular ring and annular cylindrical array for continuous as well as pulse excited signals is discussed in this chapter. The effective acoustic pressure is evaluated over the contour of the pipeline for different configurations and dimensions of the array. The axial pressure distribution of the annular ring and annular cylindrical array is also computed to optimise the radius of the array suitable for inspection of a pipeline of specified dimensions. The transmitting characteristics of the annular ring and annular cylindrical arrays are evaluated from their effective acoustic pressures. Techniques for computing the effective acoustic pressure and optimisation of different array parameters are also discussed. The annular ring array is found to have a focusing effect compared to the

linear array, which is an added advantage in defect detection.

5.1 COMPUTATION OF EFFECTIVE ACOUSTIC PRESSURE

The effective acoustic pressure is computed as the sum of the pressure contributions from the individual elements of the array. It is also computed as the sum of the Fourier transform of the impulse response of array elements. A point source of array elements are considered so that the interelement interaction is minimum when spacing is $\lambda/2$. The amount of energy reradiated from the contours of the pipeline and captured by the point sources can be considered to be negligible for all practical purposes. The effects due to the finite size of the elements are to be taken into account when constructing the array. The annular ring and annular cylindrical arrays are to be operated in such a way that the angle of incidence of the ultrasonic waves from the array elements should be less than the critical angle of the material of the pipeline.

5.1.1 Multiple point sources

The effective acoustic pressure at a point due to a simple source is expressed as

$$p = \frac{A}{r} e^{j(\omega t - kr)} \quad (5.1)$$

Where A is the rms pressure amplitude at a reference distance of 1m, k is the wave vector, ω is the angular velocity and r is the distance of the source from the field point.

For a linear array of equally spaced point sources, the elements are grouped as pairs equidistant from the centre O of the array. The effective acoustic pressure due

to these pairs are computed at a point P . The resultant pressure at a point P due to a pair of elements separated by a distance d is

$$p(\theta) = \frac{A}{r_o} e^{j(\omega t - kr_o)} \left[e^{j \frac{j\pi d}{\lambda} \sin \theta} + e^{j \frac{-j\pi d}{\lambda} \sin \theta} \right] \quad (5.2)$$

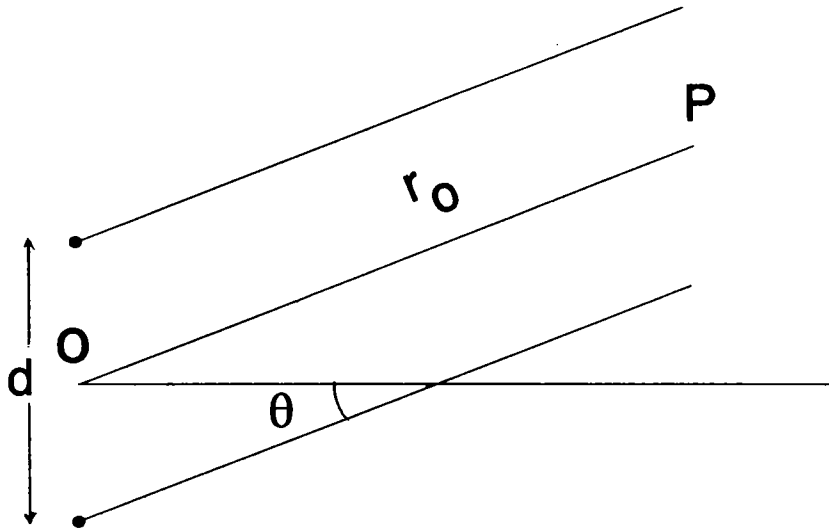


Figure 5.1 A pair of elements of a linear array

5.1.2 Annular ring array

Effective acoustic pressure developed at a distance r from a simple source has been described by Leon Camp[142]. The effective acoustic pressure at a point along the contour of the pipeline for a continuous wave excited annular ring array is the numerical sum of the weighted contributions from the selectively energised m elements. The acoustic pressure at any desired point along the pipeline can be computed as,

$$p = \sum_m \frac{A}{r_m} e^{j\omega \left[t - \frac{r_m}{v} \right]} \quad (5.3)$$

where A is the r.m.s value of pressure at a distance of 1m, r_m is the path length, v is the acoustic velocity and ω is the angular velocity. From the geometry of the array in figure.5.2 the path length r_m is,

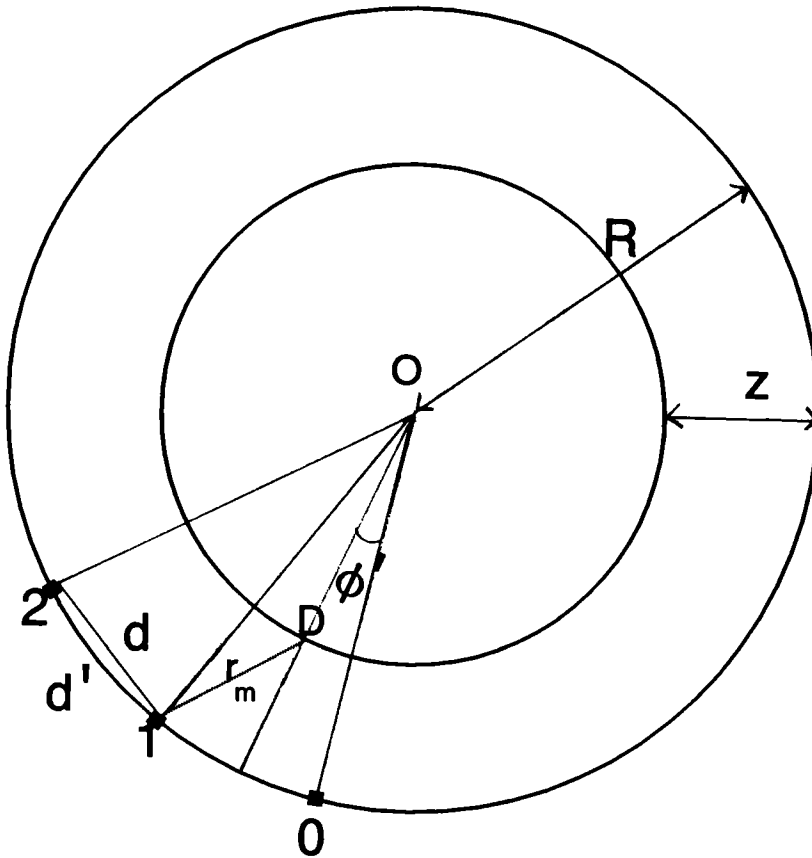


Figure 5.2 Geometrical variables used for computation

$$r_m = \sqrt{z^2 + 4R(R-z)\sin^2 \left[\frac{\left[\frac{md}{R} - \phi' \right]}{2} \right]} \quad (5.4)$$

where z is the radial distance between the array and the test pipeline and ϕ' is the angle subtended by the field point and the central element at the center of the pipeline.

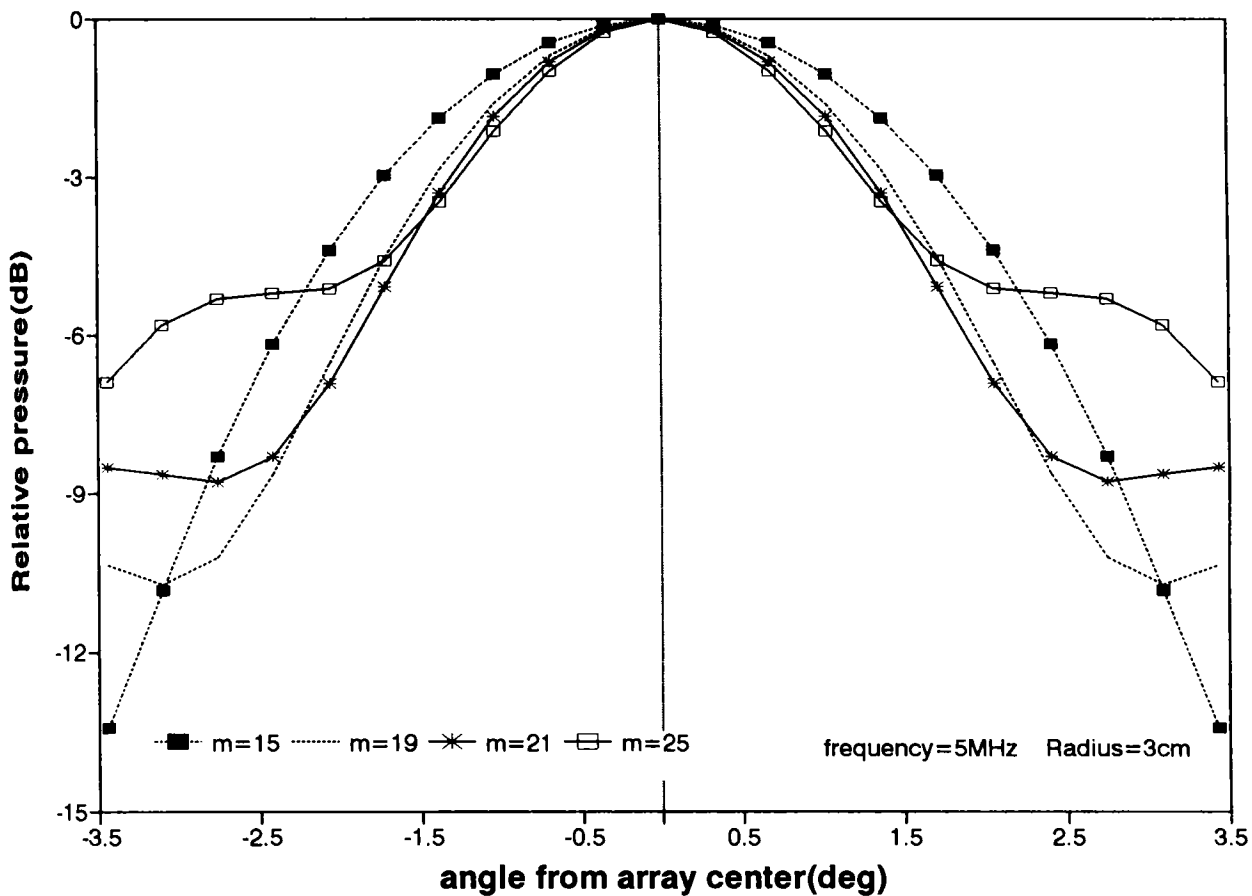


Fig.5.3 Effective acoustic pressure of an annular ring array for different configurations

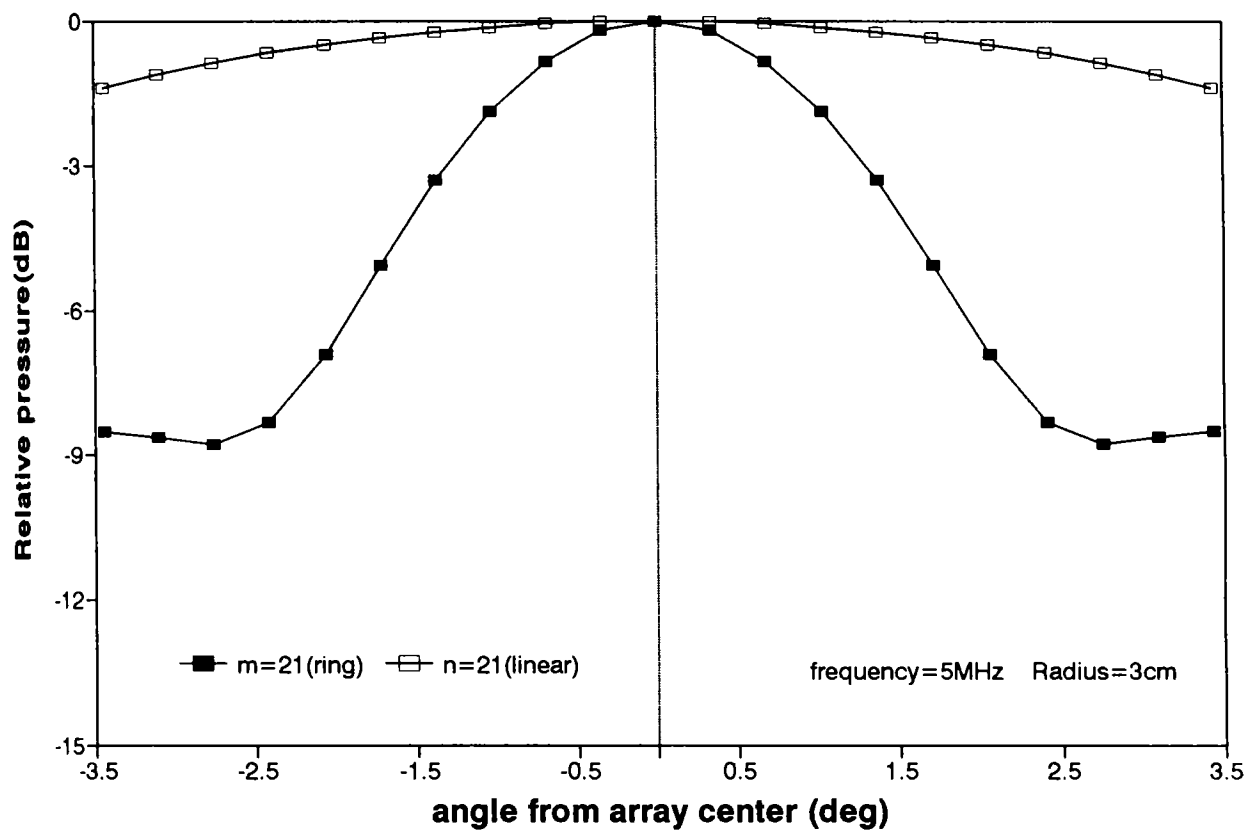


Fig.5.4 Comparison of effective acoustic pressure of a linear array and an annular ring array

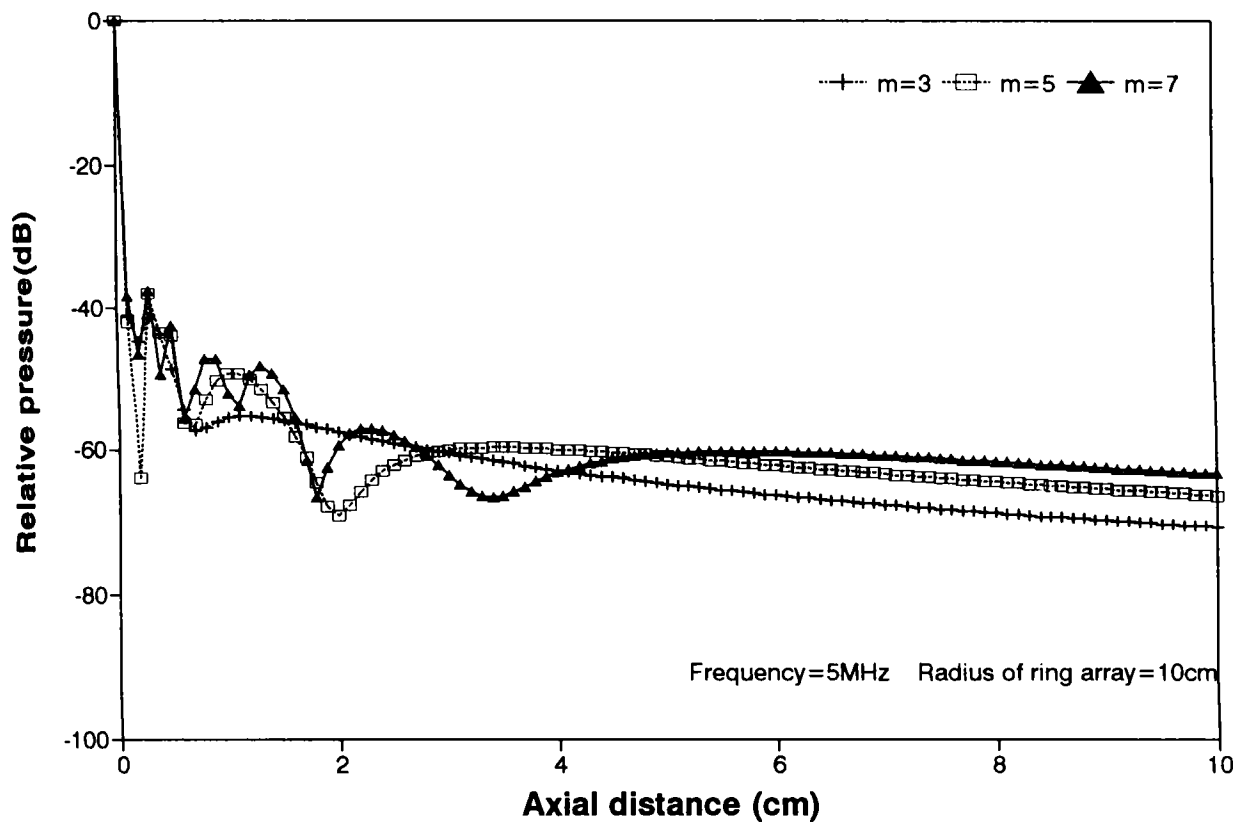


Fig.5.5a Axial pressure distribution of an annular ring array for different configurations

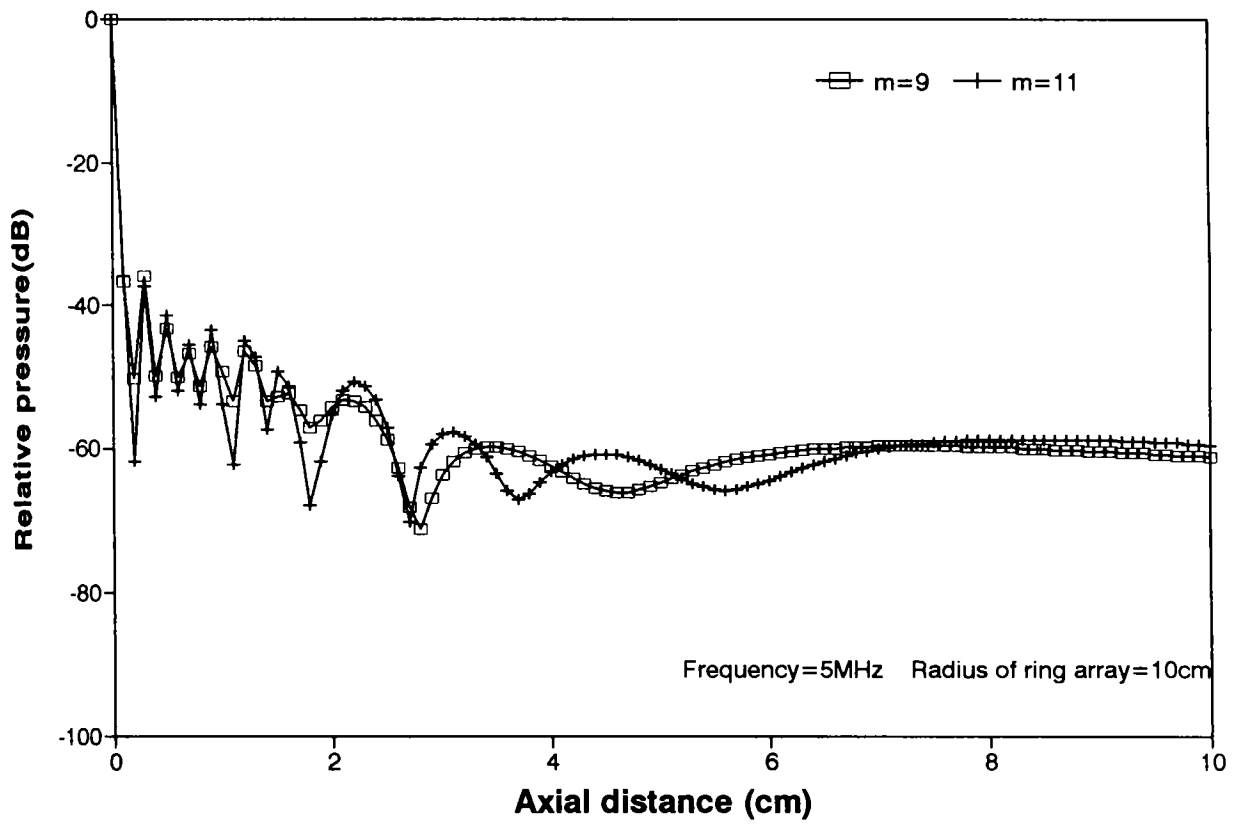


Fig.5.5b Axial pressure distribution of an annular ring array for different configurations

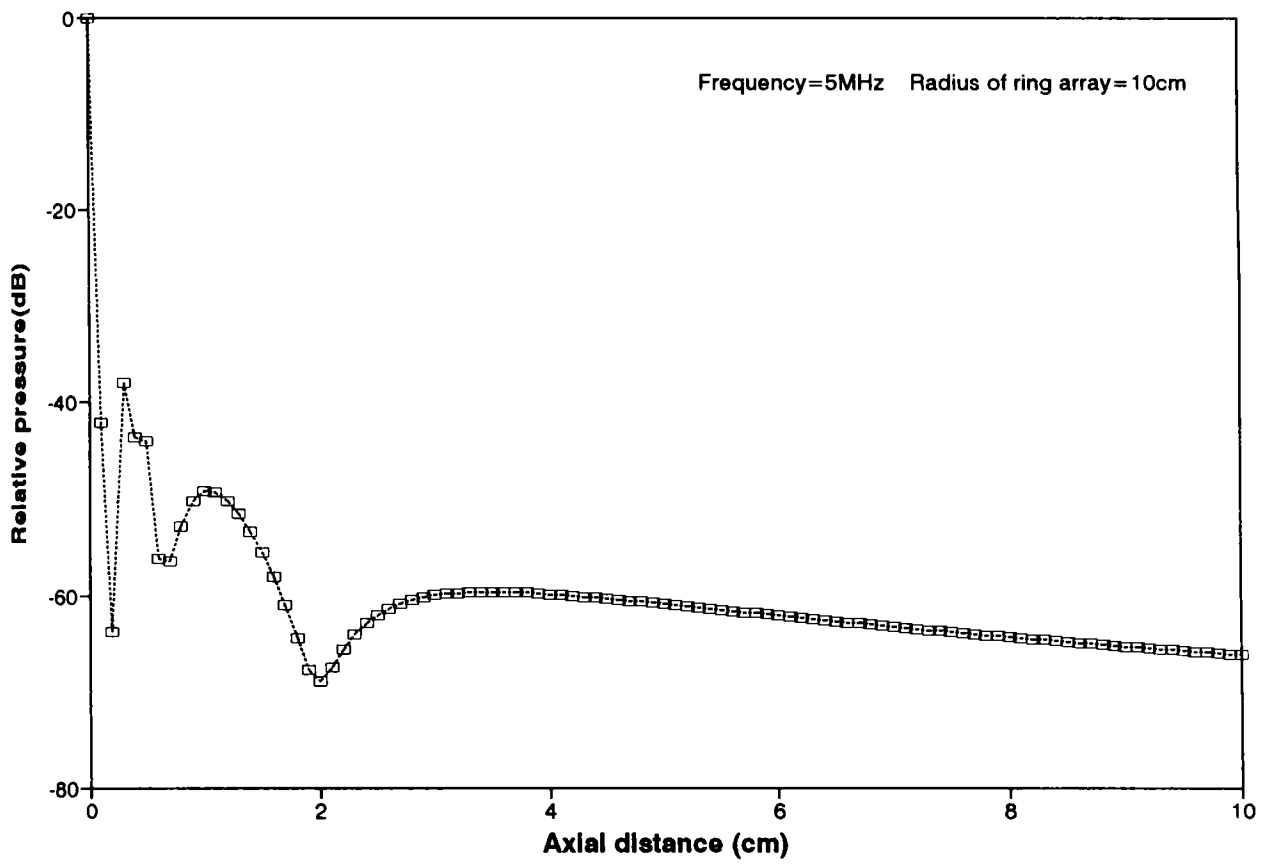


Fig.5.6 Axial pressure distribution of a 5 element annular ring array

Varying the value of ϕ' the effective acoustic pressure is evaluated over the desired portion of the pipeline.

Figure 5.3 shows the variation of effective acoustic pressure for different configurations of an annular ring array operating at 5MHz and array radius 3cm. To bring out the focusing effect of the annular ring array, a comparative study of both linear and annular ring arrays is made. A comparison of the effective acoustic pressure of a 21 element linear array and a 21 element annular ring array is shown in Figure 5.4.

The axial pressure distribution of the annular ring array is studied to optimise the array parameters such as radius and number of elements, suitable for a particular pipeline geometry. Figures 5.5a and 5.5b show the axial pressure distribution for different configurations of the array keeping the array radius fixed at 10cm. Figure 5.6 shows the axial pressure distribution for a 5 element annular ring array.

5.1.3 Annular cylindrical array

The effective acoustic pressure of an annular cylindrical array is computed similar to that of the annular ring array. For an annular cylindrical array of $m \times n$ equally spaced point source elements, the effective acoustic pressure is computed as

$$p = \sum_m \sum_n \frac{A}{r_{mn}} e^{j\omega \left(t - \frac{r_{mn}}{v} \right)} \quad (5.5)$$

where path length r_{mn} is computed from the geometry as

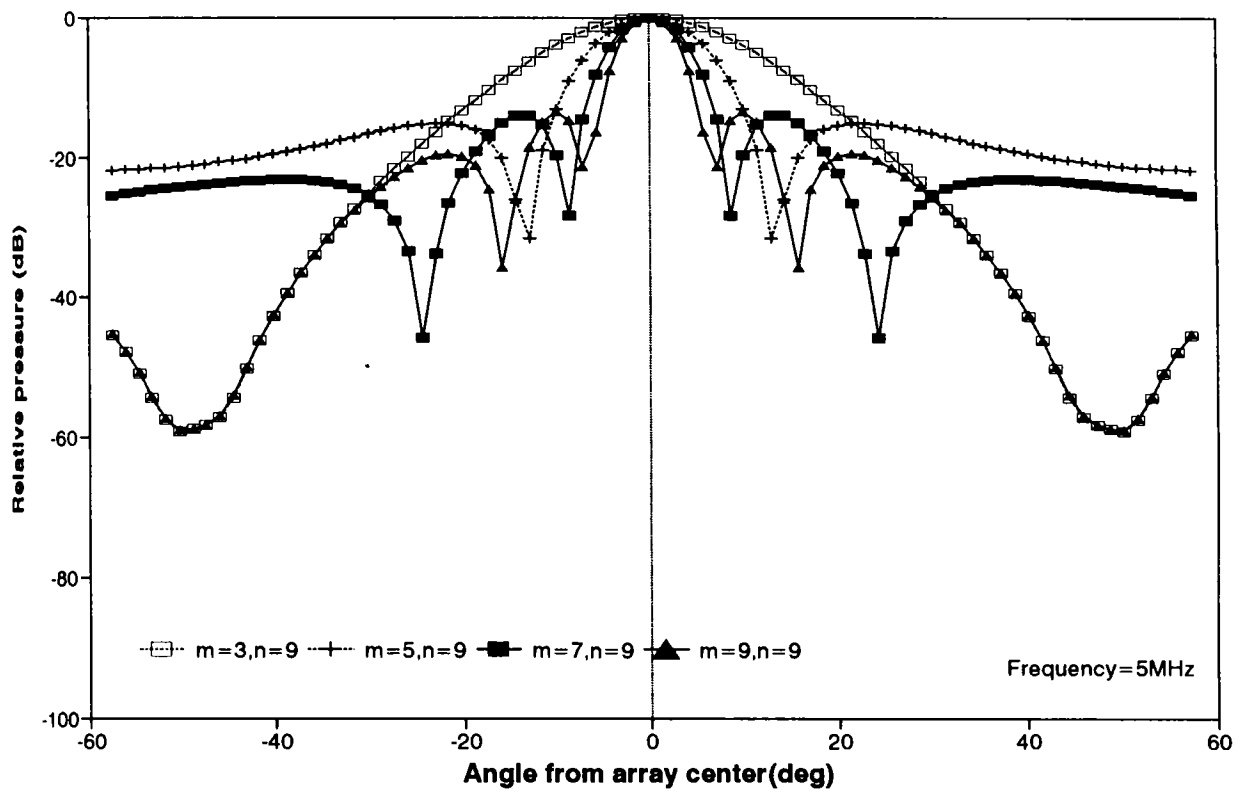


Fig.5.7 Effective acoustic pressure of an annular cylindrical array for different configurations

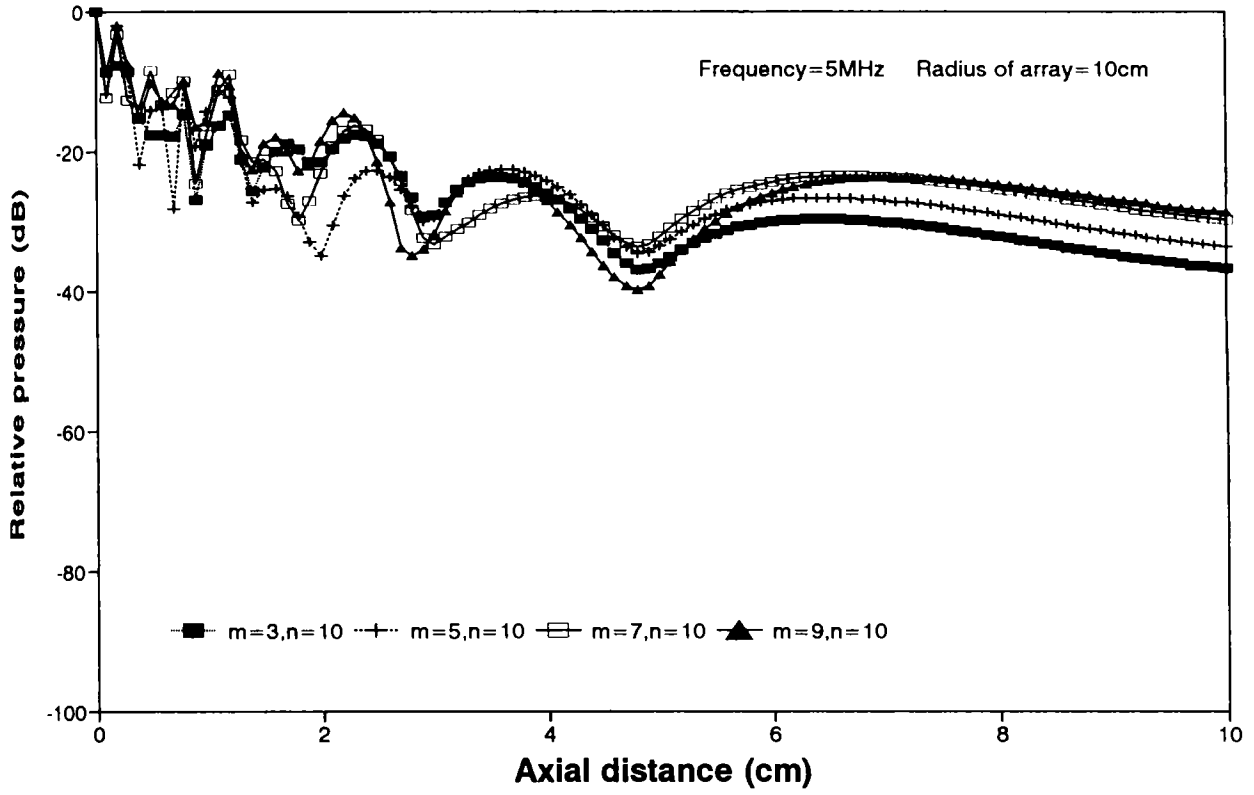


Fig.5.8 Axial pressure distribution of an annular cylindrical array for different configurations

$$r_{mn} = \sqrt{z^2 + 4R(R-z)\sin^2\left[\frac{\left[\frac{md}{R} - \phi'\right]}{2}\right]} + (nd)^2 \quad (5.6)$$

The effective acoustic pressure for different configurations of an annular cylindrical array are shown in Figure 5.7. The axial pressure distribution for different configurations of an annular cylindrical array are shown in figure 5.8.

5.2 IMPULSE RESPONSE

The instantaneous pressure at a point in the field of an ultrasound can be solved as a boundary value problem, from the classical theory of sound as

$$p(r,t) = \rho \frac{\partial \phi}{\partial t} \quad (5.7)$$

where ρ is the equilibrium density of the surrounding medium and ϕ denotes the velocity potential.

The velocity potential is also expressed as a convolution of the instantaneous normal particle velocity and the impulse response

$$\phi(r,t) = v_o(t) * h(r,t) \quad (5.8)$$

where $v_o(t)$ represents the instantaneous normal particle velocity at the face of the transducer, $h(r,t)$ is the impulse response which depends only on the shape of the radiator and * denotes the convolution.

The pressure field is expressed in terms of the impulse function as

(5.9)

$$P(r,t) = -j\omega_0 \rho_0 v_0 e^{j\omega_0 t} \int_{-\infty}^{\infty} h(r,\tau) e^{-j\omega_0 \tau} d\tau$$

The impulse response of the annular ring and annular cylindrical array are computed to determine the pressure field.

5.2.1 Impulse response of a circular piston

In the cylindrical coordinates the surface element ds is given by $\rho' d\rho' d\phi'$ and the impulse response of a circular piston is

$$h(r,t) = - \int_0^{2\pi} \int_0^a \frac{\delta(t-R'/c)}{2\pi R'} \rho' d\rho' d\phi' \quad (5.10)$$

where

$$R' = [z^2 + \rho^2 + \rho'^2 - 2\rho\rho' \cos(\phi - \phi')]^{1/2} \quad (5.11)$$

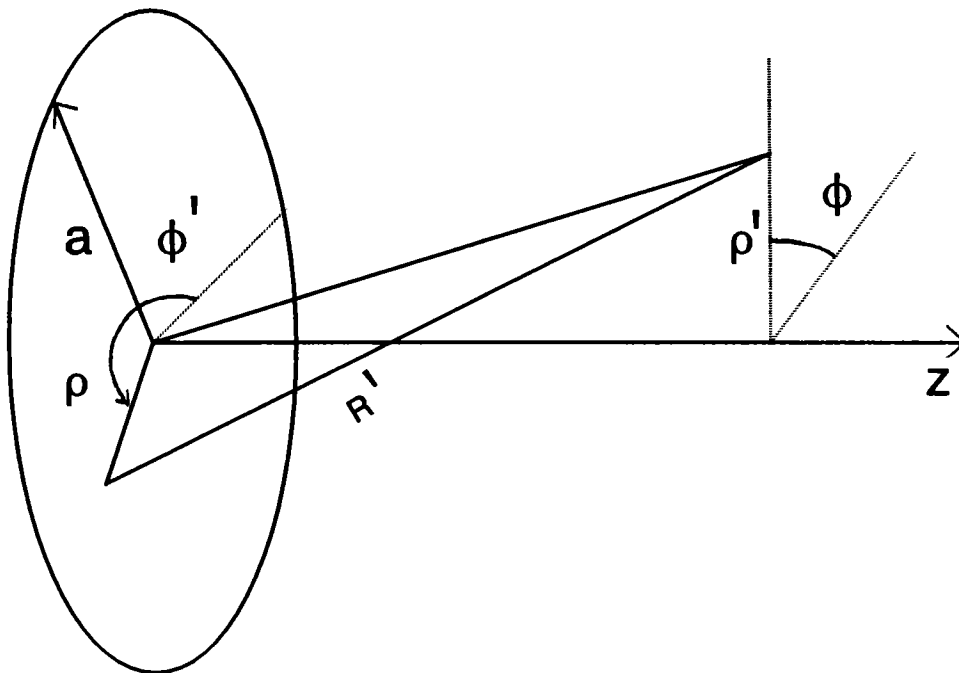


Figure 5.9 Geometrical variables used for computation

where R' is the distance from the surface of the element to the field point, ρ is the perpendicular distance from the field point to the z axis, ρ' is the radial distance to the source point from the centre of the circular piston and $(\phi-\phi')$ is the angle between ρ and ρ' .

The delta function $\delta(t-R'/c) = 0$ for $t < R'/c$ and $t > R'/c$. Therefore at each time t only those points from which the travel time $R'/c=t$ contribute to the pressure and is identically zero otherwise.

5.2.2 Impulse response of annular ring and annular cylindrical arrays

The impulse response of an array is expressed as the sum of the impulse response of the array elements. For an annular ring array of m elements the array impulse response is

$$h_a(r,t) = \sum_m h_m(r,t-\Delta t_m) \quad (5.12)$$

where h_m is the impulse response of the m^{th} element

Impulse response of the section of an annular cylindrical array consisting of $m \times n$ elements is

$$h_a(r,t) = \sum_m \sum_n h_{mn}(r,t-\Delta t_{mn}) \quad (5.13)$$

h_{mn} is the impulse response of the $(mn)^{th}$ element and Δt_{mn} is its time delay.

$$h_{mn}(r,t) = - \int_0^{2\pi a} \int_0^{2\pi} \frac{\delta(t-R'_{mn}/c)}{2\pi R'_{mn}} \rho' d\rho' d\phi' \quad (5.14)$$

R'_{mn} is the distance of the observation point from the $(mn)^{th}$ element.

$$R'_{mn} = \sqrt{\rho_{mn}^2 + \rho'^2 - 2\rho_{mn}\rho' \cos(\phi - \phi') + [R(R-z) \cos(md'/R)]^2} \quad (5.15)$$

where R is the radius of the array, z is the perpendicular distance to the field point from the central element and $(\phi - \phi')$ is the angle between ρ' and ρ_{mn} . ρ_{mn} is the perpendicular distance of the field point to the z axis of each element. A separate z axis is defined for each element.

$$\rho_{mn} = \sqrt{(nd)^2 + [(R-z) \sin(md'/R)]^2} \quad (5.16)$$

5.3 TRANSIENT RESPONSE

A gated sinewave signal of frequency 5.0 MHz is applied to the array for a duration of $0.4\mu s$. From the expression for the effective acoustic pressure for the annular ring array, the time delay for the signal to reach the field point from the m^{th} element is

$$t_m = \frac{r_m}{v} \quad (5.17)$$

The transient pressure P , on the contour of the pipeline for the pulse excited annular ring array is

$$P = \sum_m \frac{A}{r_m} e^{j\omega(t-t_m)} \quad t_m \leq t \leq t_m + \tau \quad (5.18)$$

where τ is the pulse width. At the instant t_0 , signals from the nearest element

reaches the field point and continue to remain till an instant $t_0 + \tau$. At time t_1 signal from the next element reaches the field point and so on till t_m for the signals from the farthest element. The time of arrival from the nearest and farthest sources to the field point are t_0 and t_m respectively. Hence the weighted contributions from all the m sources are obtained from the instant t_m to $t_0 + \tau$.

Figure 5.9 shows the transient response of an annular ring array and Figure 5.10 that of an annular cylindrical array operating at 5MHz. The duration of the gated sinewave is $0.4\mu\text{s}$, the radius of the annular ring array is 3cm and the pressure is evaluated at a distance of 2cm from the central element. The time of arrival t_0 is computed to be $0.1333\mu\text{s}$ and t_m depends on the number of elements in the section of the array.

It is seen from the results obtained in Figures 5.9 and 5.10 that the effective acoustic pressures remain steady in the region t_m to $t_0 + \tau$.

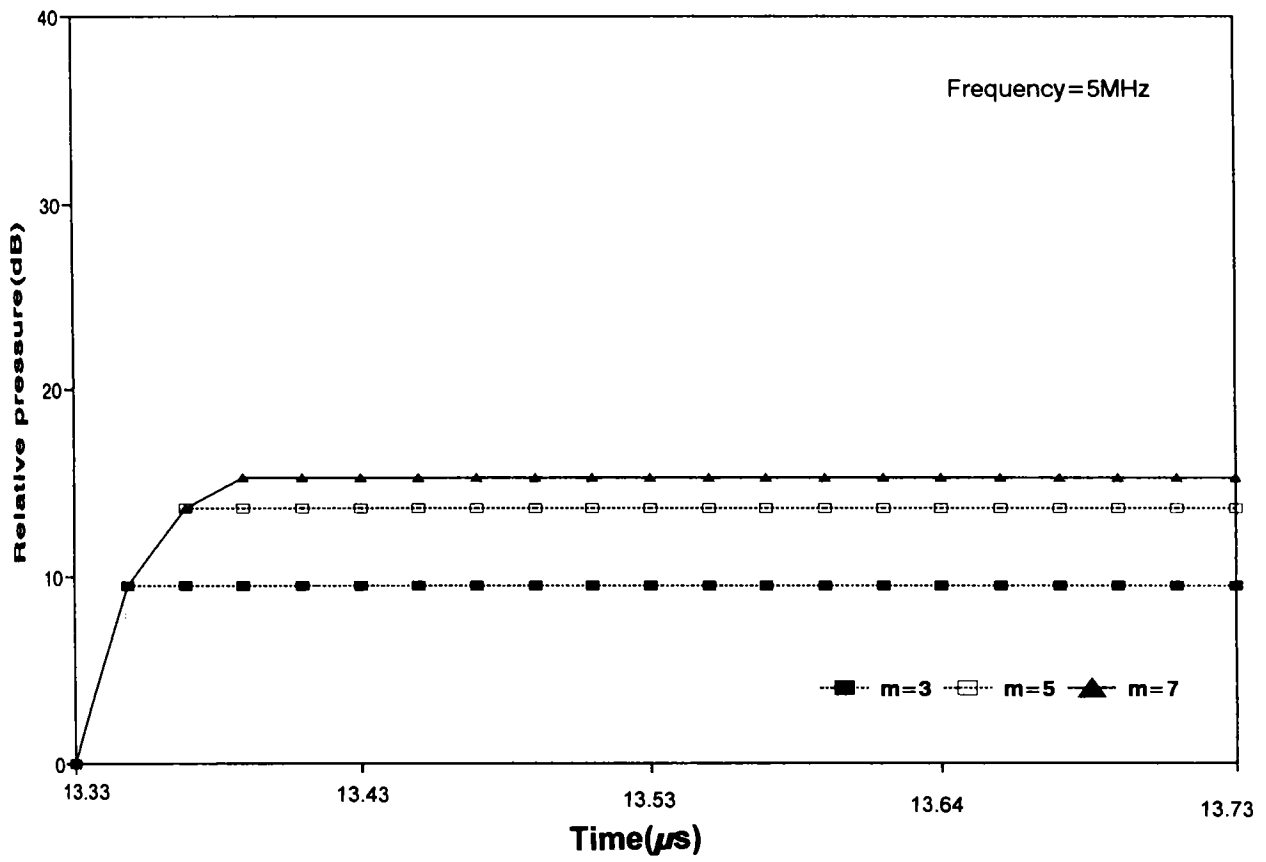


Fig.5.9 Transient pressure variation of an annular ring array for different configurations.

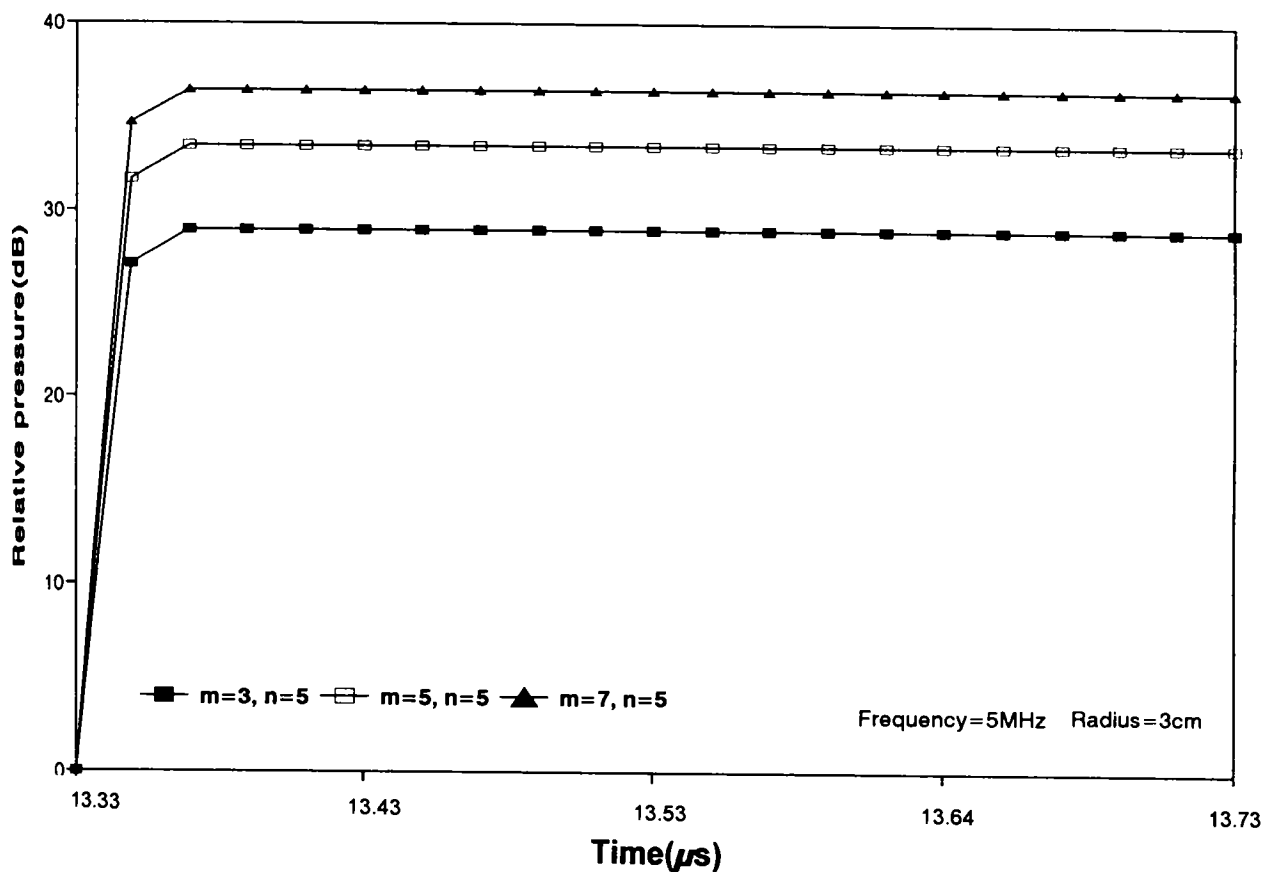


Fig.5.10 Transient pressure variation of an annular cylindrical array for different configurations.

Conclusions

The overall conclusions drawn from the various studies various studies on the annular ring and annular cylindrical arrays are presented in this chapter. The various results obtained are highlighted. This chapter concludes with a brief note on the scope for further work in this field.

Generally single probe techniques are used for underwater pipeline inspection. In this case the probe has to be rotated around the pipeline as well as moved along its length. This is a tedious and time consuming process. So there is a requirement to develop sensors which are much more efficient. The main objective of carrying out

this investigation is to develop suitable transducer array systems so that underwater pipeline inspection could be carried out in a much better way, a focused beam and electronic steering can reduce inspection time as well. Annular ring and annular cylindrical array models have been developed to be used effectively for pipeline inspection. Better results are obtained by optimising the array parameters. Selectively energised sections of the annular ring and annular cylindrical arrays placed concentric over the pipeline are studied. The beam characteristics and effective acoustic pressures of these arrays are studied for different array parameters. A theoretical model has been developed assuming point source of elements and therefore the effects due to the finite size of the elements are to be taken into account when the realisation of the array is effected. The spacing between the elements is assumed to be half the wavelength so that the interelement interaction is minimum. For NDT applications these arrays are operated at MHz range. The wavelengths become very small in these frequency ranges. Then the size of the array elements becomes very small, requiring hybrid construction techniques for their fabrication. Though single transducer elements operating in 1-10MHz range have been fabricated using PVDF as the active material, the array could not be constructed due to technical limitations. The design aspects and calibration of these transducer elements are described in the appendix.

6.1 HIGHLIGHTS

A theoretical model of a point source annular ring array and an annular cylindrical array have been developed in the course of this research work for inspection of underwater pipelines. An annular ring or annular cylindrical array with optimised array geometry and configuration can be effectively used for pipeline inspection with

a good focusing effect and reduced inspection time. The different parameters that are varied and optimised in the computations are the number of elements in the section, radius of array, radius of pipeline and axial distance between the array and pipeline. With electronic switching the ultrasound beam can be shifted over the complete contour of the pipeline. A good focusing effect of the annular ring and annular cylindrical arrays makes them much more efficient for flaw detection applications.

For an annular ring array of radius 6cm with element spacing $\lambda/2$, operating at 1MHz, the number of elements selectively energised in the section of the array is varied. The beam patterns for the different configurations are shown in Figures 4.4 and 4.5. The sidelobe levels and 3dB beamwidths for different configurations of an annular ring array are shown in Table 4.2. From these results the number of elements are optimised depending on the sidelobe level and 3dB beamwidth acceptable for a particular application.

The beam pattern of a 5 element section of an annular ring array operating at 5MHz is shown in Figure 4.6 for different array radius. The sidelobe levels and 3dB beamwidths corresponding to these variations are tabulated in Table 4.1. It is seen that the 3dB beamwidths and sidelobe levels remain constant when the array radius is $>40\lambda$.

The beam pattern of a 6x10 element annular cylindrical array compared with that of a 6 element annular ring array is shown in Figure 4.7. The parameters of the annular cylindrical array are varied similar to that of the annular ring array. The results from these computations are tabulated in Tables 4.3 and 4.4. The beam

characteristics are found to remain constant as in the annular ring array when the array radius is $\geq 40\lambda$.

The variation of effective acoustic pressure for different configurations of an annular ring array operating at 5MHz and array radius 3cm is shown in Figure 5.3. The effective acoustic pressure for different configurations of an annular cylindrical array are shown in figure 5.7. The number of elements can be optimised from these results.

A comparison of the effective acoustic pressure of a 21 element linear array and a 21 element annular ring array is shown in figure 5.4. It is seen that the annular ring array has a good focusing effect compared to the linear array.

The axial pressure distribution for different configurations of the annular ring array keeping the array radius fixed at 10cm is shown in Figure 5.5 and Figure 5.6 shows the axial pressure distribution for a 5 element annular ring array. The axial pressure distribution for different configurations of an annular cylindrical array are shown in figure 5.8. The array parameters and the array radius suitable for a particular dimension of the pipeline can be optimised for better performance.

The transient pressure variation for a pulse excited annular ring and annular cylindrical array are shown in Figures 5.9 and 5.10 respectively.

The overall conclusions drawn from the results obtained are as follows:

Performance evaluation of the annular ring and annular cylindrical array shows that the sidelobe levels and 3dB beamwidths remain unaffected for radii greater than 40λ . The evaluation of the effective acoustic pressures of the annular ring and annular cylindrical arrays show a very good focusing effect compared to the linear array.

The axial pressure distribution of the proposed arrays have been investigated for different array configurations from which the number of elements and array geometry can be optimised for different pipeline geometry. A good focusing effect can be obtained by optimizing the number of elements and the radius of the annular ring and annular cylindrical arrays. The transient response of the pulse excited annular ring and annular cylindrical arrays over the contours of the test pipeline have been evaluated.

Transducer elements have been fabricated using PVDF as the active, mild steel as the backing and conducting silver preparation as the bonding materials. The transducer is operated in the (3,3) mode. The design considerations and calibration of these transducers are discussed in the appendix. Though single transducer elements have been constructed successfully, arrays could not be fabricated due to technical limitations. The construction of a high frequency array is comparatively complicated. The interelement spacing between the transducer elements becomes considerably small when high frequencies are considered. It becomes very difficult to construct the transducer manually. The electrode connections to the elements can produce significant loading effect. The array has to be fabricated using hybrid construction techniques. The active material has to be deposited on a proper substrate and etching techniques are required to fabricate the array.

6.2 SCOPE FOR FURTHER WORK

Theoretical models of an annular ring array and an annular cylindrical array have been developed for inspection of underwater pipelines. Performance evaluation of these models have been carried out and the various array parameters have been optimised. With sophisticated fabrication techniques the annular ring and annular cylindrical arrays can be constructed based on the theoretical models developed and taking the effects due to the finite size of the array elements into consideration. Ultrasonic nondestructive testing techniques can be extended to biomedical fields as well. These days, focused ultrasound is also being considered in biomedical applications like hyperthermia treatment for cancer. The focused ultrasonic beam is directed to the affected part. The ultrasound treatment is comparatively less harmful than other radiations. The annular ring, annular cylindrical or other similar structural forms of arrays may also find applications in the near future in treatments where curved contours of the human body are affected.

T
1982-1983
1984

REFERENCES

- [1] J.Krautkrämer and H.Krautkrämer, "Ultrasonic testing of materials", Springer-Verlag, Berlin, 1969.
- [2] Don E.Bray and Roderic K.Stanley, "Nondestructive Evaluation", McGraw-Hill Inc., New York.
- [3] Paul E.Mix, "Introduction to Nondestructive testing", John Wiley & Sons, Inc., Canada,1987.
- [4] Ian R.Sinclair, "Sensors and Transducers", BSP professional books, London, 1988.
- [5] Donald E.Hall, "Basic Acoustics", John Wiley & Sons, Inc.,Canada, 1987.
- [6] J.A.Gallego-Juarez, "Piezoelectric ceramics and ultrasonic transducers", J.Phys.E: Sci. Instrum. 22 pp.804-816, 1989.
- [7] "Kynar piezofilm technical manual", Pennwalt Corporation.
- [8] Roy C.Preston, "Output Measurements for Medical Ultrasound", Springer-Verlag.
- [9] R.N.Thurston and Allan D.Pierce, "Ultrasonic measurement methods; Physical Acoustics XIX", Academic Press Inc., San Diego, 1990.
- [10] Rodney F.W.Coates, "Underwater Acoustic Systems", Macmillan Education Ltd.,

London, 1990.

- [11] Robert J.Urick, "Principles of Underwater Sound", McGraw-Hill Inc., New York, 1975.
- [12] R.Halmshaw, "Nondestructive Testing", Edward Arnold, London, 1987.
- [13] Gordon S.Kino, "Acoustic waves: Devices, imaging and analog signal processing", Prentice-Hall Inc., Englewood Cliffs, New Jersey, 1987.
- [14] John A. Adam, "Probing Beneath the Sea", IEEE Spectrum, pp.55-64, April 1985.
- [15] K.R. Wittington and C.D Cox, "Electronic Steering and Focusing of Ultrasonic Beams in Tube Inspection", Ultrasonics, pp20-25, Jan. 1969.
- [16] E.B.Steinberg, "Ultrasonics in Industry", Proceedings of the IEEE, Vol.53, No.10, pp.1292-1304, Oct. 1965.
- [17] G.S.Posakony, "Challenges for Electrical Engineering in Ultrasonic Nondestructive Testing", IEEE Trans. Sonics Ultrason., Vol. SU-21, No.4, pp.305-315, Oct. 1974.
- [18] Emmanuel P.Papadakis, "Future Growth of Nondestructive Evaluation", IEEE Trans. Sonics Ultrason., Vol. SU-23, No.5, pp.284-287, Sep. 1976.
- [19] Michael J.Buckley, "The Future Economic Role of NDE", IEEE Trans. Sonics Ultrason., Vol. SU-23, NO.5, pp.287-291, Sep. 1976.
- [20] Alan A.Winder, "Sonar System Technology", IEEE Trans. Sonics Ultrason., Vol. SU-22, No.5, pp.291-335, Sep. 1975.
- [21] Charles H.Sherman, "Underwater Sound - A Review", IEEE Trans. Sonics Ultrason., Vol. SU-22, No.5, pp.281-290, Sep. 1975.
- [22] W.J.Toulis, "Electromechanical Coupling and Composite Transducers", J.Acoust.Soc.Am., Vol.35, No.1, pp.74-80, Jan. 1963.

- [23] Gordon E.Martin, "Vibrations of Longitudinally Polarised Ferroelectric Cylindrical Tubes", J.Acoust.Soc.Am., Vol.35, No.4, pp.510-520, Apr. 1963.
- [24] Harry B.Miller, "Origin of Mechanical Bias for Transducers", pp.1455.
- [25] Le N.Bui, Herbert J. Shaw, and Louis T. Zitelli, "Study of Acoustic Wave Resonance in Piezoelectric PVF₂ Film", IEEE Trans. Sonics Ultrason., Vol. SU-24, No. 5, Sep.
- [26] Lewis F.Brown and David L. Carson, "Ultrasound Transducer Models for Piezoelectric Polymer Films", IEEE Trans. Ultrason. Ferroelec. Freq. Control, Vol.36, No.3, pp.313-318, May 1989.
- [27] Hildegard Minchenco, "High-Power Piezoelectric Transducer Design", IEEE Trans. Sonics Ultrason., Vol. SU-16, No.3, pp. , Jul. 1969.
- [28] George Kossoff, "The Effects of Backing and Matching on the Performance of Piezoelectric Ceramic Transducers", IEEE Trans. Sonics Ultrason., Vol. SU-13, No.1, pp.20-30, Mar. 1966.
- [29] Erhard K.Sittig, "Transmission Parameters of Thickness-Driven Piezoelectric Transducers Arranged in Multilayer Configurations", IEEE Trans. Sonics Ultrason. , Vol. SU-14, No.4, pp.167-174, Oct. 1967.
- [30] Erhaer K.Sittig, "Effects of Bonding and Electrode Layers on the Transmission Parameters of Piezoelectric Transducers Used in Ultrasonic Delay Lines", IEEE Trans. Sonics Ultrason., Vol. SU-16, No.1, pp.2-10, Jan. 1969.
- [31] E.A.Neppiras, "The pre-stressed piezoelectric sandwich transducer", Ultrasonics International 1973 Conference Proceedings, pp.295-301.
- [32] R.Dominguez and C.Ranz, "Sandwich Transducer, Simplified Mathematical Model (I)", Acustica, Vol.29, pp.156-161, 1973.
- [33] R.Dominguez and C.Ranz, "Sandwich Transducer, Simplified Mathematical

- Model (II)", *Acustica*, Vol.29, pp.161-167, 1973.
- [34] Jeffrey H.Goll and Bertram A.Auld, "Multilayer Impedance Matching Schemes for Broadbanding of Water Loaded Piezoelectric Transducers and High Q Electric Resonators", *IEEE Trans. Sonics Ultrason.*, Vol. SU-22, No.1, pp.52-53, Jan. 1975.
- [35] Rubens A.Sigelmann and Arvind Caprihan, "Design method for ultrasound transducers using experimental data and computers", *J.Acoust.Soc.Am.*, Vol.62, No.6, pp.1491-1501, December 1977.
- [36] K.L.Narayana, K.M.Swamy and R.S.Rohella, "Sandwich Transducer Design and its Testing", *J. Instn. Electronics & Telecom. Engrs*, Vol. 24, No. 6, pp. 260-262, 1978
- [37] Charles S. Desilets, John D. Fraser and Gordon S. Kino, "The Design of Efficient Broad-Band Piezoelectric Transducers", *IEEE Trans. Sonics Ultrason.* SU-25, No.3, pp. 115-125, May 1978.
- [38] Jeffery H Goll, "The Design of Broad-Band Fluid-Loaded Ultrasonic Transducers", *IEEE Trans. Sonics Ultrason.*, Vol.SU-26, No.6, pp.385-393, Nov. 1979.
- [39] A.J.Hayman and J.P.Weight, "Transmission and Reception of Short Ultrasonic Pulses by Circular and Square Transducers", *J.Acoust.Soc.Am.*, Vol.66, No.4, pp. 945-951, Oct. 1979.
- [40] W.M.R. Smith and A.O. Awojobi, "Factors in the Design of Ultrasonic Probes", *Ultrasonics*, pp. 21-26, Jan. 1979.
- [41] Jacques Souquet, Philippe Defranould and Jeans Desbois, "Design of Low-Loss Wide-Band Ultrasonic Transducers for Noninvasive Medical Application", *IEEE Trans. Sonics Ultrason.* SU-26, No. 2, pp. 75-81, March 1979. *IEEE Trans.*

- Sonics Ultrason., Vol.SU-26, No.6, pp.385-393, Nov. 1979.
- [42] P TH A Klaase, "Low-Frequency and Ultrasonic Applications of Piezoelectric PVDF-Films", *Ferroelectrics*, Vol.60, pp.215-225, 1984.
- [43] Ralph S.Woollett, "Power Limitations of Sonic Transducers", *IEEE Trans. Sonics Ultrason.*, Vol. SU-15, No.4, pp.218-230, Oct. 1968.
- [44] Franklin D.Martin and M.A.Breazeale, "Simple Way to Eliminate Diffraction Lobes Emitted by Ultrasonic Transducers", *J.Acoust.Soc.Am.*, Vol.49, No.5, Aug. 1970.
- [45] A.P.Hulst, "On a family of high power transducers", *Ultrasonics International 1973 Conference Proceedings*, pp.283-293.
- [46] G.Du and J.Wu, "A Design of Ultrasonic Transducers with Curved Back-Electrodes", *IEEE Ultrasonic Symposium*, pp.709-711, 1989.
- [47] C.T.Mollow, "Calculation of Directivity Index for Various Types of Radiators", *J.Acoust.Soc.Am.*, Vol.20, No.4, pp.387- 1948.
- [48] W.James Trott, "A Portable Hydrophone Calibrator", *J.Acoust.Soc.Am.*, Vol.49, No.3, pp.850-855, Jul. 1971.
- [49] Peter A. Lewin, "Miniature Piezoelectric Polymer Hydrophones in Biomedical Ultrasonics", *Ferroelectrics*, Vol.60, pp.127-139, 1984.
- [50] V.N. Bindal, T.K.Saxena and S.K. Singhal, "A Simple Method for the Designing of a Half-Wave Resonator-Transducer Assembly", *Indian Journal of Pure & Applied Physics*, Vol.22, pp.642-646, Nov. 1984.
- [51] S.Leeman, E.T.Costa and A.J.Healy, "Large Aperture Hydrophones for Field Characterisation", *IEEE Ultrasonics Symposium*, pp.679-681, 1991.
- [52] P.J 't Hoen, "Aperture Apodization to Reduce the Off-axis Intensity of the Pulsed-mode Directivity Function of Linear Arrays", *Ultrasonics*, pp.231-236,

Sep. 1982.

- [53] H.Kawai, "The Piezoelectricity of Polyvinylidene Fluoride", Japan. J.Appl.Physics. 8, pp.975-976, 1969.
- [54] J.H.McFee, J.G.Bergman,Jr and G.R.Crane, "Pyroelectric and nonlinear optical properties of poled polyvinylidene fluoride films", IEEE Trans. Sonics Ultrason. SU-19, pp.305-313, 1972.
- [55] H.R Gallantree, "PVDF Membrane Hydrophones - An Ultrasonic Characterisation tool", Materials Applications and Devices Lab., Marconi Research Centre, Essex, UK, PP.1-10, April 1987.
- [56] J. Inderherbergh, "Polyvinylidene Fluoride (PVDF) Appearance, General Properties and Processing", Ferroelectrics, Vol.115, pp.295-302, 1991.
- [57] S.Edelman, L.R.Grisham, S.C.Roth and J.Cohen, "Improved Piezoelectric Effects in Polymers", J.Acoust.Soc.Am., Vol.48, No.5, pp.1040-1043, Jun. 1970.
- [58] B.Woodward, "The Suitability of Polyvinylidene Fluoride as an Underwater Transducer Material", Acustica, Vol.38, pp.265-268, 1977.
- [59] A.N Hadjicostis, C.F.Hottinger, J.J.Rosen and P.N.T. Wells, "Ultrasonic Transducer Materials for Medical Applications", Ferroelectrics, Vol.60, pp.107-126, 1984.
- [60] P.Dario, D.De Rossi, R.Bedini, R.Francesconi and M.G.Trivella, "PVF₂ Catheter-tip Transducers for Pressure, Sound and Flow Measurements", Ferroelectrics, Vol.60, pp. 149-162, 1984.
- [61] Kuniko Kimura, Nobuo Hashimoto and Hiroji Ohigashi, "Performance of a Linear Array Transducer of Vinylidene Fluoride Trifluoroethylene Copolymer", IEEE Trans. Ultrason. Ferroelec. Freq. Control, Vol.SU-32, No.4 pp.566-573, July 1985.

- [62] A.A. Schoenberg, D.M.Sullivan, C.D.Baker, H.E.Booth and C.Galway, "Ultrasonic PVF₂ Transducers for Sensing Tactile Force", *Ferroelectrics*, Vol.60, pp. 239-250, 1984.
- [63] Masahiko Tamura, Tadahiro Yamaguchi, Takashi Oyaba and Toshikazu Yoshimi, "Electroacoustic Transducers with Piezoelectric High Polymer Films", *Audio Engineering Society Journal*, vol.23, pp.21-26, 1975.
- [64] N.Chubachi and T.Sonnomiya, "Composite Resonator Using PVF₂ Film and Its Application to Concave Transducer for Focusing Radiation of VHF Ultrasonic Waves", *Ultrasonic Symposium Proceedings*, pp. 119-123, 1977.
- [65] N.Murayama, K.Nakamura, H.Obara and M.Segawa, "The strong piezoelectricity in polyvinylidene fluoride (PVDF)", *Ultrasonics*, pp.15-23, January 1976.
- [66] N.C Sasady, A. Hartig and L. Bjorno, "Development of Some Transducers Based on Polyvinylidene Fluoride", *Ultrasonics*, pp. 468-475, 1979.
- [67] T.D.Sullivan and J.M.Powers, "Piezoelectric polymer flexural disk hydrophone", *J.Acoust.Soc.Am.*, Vol.63, No.5, pp.1396-1401, 1978.
- [68] Reinhard Lerch, "Acoustic Transducers Using Piezoelectric Polyvinylidene fluoride Films", *J.Acoust.Soc.Am.*, vol. 66, No. 4, pp. 952-954, Oct. 1979.
- [69] R. Lerch and G.M.Sessler, "Microphones with Rigidly Supported Piezopolymer Membranes", *J.Acoust.Soc.Am.*, Vol.67, No.4, pp.1379-1381, April 1980.
- [70] Theodore A. Henriquez, "Application of Tubular PVDF to Shock Resistant hydrophones", *Ferroelectrics*, Vol.50, pp.39-44, 1983.
- [71] A.S.DeReggi, S.C.Roth, J.M.Kenney and S.Edelman,"Piezoelectric Polymer Probe for Ultrasonic Applications", *J.Acoust.Soc.Am.*, Vol.69, No.3, pp.853-859, March 1981.
- [72] R.Lerch "Piezopolymer Transducers with Point-supported Membranes", *J.*

- Acoust. Soc. Am., Vol.70, No.5, pp.1229-1235, Nov. 1981.
- [73] Norman F.Foster, "Piezoelectricity in Thin Film Materials", J.Acoust.Soc.Am., Vol. 70, No.6, pp.1609-1614, Dec. 1981.
- [74] Michael A. Marcus, "Ferroelectric Polymers and Their Applications", J.Acoust.Soc.Am., Vol.69, No.3, pp.846-859, March 1981.
- [75] Gerald.R.Haris, "Sensitivity Considerations for PVDF Hydrophones Using the Spot-Poled Membrane Design", IEEE Trans. Sonics Ultrason., Vol.SU-29, No.6, pp.370-377, Nov. 1982.
- [76] Sidney Lees, Robert S.Gilmore, and Paul R.Kranz, "Acoustic Properties of Tungsten-Vinyl Composites", IEEE Trans. Sonics Ultrason., Vol. SU-20, No.1, pp.1-2, Jan. 1973.
- [77] J.Hossack, Y.Gorfu and G.Hayward, "The Modelling and Design of Composite Piezoelectric Arrays", IEEE Ultrasonics Symposium, pp.793-796, 1989.
- [78] H.J.McSkimin, "Transducer Design for Ultrasonic Delay Lines", J.Acoust.Soc.Am., Vol.27, No.2, pp.302-309, Mar. 1955.
- [79] Morio Onoe, "Theory of Ultrasonic Delay Lines for Direct-Current Pulse Transmission", J.Acoust.Soc.Am., Vol.34, No.9, pp.1247-1253, Sep. 1962.
- [80] Goodman J.W, "Foundations of Scalar Diffraction Theory", Introduction to Fourier Optics, McGraw Hill New York, pp. 30-75, 1969.
- [81] A.R.Selfridge, G.S.Kino and Khuri-Yakub, "A Theory for the Radiation Pattern of a Narrow-strip Acoustic Transducer", Appl.Phy.Lett., Vol.37, No.1, pp.35-36, Jul. 1980.
- [82] H.T.O'Neil, "Theory of Focusing Radiators", J.Acoust.Soc.Am., Vol.21, No.5, pp. 516-526, 1949.
- [83] Peter R.Stepanishen, "Transient Radiations from Pistons in an Infinite Planar

- Baffle", *J.Acoust.Soc.Am.*, Vol.49, No.5(part 2), pp.1629-1638, 1971.
- [84] P.R.Stepanishen, "An Approach to Computing Time-Dependent Interaction Forces and Mutual Radiation Impedances between Pistons in a Rigid Planar Baffle", *J.Acoust.Soc.Am.*, Vol.49, No.1 (part 2), pp.283-292, 1971.
- [85] J.C.Lockwood and J.G.Willette, "High-speed method for computing the exact solution for the pressure variations in the near field of a baffled piston", *J.Acoust.Soc.Am.*, Vol.53, No.3, pp.735-741, 1973.
- [86] A.Penttinen and M.Luukkala, "The impulse response and pressure nearfield of a curved ultrasonic radiator", *J.Phys.D:Appl.Phys.*, Vol.9, pp.1547-1557, 1976.
- [87] John W.Hunt, Marcel Arditi and F Stuart Foster, "Ultrasound Transducers for Pulse-Echo Medical Imaging", *IEEE Trans. on Biomedical Engg.* Vol. Bme-30, No. 8, pp. 453-481, Aug. 1983.
- [88] Lin Xin Yao, James A. Zagzebski and Evan J. Boote, "A Fast algorithm to Calculate Ultrasound Pressure Fields from Single Element Transducers", *IEEE Trans. Ultrason. Ferroelec. Freq. Control*, Vol. 36, No.4, pp. 446-451, July 1989.
- [89] Kenneth B.Ocheltree and Leon A.Frezzell, "Sound Field Calculation for Rectangular Sources", *IEEE Trans. Ultrason. Ferroelec. Freq. Control*, Vol. 36, No.2, pp. 242-248, March 1989.
- [90] Hong Zhang Wang, Yun He and Yi Hong Yang, "Ultrasound Characteristic of Focused Axisymmetrically Curved Surface Transducers", *IEEE Trans. Ultrason. Ferroelec. Freq. Control*, Vol. 36, No.1, pp.63-72,Jan. 1989.
- [91] Jorgen Arendt Jensen and Niels Bruun Svendsen, "Calculation of Pressure Fields from Arbitrarily Shaped, Apodized, and Excited Ultrasound Transducers",*IEEE Trans. Ultrason. Ferroelec. Freq. Control*, Vol.39, No.2, pp.262-267, March 1992.

- [92] Young J.Yoon and Paul J.Benkese, "Sound Field Calculations for an Ultrasonic Linear Phased Array with a Spherical Liquid Lens", IEEE Trans. Ultrason. Ferroelec. Freq. Control, Vol.39, No.2, pp.268-278, March 1992.
- [93] G.Kossoff, "The measurement of peak acoustic intensity generated by pulsed ultrasonic equipment", Ultrasonics, pp.249-251, 1969.
- [94] F.S.Foster and J.W.Hunt, "The design and characterisation of short pulse ultrasound transducers", Ultrasonics, pp.116-122. May 1978.
- [95] Gerald R Haris, Edward E.Carome and Henry D.Dardy, "An Analysis of Pulsed Ultrasonic Fields as measured by PVDF Spot-Poled Membrane Hydrophones", IEEE Trans. Sonics Ultrason., Vol. SU-30, No.5, pp.295-303, Sep. 1983.
- [96] D.A. Hutchins, H.D.Mair and R.G. Taylor, "Transient Pressure Fields of PVDF Transducers", J.Acoust.Soc.Am., Vol.82, No.1, pp.183-192, July 1987.
- [97] M.R. Smith and A.k.Dunhill, "The Design and Performance of PVDF Transducers", IEEE Ultrasonic Symposium, pp.675-679, 1987.
- [98] Peter R.Stepanishen, "Pulsed Transmit/Receive Response of Ultrasonic Piezoelectric Transducers", J.Acoust.Soc.Am., Vol.69, No.6, pp.1815-1827, June 1981.
- [99] M.Redwood, "Transient Performance of a Piezoelectric Transducer", J.Acoust.Soc.Am., Vol.33, No.4, pp.527-536, Apr. 1961.
- [100] A.F.Brown and J.P.Weight, "Generation and reception of wideband ultrasound", Ultrasonics, pp.161-167, July 1974.
- [101] L.Bui,H.J.Shaw and L.T.Zitelli, "Experimental broadband ultrasonic transducers using PVDF piezoelectric film", Electronics Letters, Vol.12, No.16, pp.393-394, 5th August 1976.
- [102] K.C.Shotton, D.R.Bacon and R.M.Quilliam, "A PVDF Membrane Hydrophone for

- Operation in the Range 0.5 MHz to 15 MHz", *Ultrasonics*, pp.123-126, May 1980.
- [103] David R.Bacon, "Characteristics of a PVDF Membrane Hydrophone for Use in the Range 1-100 MHz", *IEEE Trans. Sonics Ultrason.*, Vol. SU-29, No.1, pp.18-25, Jan. 1982.
- [104] Velayutham Rajendran, Mitsuru Yamamoto, Ken-ya Hashimoto and Masatsune Yamaguchi, "Ultrasonic Transducer Employing ZnO-Film/Al-Foil Composite Structure and Their Application to Acoustic Microscopes", *Trans. IEEE of Japan*, Vol.111-C, No.9, pp.433-438, Sep. 1991.
- [105] Robert G. Swartz and James D. Plummer, "On the Generation of High-Frequency Acoustic Energy with Polyvinylidene Fluoride", *IEEE Trans. Sonics Ultrason.* SU-27, No.6, pp. 295-302, Nov. 1980.
- [106] R.Bruce Thompson and Donald O.Thompson, "Ultrasonics In Nondestructive Evaluation", *Proceedings of IEEE*, Vol.73, No.12, pp. 1716-1754, Dec. 1985.
- [107] M.Onozawa, A. Katamine, Y. Ishii and G Ohira, "Ultrasonic Testing for Near Surface Flaws in Castings", *British Journal of NDT*, Vol. 31, No.11, pp.611-616, Nov. 1989.
- [108] M.A.Garcia-Olias and F.R.Montero de Espinosa, "Non-Destructive Testing Transducer for High Temperature Applications", *Ultrasonics*, Vol.28, pp.50-51, Jan. 1990.
- [109] Richard M.White , C.T.Chuang and Adrian C.C.Lee, "Bulk Ultrasonic Transducer Employing Piezoelectric Film on Thin Metal Sheet", *IEEE Trans. Sonics Ultrason.*, Vol. SU-28, No.1, pp.9-13, Jan. 1981.
- [110] Martin Greenspan and Raymond M.Wilmotte, "Distributed Transducer", *J.Acoust.Soc.Am.*, Vol.30, No.6, pp.528-532, Jun. 1958.

- [111] James D.Plummer, Robert G.Swartz, Jacques R.Beaudouin and James D.Meindl, "Two-Dimensional Transmit/Receive Ceramic Piezoelectric Arrays: Construction and Performance", IEEE Trans. Sonics Ultrason. Vol.SU-25, No.5, pp.273-280, 1978.
- [112] Wei-Ming Wang, "Radiation Patterns of Acoustic Transducer elements in an Infinite Array", IEEE Trans. Sonics Ultrason. Vol.SU-19, No.1, pp.31-33, January 1972.
- [113] A. McNab and M.J. Campbell, "Ultrasonic Phased Arrays for Nondestructive Testing", NDT International, Vol.20, No.6, pp.333-337, Dec. 1987.
- [114] A.Cochran, D.Reilly, G.Hayward and A.McNab, "Beam Forming in Solids Using Monolithic Ultrasonic Arrays", IEEE Ultrasonic Symposium, pp.695-698, 1989.
- [115] D.McGhee and J.S.Jaffe, "A Spatially Shaded PVDF Acoustic Transducer", IEEE Ultrasonics Symposium, pp. 589-592, 1992.
- [116] H.P. Schwarz, "Development of a Divided Ring Array for Three-Dimensional Beam Steering in Ultrasonic Nondestructive Testing", IEEE Ultrasonics Symposium, pp.859-861, 1987.
- [117] S.Shibata, T.Koda and J.Yamaga, "C-mode ultrasonic imaging by an electronically scanned coaxial circular spherical receiving array", Ultrasonics, pp. 65-68, March 1978.
- [118] J.P.Huissoon and D.Moziar, "Simulation and Design of Curved Array Transducers for Airborne Sonar", IEEE Ultrasonic Symposium, pp.691-694, 1989.
- [119] J.T. Yitalo, T. Hanhineva, P.Kekkonen and Z.D. Qin, "A 1 MHz Multielement Curved Transducer for Transskull Imaging", IEEE Ultrasonics Symposium, pp.687-690, 1991.

- [120] Emad S. Ebbini and Charles A. Cain, "Experimental Evaluation of a Prototype Cylindrical Section Ultrasound Hyperthermia Phased-Array Applicator", IEEE Trans. Ultrason. Ferroelec. Freq. Control, Vol.38, No.5, pp.510-531, Sep. 1991.
- [121] H.Wang, E.Ebbini, M.O'Donnell, R.Seip and C.Cain, "Adaptive 2-D Cylindrical section Phased Array System for Ultrasonic Hyperthermia", IEEE Ultrasonics Symposium, pp.1261-1264, 1992.
- [122] S.D.Bennet and J.Chambers, "Novel Variable-Focus Ultrasonic Transducer", Electronic Letters, Vol.13, No.4, pp.110-111, Feb. 1977.
- [123] Gordon S. Kino, "Acoustic Imaging for Nondestructive Evaluation", Proceedings of IEEE, Vol. 67, No.4, pp. 510-525, April 1979.
- [124] Olaf T.Von Ramm and Stephen W. Smith, "Beam Steering with Linear Arrays", IEEE Trans. on Biomedical Engg., Vol. BME-30, No.8, pp.438-452, Aug. 1983.
- [125] Daniel H. Turnbull and F. Stuart Foster, "Theoretical Steered Beam Profiles from a Two-Dimensional Transducer Array", IEEE Ultrasonic Symposium, pp.699-704, 1989.
- [126] H.P Schwarz, H.J. Welsch, P.Becker, M.Biebinger and R.M.Schmitt, "Development of a new Ultrasonic Circular Array for Endoscopic Application in Medicine and NDT", IEEE Ultrasonic Symposium, pp.687-690, 1989.
- [127] J.Adach and R.C Chivers, "A Detailed Investigation of Effective Geometrical Parameters for Weakly Focused Ultrasonic Transducers. Part I: Optimization of Experimental Procedures", Acustica, Vol.70, pp.12-22, 1990.
- [128] S.Hurmila, H.Stubb, J.Pitkanen, K.Lahdenpera, A.Penttinen, V.Suorsa and A.Tauriainen, "Ultrasonic Transducers Using PVDF", Ferroelectrics, Vol.115, pp. 267-278, 1991.
- [129] Zheng Di Qin, Juha Ylitalo, Juhani Oksman and Weixue Lu, "Circular Array

- Ultrasound Holography Imaging Using the Linear Array Approach", IEEE Trans. Ultrason. Ferroelec. Freq. Control, Vol.36, No.5, pp.485-493, Sep. 1989.
- [130] B.G.Kim, J.O.Lee and S.Lee, "Development of Surface Point-Focusing Ultrasonic Transducer Using PVDF", IEEE Ultrasonics Symposium, pp. 609-612, 1989.
- [131] Emad S. Ebbini and Charles A. Cain, "Multiple-Focus Ultrasound Phased-Array Pattern Synthesis: Optimal Driving Signal Distributions for Hyperthermia", IEEE Trans. Ultrason. Ferroelec. Freq. Control, Vol. 36, No.5, pp. 540-548, Sep. 1989.
- [132] Mohammed S. Ibbini, Emad S. Ebbini and Charles A. Cain, "N X N Square-Element Ultrasound Phased Array Applicator: Simulated Temperature Distributions Associated With Directly Synthesized Heating Patterns", IEEE Trans. Ultrason. Ferroelec. Freq. Control, Vol.37, No.6, pp.491-500, Nov. 1990.
- [133] R.Reibold and R.Kazys, "Radiation of a Rectangular Strip-like Focusing Transducer:Part 1:Harmonic Excitation", Ultrasonics, Vol.30, No.1, pp.49-55, 1992.
- [134] R.Reibold and R.Kazys, "Radiation of a Rectangular Strip-like Focusing Transducer: Part 2: Transient Excitation", Ultrasonics, Vol.30, No.1, pp.56-59, 1992.
- [135] Danniell H. Turnbull and Stuart Foster, "Beam Steering with Pulsed Two-Dimensional Transducer Arrays", IEEE Trans. Ultrason. Ferroelec. Freq. Control, Vol.38, No.4, pp.320-333, July 1991.
- [136] V.R.Singh and Sanjay Yadav, "A Multi-Frequency Multi-Focal Length Ultrasonic Therapy Transducer", IETE Technical Review Vol.9 No.2 pp.121-127, March-April 1992.
- [137] Jerry L. Sutton, "Underwater acoustic imaging", Proceedings of IEEE, Vol.67,

No.4, pp.554-566, April 1979.

- [138] Albert Macovski, "Ultrasonic Imaging Using Arrays", Proceedings of the IEEE, Vol. 67, No. 4, pp. 484-495, April 1979.
- [139] P.H.Brown, "Ultrasonic Imaging with an Electron Beam Scanned PVDF Sensor", Ferroelectrics, Vol.60, pp.251-261, 1984.
- [140] S.W Smith, G.E.Trahey and O.T. von Ramm, "Two Dimensional Arrays for Medical Ultrasound", IEEE Ultrasonic Symposium, pp.625-628, 1991.
- [141] Mathew O'Donnell, "A Proposed Annular Array Imaging System for Contact B-scan Applications", IEEE Trans. Sonics Ultrason., Vol. SU-29. No.6, pp.331-339, Nov 1982.
- [142] Leon Camp, "Underwater Acoustics", Wiley-Interscience, New York, 1970.

INDEX

(3,3) mode	10	Biomedical	9
Aberration	18	Bock,	2
absorption	1, 23, 26	Bonding	15
Absorption.	1	Boundaries	21
Accurate	8	Boundaries.	21
ACEC	2	Bradfield	3
Acoustic emissions	1	Breakthrough	11
acoustic pressure	5, 6, 9, 20, 30, 75-77, 84, 87, 90, 97	Brightness scan	27
active material	5, 14, 95, 99	Broad band	12
Adach	18	Brown	16, 19
alignment	7	Buckley	11
amplitude	2, 3, 7, 26-28, 30, 76	Bui	12, 16
Angle beam	6	calibration	10, 12, 13, 95, 98, 103, 104, 106
Angle probes	7	Characterisation	1
annular array	19, 128, 71	Characterisation,	1
Aperture	13	Charloi,	2
Apodization	13	Chilowski	3
APPENDIX	100	Chubachi	14
Araldite	101	Cleaning	2
array gain	6, 9, 20, 27, 31, 34	Cochran	17
Attenuated	1	communication	5, 11
Attenuation	1	Comparison method	103
axis	4, 6, 13, 15, 16, 18, 30, 89, 90, 118	Compliance.	5
Backing	12, 23	composites	4, 5, 15, 23, 120
Bacons	17	Composites.	4
Barium titanate	4	Compressional wave	21
barrier	7	Computation	9
Bats	3	Concentrate	28
Beam angle	29	concentric	9, 31, 71, 95
Beam divergence	6	Conducting cement	100
beam pattern	6, 9, 18, 20, 28, 30, 31, 34-36, 71-73, 96	configuration	12, 31, 32, 96
Beamsread,	20	Conical transducer	18
Beamsteering	6	Consistent	7
Belgium	2	contour	8, 9, 32, 75, 77, 91, 96, 9
Bennett	18	Convolution	16
Berthold	2	Copolymer,	14
Bindal	13	coupling	7, 8, 12, 14, 19, 23, 26, 115
		Cox	8
		crack	2

Creeping waves	21	field	1, 2, 4-6, 8, 9, 11, 13-16,
crosscorrelation	27, 28, 32-34		18, 20, 29, 30, 76, 79, 87-91, 94, 100,
Cunningham	2		118, 121, 122
Cylindrical	6	Firestone	3
Czerlinsky,	2	flaw	3, 5-8, 25-27, 96, 100, 101, 7
Damp	23	Flexibility	14
Dario	14	Flexural	12, 14
decibel	5	focusing	3, 5, 9, 16, 18, 19, 76, 84,
Density,	1, 2		96-98, 114, 119, 121, 126, 127, 5
design	5, 9-17, 19, 20, 23, 28, 95, 98,	Formulation	9
	100, 106, 115, 116, 117, 120, 122,	Foster	15, 16
	123, 125	fourier transform	9, 15, 16, 76
Desilets	13	Frequency response	2
detection	1, 2, 5-8, 11, 15, 18, 21,	Gallantree	14
	25-27, 29, 31, 76, 96, 100, 21	Gallego	12
Diaphragm	14	Garcia	17
Dielectric	12	Gaussian	13
diffraction	1, 5, 7, 13, 15, 117, 121	Goll	13
Dipole	4	Goodman	15
directivity	5, 6, 13, 17, 26, 29, 30,	Götz	2
	117, 118	Grating lobes	32
Directivity index	6	Greanleaf	4
discontinuity	2	Green's function	15
Disks	13	Greenspan	17
display	8, 9, 26, 101	Greguss,	3
Dominiques	12	Griffin.	3
Donald	3	Hadjicostis	14
Drilling	2	Harris	15, 16
Du	13	Hatfield	2
Dussik	3	Hayman	13
Ebbini	18	Head wave	13
echo	2, 3, 6, 7, 16, 25-27, 101, 121	Head waves	21
Echograms	14	Henriquez	15
Edelman	14	Heppenheim,	2
effective acoustic pressure	9, 20, 30,	Hoer	13
	75-77, 84, 87, 90, 97	Hossack	15
Elastic properties	1	Housing	24
Electroacoustic	14	Huissan	18
Electrode	12	Hulst	13
Electrodes	4	Hunt	15, 16
Electromagnetic waves	1	Hurmila	18
Electromechanical	12, 15	Hutchins	16
Emulsifying	2	hydrophone	5, 13, 14, 16, 17,
estimation	1, 8, 11, 1		117, 119, 123
evaluated	9, 15, 18, 75, 84, 91, 98	Hyperthermia	4, 18
Excitation	5	Ibbini	18
fabrication	5, 9, 11, 17, 19, 31, 95,	Icebergs	3
	99, 106, 5	Illuminated	28
Facilitated	3	imaging	2-5, 17-19, 27,

	114, 121, 125-128	Logarithmic	5
Impedance	4	longitudinal waves	3, 20, 22, 20
impenetrable	7	Longitudinal,	1
Implantable	18	Lord Rayleigh	3
impulse response	9, 13, 15, 76, 87-90, 121	Love waves	21
Inderherbergh	14	Macrosonic	13
Indispensable	11	Main lobe	6
Infrasound.	20	Maintenance	11
inspection	1, 8, 9, 11, 20, 31, 32, 75, 94-96, 99, 106, 114, 20	Manipulator arms	8
Instrument	2	Manipulator devices	4
intensity	2, 5, 7, 13, 16, 25, 27, 118, 122	Marcus	15
Interaction	15	Martin	12, 13
Interelement	28	Masahiko Tamura	14
interface	7, 9, 20-22	Mason,	2
Interface,	20	Matching	12
interference	1	Materials	1
Interferometry.	3	Mc Skimin	2, 15
Intracardiac	14	McFee	14
Introduction	1	McGehee	17
Jacques	3	McLean	3
James Troff	13	McNab	17
Jensen	16	Measurement	103
Kaiser	2	Mechanical	1
Kawai	14	Medical diagnostics	1
Kim	18	Membrane hydrophones	14
Kimura	14	Methodology	20
Kino	18	Meyer,	2
Klaase	13	Mezrich	3
Korpel	4	Microphone	4
Kossoff	12, 16	Microphones	14
Kruse,	2	Micropositioners	4
Langevin	3	Microstructure,	1
Lateral waves	21	Minchenko	12
Lead Niobate	4	Mine hunting	5
Leaky waves	21	Mode conversion	20
Leeman	13	Models	3
Lehfeldt	2	Mollow	13
Lerch	14, 15	Morio Onoe	15
Lewin	13	Mounted	100
LiNbO3	14	Mueller,	3
Linear array	13	Mühlhäuser	2
Lithium sulphate	4	Multielement	5, 12
Lithotripsy	2	Murayama	14
localisation	8, 11	Narayana	13
Location	3	NDT	1, 4, 6, 8, 17, 18, 95, 124, 126
Lockwood	15	Neal	3
		near field	5, 8, 16, 121
		Neppiras	12
		noise	5, 6, 15, 27, 28, 32, 33

Nondestructive testing	1	probes	3, 6-9, 13, 15, 20, 24, 31, 117
Nondirectional	6	Production,	11
Normal probe	24	projector	6, 28, 30, 28
O'Neil	15	Projectors.	4
O'Donell	19	propagation	3, 20, 21, 27
obstacle	7	Prospects	11
Ocheltree	16	Proximity	2
Ogura	2	pulse echo	2, 3, 6, 7, 16, 25, 26
Onozawa	17	Pulse shape	1
Optimum	2	Pulse size	1
Orientate	3	pulse width	2, 91
orientation	7, 31, 32	PVDF	4, 5, 10, 12-19, 95, 98, 100, 106, 117-120, 122, 123, 125-127
Oscillations	3	Pyroelectric	14
Osteogenesis	4	Qin	18
P waves	21	Quality control	11
P(VDF-TrFE)	12	Quartz	2
Papadakis	11	Quate	2, 4
Parameters	6	Radiation pattern	28
path	7, 8, 21, 25, 34, 35, 78, 85	Radiation source	1
Penetrate.	1	Radiography	1
Penttinen	15	Radiography,	1
Performance	12, 15	Rajendra	17
Perspex	19	Rayleigh waves	18, 21
Phase	2	Realisation	3
Phase reversal	28	Receivers.	3
Phase-measuring	2	Receiving sensitivity	106
Phased array	3	Reciprocity	13
Pierce	3	Reciprocity method	103
Pierre	3	Redwood	16
piezoceramics	3, 23	Reflected	2
Piezoelectric effect	3	reflection	1, 2, 7, 14, 19, 20, 23
piezopolymers	3, 4, 23	Reibold	18
pipeline	8, 9, 31, 32, 71, 75-77, 79, 84, 91, 94-98	Reliable,	8
Plane waves	20	Relief method	2
Plate waves	21	Reproducibility,	11
Plummer	17	Resins	23
Pohlman cell	2	resolution	6, 14, 16, 18, 19, 18
Point source	8	resonance	2, 6, 7, 25, 26, 115
Polarised	21	Response	28
Poling	14	ring array	6, 8, 9, 17, 31-35, 69-73, 76, 77, 84, 89-91, 95-97, 99, 125
Polymer films	14	Rod waves	21
Porosity,	1	Rubens	12
Portable	13	Ruggedness.	14
Posakony	11	SAFT-UT	3
power	1, 12, 13, 17, 26, 115, 117	Sandwich	12
Powers	14	Sasady	14
pressure field	9, 16, 30, 88	scanning	2, 3, 17
Prestressed	13		

Scattered	2	Stretching	15
scattering	1, 26, 32, 1	structures	8, 12, 15, 27
Schallsichtgerät	2	Submarines	3
Schlieren method	3	Suckling	3
Schoenberg	14	Sullivan	14
Schotton	16	superdirectivity	6, 28
Schwarz	17, 18	Surface characteristics	1
Seismic	20	Surface waves	1, 15
Selfridge	15	Surgery	2
sensitivity	3, 5, 6, 14, 15, 28, 103, 104, 106, 120	Sutton	19
sensor	2, 8, 14, 19, 127	Swartz	17
shading	6, 17, 28, 29	Switching	32
shadow	2, 7, 25, 26	Tactile sensors	4
Shaping	5	target	5, 6, 29, 101
Shear	1	Target detection	29
Sheridan	3	Techniques	1
Sherman	11	Testing	1
Shibata	17	Therapy.	2
Shockley	2	Thickness	2
Shraiber	2	Thompson	17
sidelobe	6, 9, 29, 31, 69-71, 73, 74, 96, 98	through transmission	6, 7, 25
Sidney Lees	15	Thurstone	3
signal	2, 5-7, 15, 26-28, 32, 33, 90, 91, 101-104, 114, 126	tomography	4
Singh	19	Toulis	12
Sinusoidal	5	transducer	2, 4-20, 23-27, 31, 32, 34, 88, 95, 98-104, 106, 115, 116, 118-121, 123-127
Sittig	12	Transduction	11
Smith	13, 19	Transform	2
Sokolov	2	transient	9, 15, 16, 90, 91, 97, 98, 121-123, 127
Soldering	2	Transient pressure	91
Sonar	6	Transit time	3
Sonomicroscope	2	transmission	1, 6, 7, 12-14, 19, 25, 27, 115, 116, 121
Sonoscan,	2	Transmitters	3
Sound-emission	2	Transmitting response	106
Souquet	13	Transparent	3
Source strength	104	transverse waves	3, 20-22, 20
Spacing	19	Trost	2
Spallanza	3	Tubular PVDF	15
Specimen,	2	Tuned,	3
Spherical	5	Tungsten	23
Spot poled PVDF	15	Turnbull	18, 19
Sproule	3	Tweeters	14
Stacking	12	Twin probe	7
Steering	18	Ultrasonic beam	2
Steinberg.	11	Ultrasonic microscopy	2
Stepanishen	15, 16	ultrasonic testing	1-3, 6, 9, 17,
Stiffness,	12		

	20, 25, 113, 124	
Underwater		1
Unidirectional		28
velocity	2, 7, 15, 20, 21, 26-29, 33, 76, 78, 87, 88	
Vibration		11
Viscosity,		2
Visual image		2
visualisation		8
Von Ramm		18
Wang		18
Wave		1
Wave number		30
Wavefront		34
wavelength	7, 12, 13, 20, 21, 23, 32, 35, 70, 95	
Wedge		24
Wei-Ming Wang		17
Weight		16
Weighting		6
Welding		2
White		17
Whittington		8
Wild		3
Willette		15
Woodward		14
Woollett		13
Yao		16
Ylitalo		18
Yoon		16

REPRINTS OF JOURNAL PAPERS PUBLISHED

BY THE AUTHOR

DESIGN CONSIDERATIONS OF TRANSDUCER ARRAY SYSTEMS FOR ULTRASONIC TESTING OF UNDERWATER PIPELINES

R. Sumangala and P.R. Saseendran Pillai

*Department of Electronics, Cochin University of Science and Technology,
Cochin 682 022, India.*

Abstract

Ultrasonic nondestructive evaluation of ocean structures and underwater pipelines will help in preventing catastrophic failures. Probes of various types have been developed for ultrasonic NDE of underwater pipelines, which require rotational as well as linear movements for the complete inspection and evaluation. This method being a time consuming one, an attempt has been made to design an annular cylindrical array, which will reduce the probe movements as much as possible. This paper presents a study of the usefulness of such an array for underwater pipeline inspection.

Introduction

Nondestructive evaluation (NDE) is one of the most challenging fields of research and development. NDE plays a significant role in the prevention of catastrophic failures, quality control and cost savings. NDE can ensure products that are more efficient, cost effective and safer for the consumer and the environment [1, 2]. Ultrasonic NDE is a more handy technique than X-rays and gamma rays. Ultrasonics is also employed in medical diagnosis and imaging applications [3]. The potential of ultrasonic technology provides an advanced means of describing the size, population, geometry and location of material anomalies. Ultrasonic NDE technique has wide applications and a considerable economic impact. This paper describes the design and development of an annular cylindrical array, which can be used for the ultrasonic NDE of underwater pipeline flaws. The beam characteristics and gain of the proposed array are studied.

High ultrasonic frequencies in the 1 – 10MHz range are often desired for NDE, to achieve a reasonable resolution of flaws or cracks. It is a low power application because the ultrasonic energy explores the test material and is modified. Ultrasonic waves are introduced into the region to be tested, and are reflected at the interfaces of materials having different acoustic properties [4]. Ultrasonic testing employs the fundamental relationship of distance, velocity and time. The various techniques used for ultrasonic testing are: the pulse echo technique, the through transmission technique and the resonance technique.

The pulse echo technique is the most versatile. A short burst of ultrasonic waves is sent into the object to be tested; echoes from the discontinuities or defects are processed and displayed on a CRT, which displays their amplitude and time of flight. In through transmission, the transmitter probe is placed on one side of the object and the ultrasound is monitored using another probe. A flaw in the path constitutes a barrier for the ultrasound, casting an acoustic shadow on the receiver probe, which thus reveals the defect. The resonance method requires two adjacent resonances for thickness determination [4].

Detection of pipeline flaws

A single probe method is in widespread use for the detection of flaws, in the pulse echo method. The probe is moved around and along the pipeline in the transmit/receive mode. A narrow beam of ultrasound generated by the probe is transmitted as pressure waves

through the coupling medium and the wall of the pipeline. A flaw present in the pipeline reflects a part of the sound energy, which is received as an echo pulse, either by the transmitting probe in the transmit/receive mode or by a separate receiving probe [5]. In this method, the probe head is required to rotate for complete inspection of the pipeline, which severely limits the speed of inspection.

These limitations can be overcome by the use of either a ring array or an annular cylindrical array. The annular cylindrical array can be seen to have improved performance.

Annular cylindrical array

The configuration of the annular cylindrical array is shown in Figure 1. It consists of m n -element linear arrays (staves), arranged in a circular configuration. In the approach presented in this paper, the desired portion of the annular cylindrical array, consisting of l n -element linear arrays can be energised, which will generate a focussed beam. An appropriately grouped set of the remaining staves of the annular cylindrical array will be used for receiving the echo pulse. The beam pattern $B(\theta)$ of the portion of the annular cylindrical array, consisting of l staves, can be expressed to a good approximation using [6]:

$$B(\theta) = b(\theta) b'(\theta) ,$$

where $b(\theta)$ and $b'(\theta)$ are the beam patterns of the n -element linear array and l -element curved array. The value of l should be typically less than 6.

Consider two adjacent elements A and B in the ring array, as shown in Figure 2. The path difference between A and B is

$$U = R \{ [\sin(\theta' + d'/R) - \sin \theta'] \sin \phi \} .$$

The path difference for the l th element along the circumference is

$$U_{l-1} = R \{ [\sin(\theta' + \overline{l-1} d'/R) - \sin \theta'] \sin \phi \} ,$$

where d is the inter-element spacing, d' is the arc length between A and B, R is the radius of the annular cylindrical array and $k = 2\pi/\lambda$, the wave vector; λ being the wavelength of the acoustic radiation. The total output voltage developed in the l -element curved array is

$$\begin{aligned} V &= e^{jU_0} + e^{jU_1} + \dots + e^{jU_{(l-1)}} \\ &= \sum_{i=0}^{l-1} \cos kR \{ [\sin(\theta' + id'/R) - \sin \theta'] \sin \phi \} \\ &\quad + j \sum_{i=0}^{l-1} \sin kR \{ [\sin(\theta' + id'/R) - \sin \theta'] \sin \phi \} . \end{aligned}$$

The beam pattern of l elements along the circumference is

$$b'(\theta) = [V/l]^2 ,$$

and the beam pattern of the n -element linear array is

$$b(\theta) = \left[\frac{\sin(n\pi d \sin \theta \cos \phi)}{n \sin(\pi d \sin \theta \cos \phi)} \right]^2 .$$

Hence, using [6]

$$\begin{aligned} B(\theta) &= \left[\frac{\sin(n\pi d \sin \theta \cos \phi)}{n \sin(\pi d \sin \theta \cos \phi)} \right]^2 \times \\ &\quad \frac{1}{l^2} \left\{ \left[\sum_{i=0}^{l-1} \cos kR \{ [\sin(\theta' + id'/R) - \sin \theta'] \sin \phi \} \right]^2 \right. \\ &\quad \left. + \left[\sum_{i=0}^{l-1} \sin kR \{ [\sin(\theta' + id'/R) - \sin \theta'] \sin \phi \} \right]^2 \right\} . \end{aligned}$$

The beam pattern for the case $n = 10$ and $l = 3$ is shown in Figure 3. The array gain of the proposed array is computed using the cross-correlation coefficients of the signal and noise. The cross-correlation coefficient for single frequency, zero time delay, uni-directional signal and the cross-correlation coefficient of isotropic noise are computed using [7].

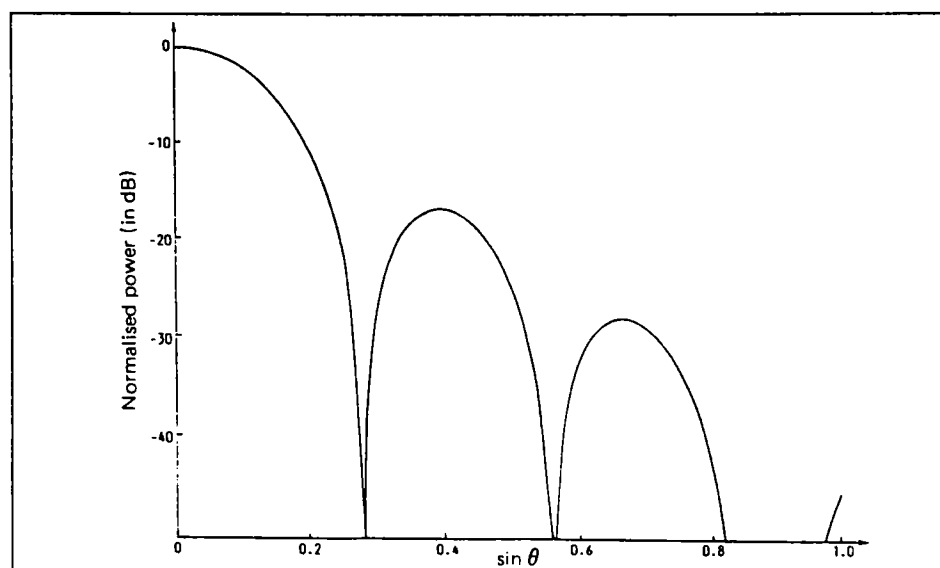
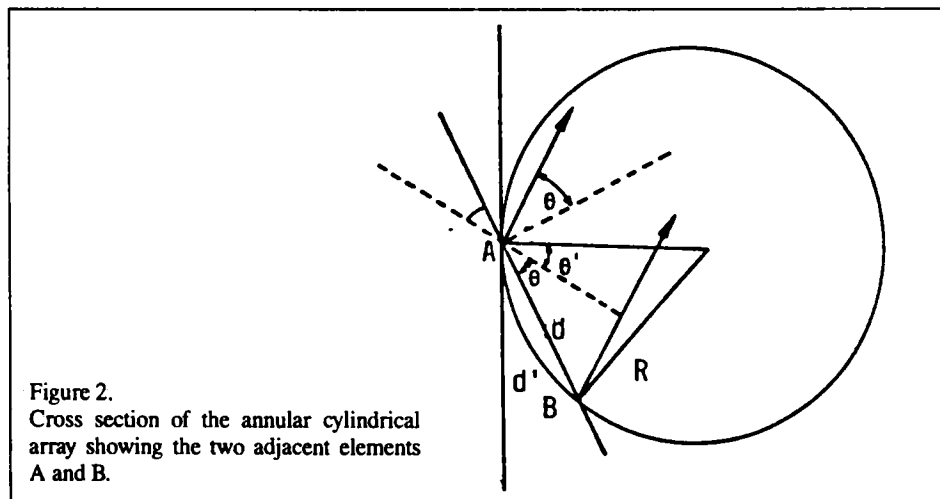
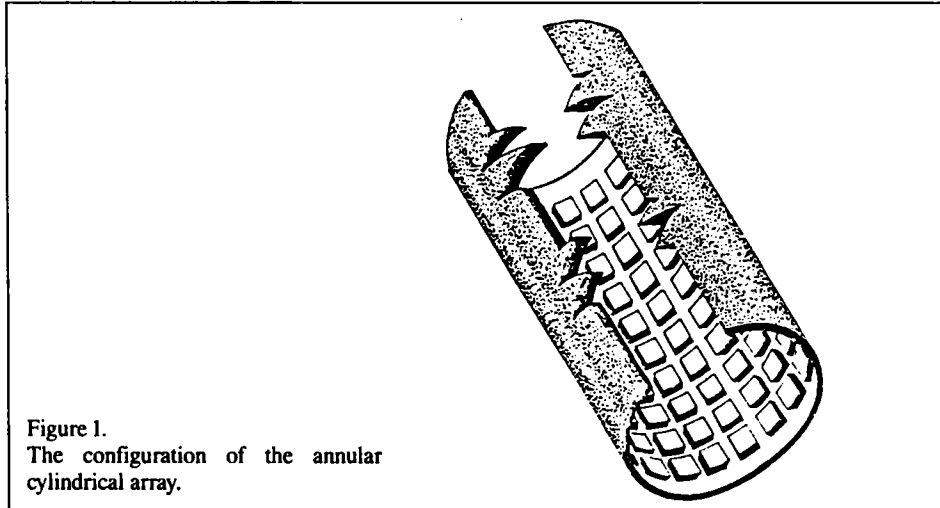


Figure 3. Beam pattern of the portion of the annular cylindrical array consisting of $n = 10$ and $l = 3$.

Results and discussion

The effect of variation of the radius of the annular cylindrical array on its beam characteristics for $n = 10$ and $l = 3$ is given in table 1. It can be seen from the table that the half-power beamwidth, the most intense sidelobe level and the sidelobe level at 90 degrees to the beam axis remain constant, when R exceeds 40λ .

Table 1.
Effect of radius of the annular cylindrical array on the beam characteristics.

Radius R (in λ)	Most intense sidelobe level (in dB)	Sidelobe level at 90° (in dB)	3dB beamwidth (in degrees)
5	-14.84	-42.49	-14.4
10	-15.14	-42.25	-14.2
20	-15.29	-42.19	-14.1
30	-15.34	-42.18	-14.1
40	-15.36	-42.17	-14.0
50	-15.38	-42.17	-14.0
60	-15.39	-42.17	-14.0
100	-15.40	-42.17	-14.0

The array performance summarised in table 2 shows the effect of the number of staves l for $n = 10$ and $\phi = \pi/4$. Annular cylindrical arrays can be found to have better array gains, when compared to planar arrays of the same size.

Table 2.
Effect of the number of staves on the array performance.

Number of staves in the array l	Most intense sidelobe level (in dB)	3dB bandwidth (in degrees)	Sidelobe level at 90° (in dB)	Array gain for $\theta = \pi/4$ $\phi = \pi/2$ (in dB)
2	-13.90	14.2	-26.17	9.79
3	-15.40	14.0	-42.17	10.13
4	-17.61	13.6	-30.53	10.23
5	-20.50	13.2	-35.67	10.39

Taking into account the design considerations and the acoustic impedance match to water, piezo-film transducers are being evolved for the performance evaluation of the proposed array. Diametrically opposite set of staves can be used as transmitting and receiving arrays.

Conclusions

The half-power beamwidth and the sidelobe levels of annular cylindrical arrays remain unaffected beyond $R = 40\lambda$. Annular cylindrical arrays are seen to have better gain and array performance.

Acknowledgements

The authors gratefully thank the authorities of the Cochin University of Science and Technology for providing the necessary facilities to carry out this work and the Ministry of Human Resource Development, Government of India, for financial assistance.

References

- [1] Papadakis, E.P., *Future Growth of Nondestructive Evaluation*, *IEEE Trans. on Sonics and Ultrasonics*, SU-23, 5, 284-287, (1976).

- [2] Buckley, M.J., *The Future Economic Role of NDE*, *IEEE Trans. on Sonics and Ultrasonics*, SU-23, 5, 287–291, (1976).
- [3] Havlice, J.E. and Taenzer, J.C., *Medical Ultrasonic Imaging: An Overview of Principles and Instrumentation*, *Proc. of IEEE*, 67, 4, 620–641 (1979).
- [4] Szilard, J., *Ultrasonic Testing*, John Wiley & Sons, Ltd., pp.32–51, (1982).
- [5] Steinberg, E.B., *Ultrasonics in Industry*, *Proc. of IEEE*, 53, 10, 1292–1304, (1965).
- [6] Johnson, R.C. and Jasik, H., *Antenna Engineering Handbook*, McGraw Hill Book Company, pp.20–16, (1984).
- [7] Urlick, R.J., *Principles of Underwater Sound*, McGraw Hill Book Company, pp.30–37 & 51–53, (1967).

(Received 23 June 1991)

2:30

2pEA7. Close-packed acoustic array element interaction. John B. Blottman III (Naval Undersea Warfare Ctr., New London Detachment, New London, CT 06320) and Jean-Noël Decarpigny (Inst. Supérieur d'Electron. du Nord, 59046 Lille Cedex, France)

The acoustic array element interaction is an essential parameter determining transducer array behavior. It is characterized by the mutual radiation impedance. Low-frequency transducers in a volumetric array with small size constraints are subject to much larger interaction and scattering than in conventional arrays. This paper provides an overview of an investigation of the modal components of mutual radiation impedance. The *in vacuo* eigenmodes of a single element are determined using the ATILA finite-element method. Selection of the modal expansion terms will be based on their radiation efficiencies. Modal radiation impedances are generated using the EQI boundary integral equation method. A simple multi-mode equivalent circuit model of the *in situ* projectors, including the interaction effects, is proposed. Comparison of the results to a full finite-element model of an array is presented.

2:45–3:00 Break

3:00

2pEA8. Sensor-actuator interactions in the NRL-ABC platform. Robert D. Corsaro and Brian Houston (Naval Res. Lab., Code 7130, Washington, DC 20375-5350)

The ABC research platform consists of a large array of multifunctional transducers mounted on a backing structure. It was specifically constructed for underwater studies of sensor/actuator coupling mechanisms. The platform transducers are represented as a 15 tile array of ABC tiles, where each tile contains a large area actuator, pressure sensor, and velocity sensor, where the latter is constructed by summing and integrating the outputs of four accelerometers. Acoustic characteristics of the ABC tiles and platform were evaluated in the NRL Large Pool Facility, both in the freefield and when mounted on a backing structure. This paper presents results and analysis of inter- and intra-tile coupling mechanisms, including particularly an evaluation of the role of the backing structure.

3:15

2pEA9. Acoustic pressure field evaluation of an annular cylindrical array for underwater pipeline inspection. R. Sumangala and P. R. Saseendran Pillai (Dept. of Electron., Cochin Univ. of Sci. and Technol., Cochin-682 022, India)

Evaluation of the effective acoustic pressure field of a continuous wave, optimum spaced, point source, annular cylindrical array for underwater pipeline inspection is featured in this paper. A section of the array comprised of $m \times n$ elements is selectively energized to illuminate the region to be tested and a similarly grouped set of remaining array elements function as receivers. A steady half-power beamwidth and sidelobe levels were obtained for a radius of the array greater than 40λ . The portion of the energy reflected or reradiated from the contours of the pipeline and captured by the point source elements being nominally small can be neglected for all practical purposes. Effective acoustic pressure is computed as the Fourier transform of the impulse response of the array elements $h_m(r, t)$ determined using the Green's function approach. The total effective acoustic pressure over the contour of the pipeline is the sum of the weighted contributions from all radiating set of elements. A good focusing effect can be achieved by optimizing the number of elements and the radius of the array. [Work supported by CSIR INDIA.]

2pEA10. Transmission and reception performance of multilayered transducer structures. David J. Powell (Dept. of Ocean Eng., Florida Atlantic Univ., Boca Raton, FL 33431), Robert Y. Ting (Naval Undersea Warfare Ctr., Orlando, FL 32856-8337), and Thomas R. Howarth (Naval Res. Labs., Washington, DC 20375)

Multilayered transducer structures offer the potential for greater performance in terms of increased radiated acoustic power and improved reception characteristics. In earlier work, a unidimensional modeling approach was presented, that was shown to provide a means of accurately predicting the in-air electrical impedance characteristics of a range of different laminated transducer structures [J. Acoust. Soc. Am. 97, 3299(A) (1995)]. These prototype devices have since been encapsulated within polyurethane rubber ready for in-water acoustic testing. This paper presents a theoretical and experimental analysis of both the transmission and reception performance characteristics of this group of multilayered devices. The effects of intermediate bondlines and electrode layers will be considered in terms of changes to both the device's sensitivity and its resonant frequency. Transducer performance will be assessed via the standard figures of merit, TVR and FFVS, in conjunction with its pulse-echo transient response. Theoretical predictions from the unidimensional model are in good agreement with experimentally obtained values. The polyurethane encapsulant was found to have detrimental effects on overall transducer performance. Beam profiles for the laminated devices have been recorded experimentally and are compared to the responses of their single-layer counterparts. [Work sponsored by the Office of Naval Research.]

3:45

2pEA11. A reinforced Neoprene rubber boot for the barrel-stave flextensional projector. Dennis F. Jones (Defence Res. Establishment Atlantic, P.O. Box 1012, Dartmouth, NS B2Y 3Z7, Canada)

The Class I barrel-stave flextensional projector is a lightweight and compact underwater sound source that is well-suited to low-frequency sonar and oceanographic applications. By modifying a few of the parts used in the Class I projector, a high-power Class II or broadband Class III barrel-stave projector can be constructed, which is testimony to the versatility of the basic barrel-stave design. These projectors require gaps, between adjacent staves, that are sufficiently wide for free-stave vibration at the operating drive levels and water depths. Gap widths of about 1 mm are typical. A rubber boot is stretched over the projector to inhibit the ingress of seawater through the gaps. However, since the gap widths and boot wall thicknesses are similar, the boots can be forced into the gaps by hydrostatic pressure, causing significant variations in the projector performance parameters with water depth [D. F. Jones and M. B. Moffett, J. Acoust. Soc. Am. 93, 2305(A) (1993)]. To minimize these variations, a new rubber boot with reinforcements in the vicinity of the gaps has been fabricated and tested on a Class II barrel-stave projector. Measured results showing performance stability with depth are presented.

4:00

2pEA12. Assessment of a fractal model for corona discharges in salt water. H. M. Jones, J. C. Epsinoso, M. L. Galloway, A. M. Gleeson, and R. L. Rogers (Appl. Res. Labs., Univ. of Texas, P.O. Box 8029, Austin, TX 78713-8029)

The prebreakdown corona phase of a spark discharge in salt water produces a measurable acoustic pulse. This pulse is produced by the formation and collapse of a vapor bubble. The plasma has a multiply fingered shape, and it creates a bubble with a corresponding acoustic pulse. The rate of formation of plasma fingers may be a fractal dimension of the size of the discharge. A fractal model of the growth of the corona discharge can be used to connect the variables of voltage, current, and bubble wall acceleration. The dependence of the acoustic and electrical response and thus the fractal dimension of the corona growth on liquid conductivity, and applied voltage are investigated. The acoustic data are used to infer the bubble wall acceleration while the current-voltage data are measured directly and used to determine the total resistance of the plasma. The corona is formed by the application of high-amplitude electric fields to a set of electrodes that are immersed in the liquid. [Work supported by the Office of Naval Research under Grant No. N00014-94-1-0150.]

Transient Pressure Variation of Pulse Excited Ring Array for Pipeline Testing

R. Sumangala and P.R. Saseendran Pillai
Department of Electronics
Cochin University of Science and Technology
Cochin - 682 022, INDIA

Abstract

An ultrasonic transducer array comprising a selectively energised section of a ring array concentric to the test pipeline, with the ultrasound focused on its contour is used for underwater pipeline inspection. Beam characteristics, sidelobe levels and effective acoustic pressure of the array is evaluated. The transient response as well as the continuous wave effective acoustic pressure of a section of the ring array is computed for different configurations. A comparison of the acoustic pressure field of the ring array with a linear array demonstrates the focusing effect of the ring array for such applications.

INTRODUCTION

Ultrasound transducers find major applications in flaw detection and medical diagnosis. A large number of ultrasonic probes have been developed suitable for various applications[1]. Generally single probe transducers are being used for inspection and detection of flaws in underwater pipelines, but a substantial time saving in the inspection can be achieved by using suitable arrays. Investigations on phased array configurations as potential applicators for ultrasound hyperthermia cancer therapy are also in progress[2]. By adjusting the driving signal to each array element, the focused beam of the phased array can be translocated to the desired region, thereby eliminating the mechanical movement of the applicator that must be continuously moved[3]. Fabrication of ultrasonic arrays is feasible using integrated circuit and hybrid construction techniques.

Generally used NDE techniques are the reflected pulse and the beam obscuration techniques. In the reflected pulse amplitude technique, the amplitude of the reflected pulse is affected by defect type, shape, size, orientation and diffraction of ultrasonic beam and also the test piece geometry, surface conditions and material characteristics. Successful and reliable defect detection can be achieved, taking into account, diffraction around the edges of the defect, distance from the surface of detection, consistent acoustic coupling and formation of standing waves [5,6].

The pressure field of short pulse transducers have been evaluated using the convolution as well as Fourier transform technique[4]. Turnbull, Foster, Ebbini etc have carried out valuable studies on ultrasound phased arrays as promising tools in biomedical imaging. Convolution and Fourier transform techniques have been employed for the prediction of the field of a short pulse device as reported by Stephanishen, Freedman, Robinson, Foster, Hunt etc., [4,7-10]. Pulsed two dimensional transducer arrays suited for medical imaging have been studied by Turnbull and Foster [3]. In a narrow band or continuous wave excited two dimensional array system, the pressure distribution is computed as the product of axial pressure distribution, element factor and array factor. The transient field is obtained as the convolution of the ultrasound waveform with the impulse response of the acoustic source. Another approach using the Fourier transform technique has been employed by Foster and Hunt, in which the pressure pulse leaving the transducer is split into its continuous wave components and allowed to propagate to the field point and then reassembled in the correct phase [4]. A widely spaced point source ultrasound ring array working in the near field was designed, by Whittington and Cox, requiring a rotation of 10° for complete inspection of the pipe. Inspection of underwater pipelines have been carried out by single probe and twin probe transducers in the single and multiple reflection modes. The probes have to be rotated about the pipeline for complete inspection. A ring array or annular array with electronic switching reduces the need for mechanical

rotation of the transducer probes.

The formulation and computation results of array characteristics and effective acoustic pressure of a ring array for underwater pipeline inspection is featured in this paper.

PRINCIPLE

The inspection system comprises a ring array placed concentric over the pipeline and a section of M elements are selectively activated to focus the ultrasound along the contour of the pipeline. Fig.1 shows the configuration and orientation of the array about the pipeline. The array may be operated in the reflection or through transmission mode. The same section or a similarly grouped set of elements of the array may act as receivers to collect the information of the defect. The ultrasound gets reflected at the discontinuity and the reflected echo is obtained corresponding to it. In the through transmission, there is an acoustic shadow at the discontinuity. Some of the assumptions made for the computations of beam characteristics and effective acoustic pressure is that point source of elements with spacings of half the acoustic wavelength are considered. Therefore grating lobes are eliminated and interelement interaction is minimal. The amount of reradiated energy captured by the point source of elements can be neglected for all practical purposes. Finite size of the elements are to be considered when realising the array.

THEORETICAL CONSIDERATIONS

Receiving array

The beam pattern of the desired section of the receiving ring array comprising of M elements is computed as $B(\theta)$. Plane acoustic waves incident on the transducer elements generate an electrical output. Total output voltage from the section is the sum of the weighted contributions from each element [11-12]. From Fig.2, the path difference U_m due to the m^{th} element relative to the 1^{st} element is obtained from the geometry of the array shown in Fig.2 as,

$$U_m = R \left[\sin\left(\theta' + \frac{md'}{R}\right) - \sin\theta' \right] \sin\phi \quad (1)$$

where, d is the interelement spacing, d' is the spacing along the circumference of the array,

$$\phi = \pi/4, \text{ and } \theta' = \sin^{-1} \left[\frac{R}{d} \sin\left(\frac{d'}{R}\right) \right] - \theta \quad (2)$$

Hence total output voltage V can be computed as,

$$V = \sum_{m=0}^{M-1} \cos \left\{ kR \left[\sin\left(\theta' + \frac{md'}{R}\right) - \sin\theta' \right] \sin\phi \right\} \\ + j \sum_{m=0}^{M-1} \sin \left\{ kR \left[\sin\left(\theta' + \frac{md'}{R}\right) - \sin\theta' \right] \sin\phi \right\} \quad (3)$$

where $k = 2\pi/\lambda$ and λ is the acoustic wavelength.

Beam pattern of the receiving ring array is computed as

$$B(\theta) = \left(\frac{V}{M} \right)^2 \quad (4)$$

$$B(\theta) = \frac{1}{M^2} \left[\sum_{m=0}^{M-1} \cos \left\{ kR \left[\sin\left(\theta' + \frac{md'}{R}\right) - \sin\theta' \right] \sin\phi \right\} \right]^2 \\ + \frac{1}{M^2} \left[\sum_{m=0}^{M-1} \sin \left\{ kR \left[\sin\left(\theta' + \frac{md'}{R}\right) - \sin\theta' \right] \sin\phi \right\} \right]^2 \quad (5)$$

Transmitting array

Effective acoustic pressure developed at a distance r from a simple source has been described by Leon Camp [13]. The effective acoustic pressure at a point along the contour of the pipeline for a continuous wave excited ring array is the numerical sum of the weighted contributions from the selectively energised M elements. The acoustic pressure at any desired point along the pipeline can be computed as,

$$P = \sum_m \frac{A}{r_m} e^{j\omega \left(t - \frac{r_m}{v} \right)} \quad (6)$$

where A is the r.m.s value of pressure at a distance of 1m, r_m is the path length, v is the acoustic velocity and ω is the angular velocity. From the geometry of the array in Fig.2 the path length r_m is,

$$r_m = \sqrt{z^2 + 4R(R-z)\sin^2\left(\frac{md}{R} - \phi'\right)} \quad (7)$$

where z is the radial distance between the array and the test pipeline and ϕ' is the angle between the field point and the central element with the center of the pipeline.

Transient response

A gated sinewave signal of frequency 5.0 MHz is applied to the array for a duration of $0.2\mu\text{s}$. The transient pressure P , on the contour of the pipeline for the pulse excited ring array is

$$P = \sum_m \frac{A}{r_m} e^{j\omega(t-t_m)} \quad t_m < t < t_m + \tau$$

where τ is the pulse width and t_m is the time delay from the m^{th} element. The time of arrival from the nearest and farthest sources to the field point are t_0 and t_m respectively. Hence the weighted contributions from all the all the M sources are obtained from the instant t_m to $t_0 + \tau$.

RESULTS AND DISCUSSIONS

The beam characteristics of different configurations of the point source receiving ring array of radius 3cm, with interelement spacing of $\lambda/2$ and operating at 5.0 MHz is given by $B(\theta)$ a plot of which is shown against $\text{Sin}\theta$, in Fig.3. The beam characteristics of a 5 element section operating at 5.0 MHz is studied for different array radii. From Table 1. it can be seen that the sidelobe levels and 3dB beamwidth are found to remain unaffected for larger radii, typically greater than 40λ .

Total effective acoustic pressure along the contour of the pipeline at any instant is the sum of the weighted contributions from all radiating set of elements. The computation of the effective acoustic pressure over a desired portion of the contour of the pipeline using a ring array of point sources is carried out for continuous and pulsed mode of excitations. The effective acoustic pressure of a ring array at the desired portion of the test pipeline is computed for continuous waves by varying the value of ϕ' . The pressure relative to that at $\phi'=0$ is computed. Variations of the acoustic pressure fields for different configurations of the array are shown in Fig.4. The focusing effect is found to be favorable for a 21 element array.

Computation of effective acoustic pressure along the pipeline for both linear and ring array of 21 elements with an interelement spacing of $\lambda/2$ and an operating frequency of 5.0 MHz shows a narrow beam generated by the ring array, thus demonstrating its focusing effect in Fig.4.

The array geometry and pipeline geometry can be optimised from the radial pressure distribution of the array. Figure 5 shows the axial pressure distribution of a 5 element section of a ring array of radius 10cm and operating frequency 5.0 MHz. The field remains steady from a distance of 3cm onwards. Therefore this array would be suitable for inspection of pipelines of radius upto 7cms.

CONCLUSION

The radial pressure distribution of the proposed array has been investigated for different array configurations from which the number of elements and array geometry can be optimised for different

pipeline geometry. A good focusing effect can be obtained by optimizing the number of elements and the radius of a ring array. Performance evaluation of the ring array shows that the sidelobe levels and 3dB beamwidth remain unaffected for radii greater than 40λ . The transient response of a pulse excited ring array over the contours of the test pipeline has been evaluated.

Acknowledgements

The authors gratefully thank the Council of Scientific and Industrial Research, New Delhi, for financial assistance.

References

- [1] Bruce R. Thompson and Donald O. Thompson, "Ultrasonics in Nondestructive Evaluation", Proc. of IEEE, 73(12), pp.1716-1755.
- [2] Emad.S.Ebbini and Charles.A.Cain, "Experimental Evaluation of a Prototype Cylindrical Section Ultrasound Hyperthermia Phased Array Applicator", IEEE Trans. Ultrason. Ferroelec. Freq. Control UFFC Vol.38, No.5, pp.510-520, Sept.1991.
- [3] Daniel H. Turnbull and F. Stuart Foster, "Beam Steering With Pulsed Two Dimensional Transducer Array" IEEE Trans. on Ultrasonics Ferroelectrics and Frequency Control, 38(4), pp.320-333, 1981.
- [4] F.S. Foster and J.W. Hunt, "The Design and Characterisation of Short Pulse Ultrasound Transducers", Ultrasonics, May 1978, pp.116-122.
- [5] J. Krautkramer and H. Krautkramer, "Ultrasonic Testing of Materials", Springer-Verlag, pp.160-170, 196-204, 409-422, 1990.
- [6] J. Szilard, "Ultrasonic Testing" John Wiley & Sons Ltd. 1982.
- [7] Stephanishen P.R., "Transient Radiation from Pistons in an Infinite Planar Baffle", Journal of Acoust. Soc. of America 49, pp.1629-1638, 1970.
- [8] Freedman A., "Sound Field of Plane or Gently Curved Pulsed Radiators", Journal of Acoust. Soc. of America 48, pp.221-227, 1969.
- [9] Robinson D.E., "Near Field Transient Radiation Patterns for Circular Pistons", IEEE Trans. ASSP 22, pp.395-403, 1974.
- [10] Goodman J.W., "Introduction to Fourier Optics", Mc Graw-Hill, NewYork 1968.
- [11] Richard C.Johnson, Henry Jasic,"Antenna Engineering Handbook", McGraw Hill Book Company, 1984.
- [12] Robert J.Urick,"Principles of Underwater Sound", McGraw Hill Book Company, 1967,pp 30-37, 51-53.
- [13] Leon Camp, "Underwater Acoustics" Wiley Interscience 1970.

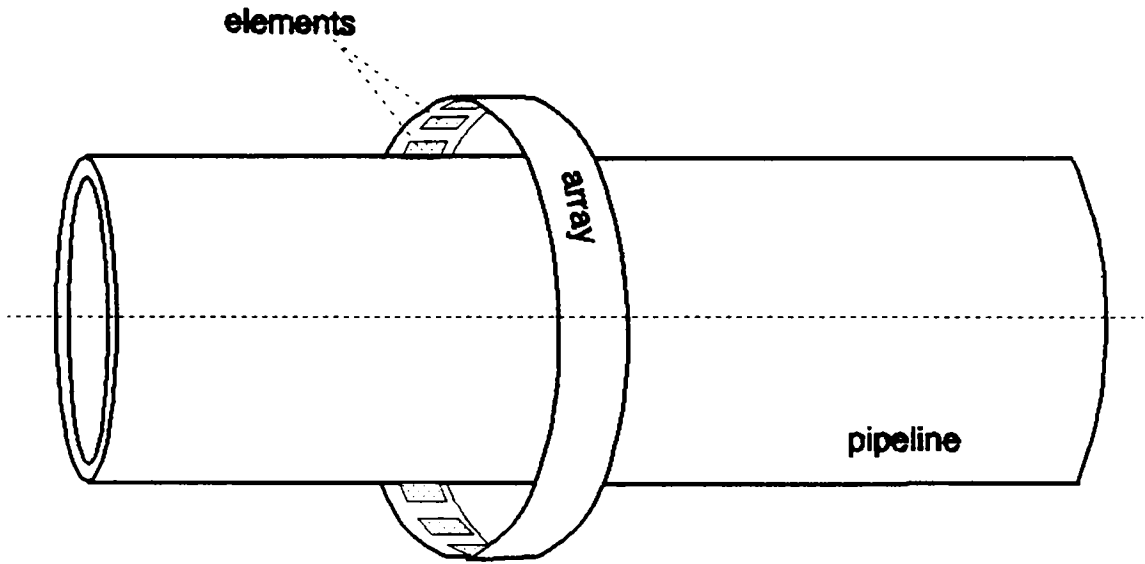


Fig. 1 Configuration and orientation of the ring array about the pipeline

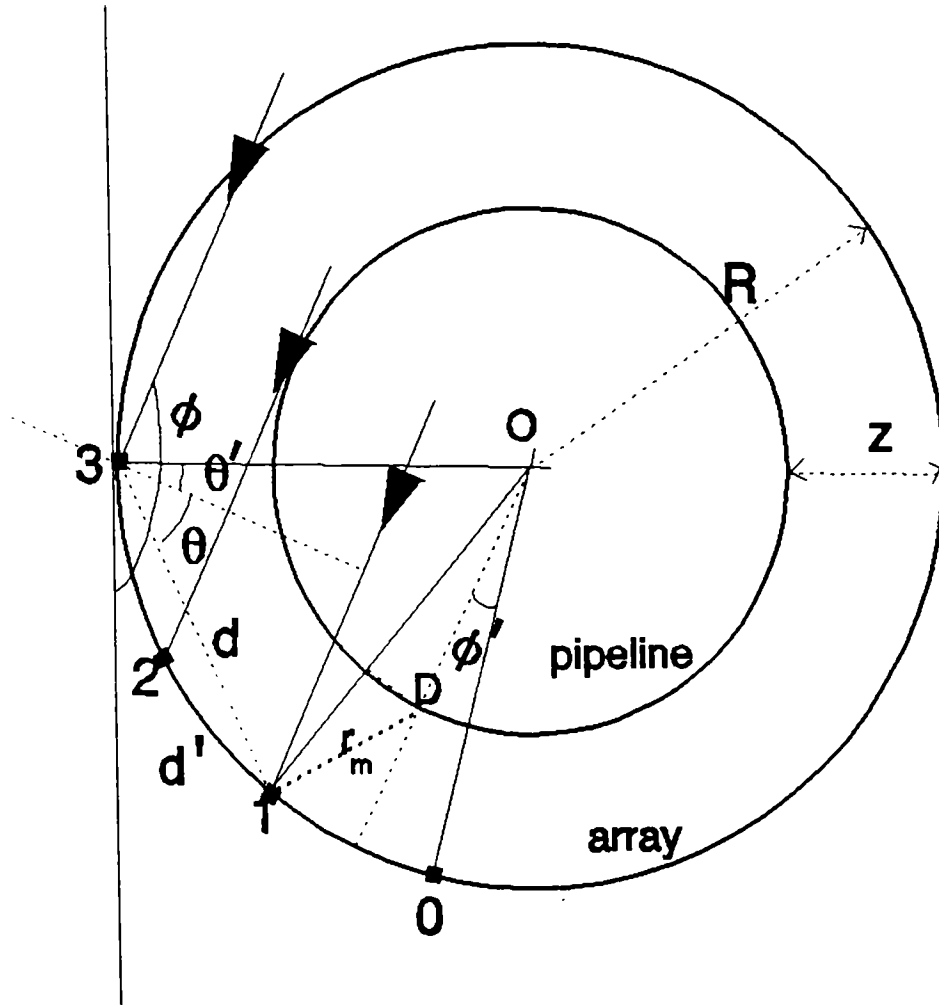


Fig. 2 Geometrical variables used for computation

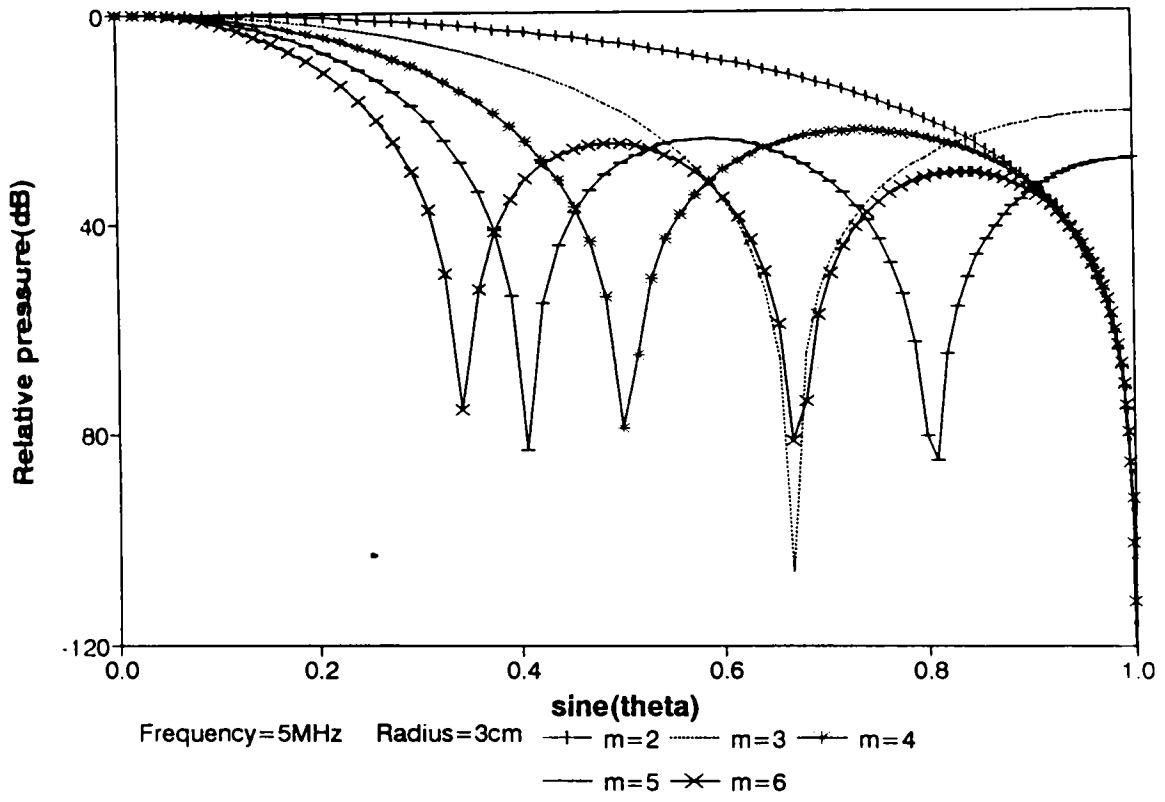


Fig. 3 Beam characteristics for different sections of the ring array

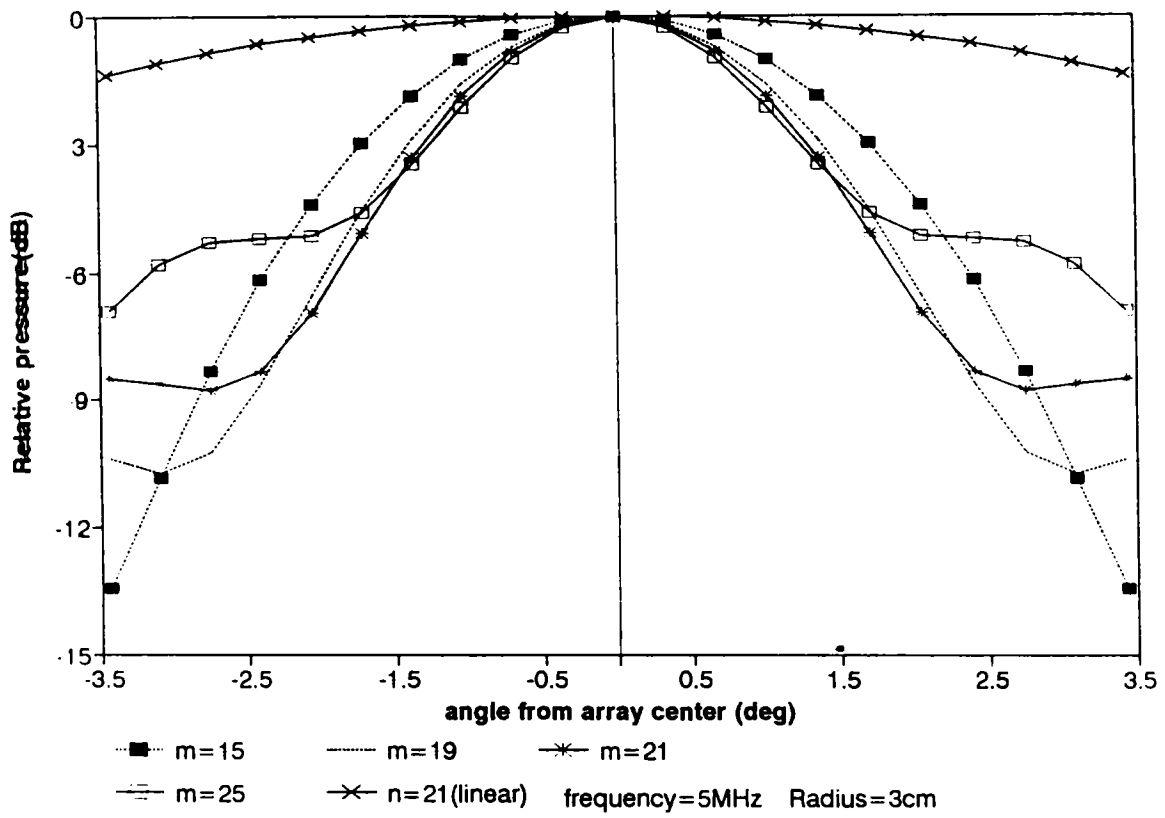
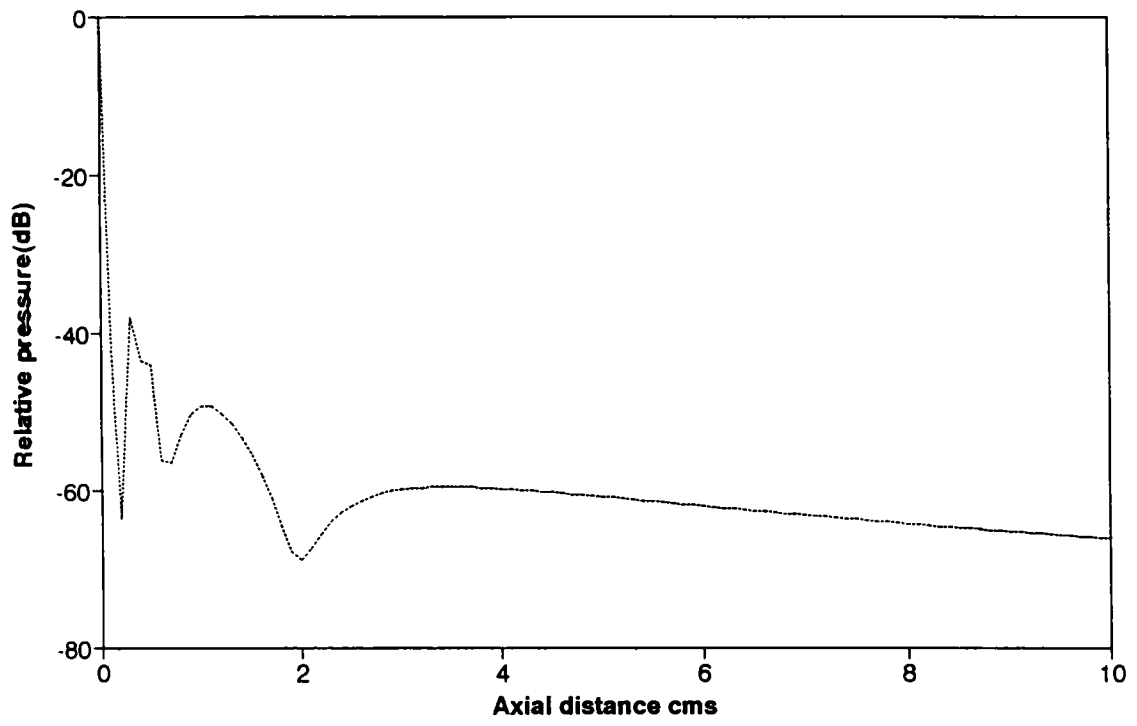


Fig. 4 Acoustic pressure field for different sections of the ring array and its focusing effect



— m=5 Frequency=5MHz Radius of ring array=10cm

Fig. 5 Axial pressure distribution of a 5 element ring array

Array Radius in wavelenths (λ)	Most Intense sibelobe level (dB)	Sidelobe level at 90° (dB)	3 dB Beamwidth (degrees)
10	-22.802	-28.107	22
20	-23.928	-28.623	20
30	-24.294	-28.719	18
40	-24.457	-28.753	17
50	-24.408	-28.768	17
60	-24.375	-28.777	17
70	-24.352	-28.782	16
80	-24.335	-28.785	16
90	-24.322	-28.788	16
100	-24.311	-28.789	16

Frequency=5MHz Radius= 100λ $d=\lambda/2$ wavelength $\lambda=0.03\text{cm}$

Table 1 Effect of radius of the array on beam characteristics of the 5 element section